

## 9

# New Strategies in the Synthesis of Grafted Supports

R. JORDAN

### 9.1

#### Introduction and Scope

The deposition of thin layers of organic compounds onto solids results in materials with the physical bulk property of the solid and the properties of the organic compound forming a new interface. The behavior of the resulting material, however, can not only be described by the mere addition of the physical and chemical properties of the solid and the deposited organic compound but the *morphology* and *dynamic behavior* of the thin layer has to be taken into account. Adsorption, wetting, adhesion and friction are strictly confined to the interface and are the origins of the macroscopic behavior of the new composite material. Rationalization of this simple fact resulted in the development of well-defined surface coatings, where the organic compound is not only *deposited* onto the solid but also *assembled*. The assembly of organic compounds into a defined layer requires firstly, a detailed knowledge of the physical properties (roughness, curvature, porosity, etc) and chemical properties (surface chemistry) of the support, ideally down to the dimension of the molecules which are to be assembled and secondly, to take into account the *interplay of order and mobility* within the layer. This is determined by the shape as well as size or molar mass of the molecules and their possible interactions along the phase boundaries. To illustrate the second point, Fig. 9.1 gives some examples of organic coatings, starting from monomolecular layers with a thickness of a few angstroms, to polymer coatings of several micrometers.

A schematic illustration of surface coatings with their typical thickness ranging from angstroms to micrometers. Selected are monomolecular layers fabricated by the transfer of Langmuir–Blodgett (LB) films onto solid substrates (1); self-assembled monolayers (SAMs) (2); multilayers thereof (3); polymer-supported (alkyl) monolayers (PSMs) (4); physisorbed or chemisorbed polymer coatings (5); polymer brushes (6) and polymer layers fabricated by macroscopic casting techniques (7) along with possible ways of their fabrication and characteristic layer dimensions.

It is beyond the scope of this Chapter to discuss all kinds of various coating techniques, properties of the supports, properties of the coatings and the various fields of application of the composites in catalysis, separation techniques, materials science, colloid science, sensor technology, biocompatible materials, biomi-

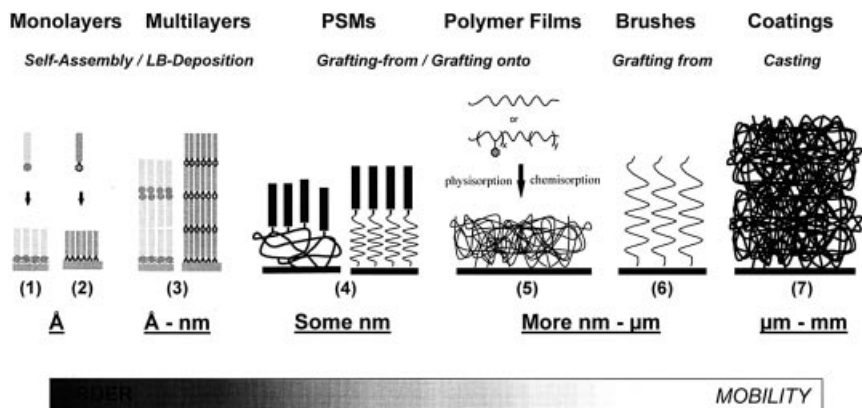


**Fig. 9.1** A schematic illustration of surface coatings with their typical thickness ranging from angstroms to micrometers. Selected are monomolecular layers fabricated by the transfer of Langmuir–Blodgett (LB) films onto solid substrates (1); self-assembled monolayers (SAMs) (2); multilayers thereof (3); polymer-

supported (alkyl) monolayers (PSMs) (4); physisorbed or chemisorbed polymer coatings (5); polymer brushes (6) and polymer layers fabricated by macroscopic casting techniques (7) along with possible ways of their fabrication and characteristic layer dimensions.

metric materials, optics etc. The scope had to be restricted to the fundamental properties of ultrathin organic layers on solid supports followed by some examples, outlining the benefit of the tailored functional surfaces such as SAM and polymer brushes for catalysis.

Taking Fig. 9.1 as a guideline, the formation and properties of monomolecular layers formed by self-assembly is discussed, followed by slightly thicker layers in which mesogenic (order-inducing) units are combined with flexible polymers and finally, new aspects in the preparation and properties of so called polymer brushes are presented. The latter will form a central subject of this Chapter, since new synthetic strategies have very recently been developed which enable the preparation of surface grafted polymer coatings of defined morphology and polymer architectures. By this, responsive functional coatings can be fabricated, being at the fine boundary between order and mobility.

## 9.2

### Self-assembled Monolayers

#### 9.2.1

##### Two Dimensional Self-assembly

Highly ordered monomolecular layers on a solid substrate were originally prepared by the so-called Langmuir–Blodgett technique. Surfactant molecules are spread at the air-water interface and pre-assemble themselves by orienting the hy-

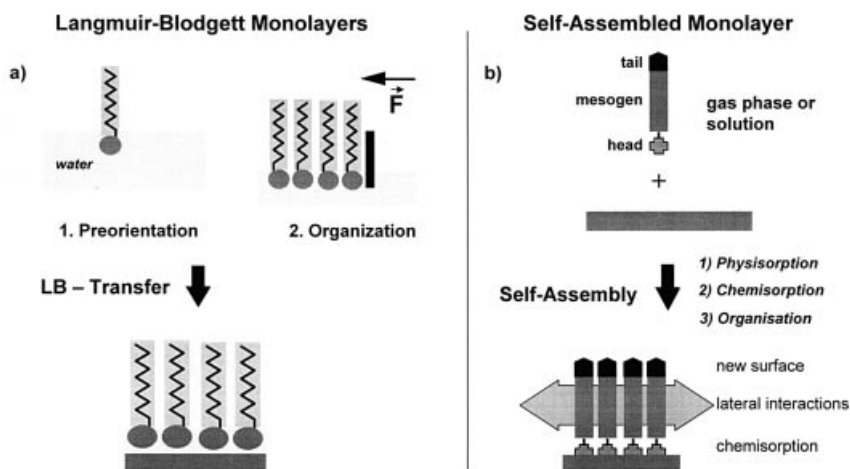


**Fig. 9.2** Preparation of oriented monomolecular layers of surface active molecules on a solid support by (a) the Langmuir–Blodgett

technique and consecutive transfer and (b) self-assembly

drophilic (polar or charged) head group towards the water and the hydrophobic tail towards the gas phase. The degree of order in this assembly can be increased by successive reduction of the available cross-sectional area for each molecule, simply by pushing the molecules together macroscopically by a movable barrier of an LB trough. During compression, the monolayer undergoes phase transition in two dimensions; analog to phase transitions in three dimensions: from the ‘gas-analog’ to the ‘liquid-analog’ up to the ‘solid-analog’ state. The phase transitions in the compression isotherms (lateral pressure,  $\Pi$ , versus area per molecule) and corresponding molecular ordering are depicted in Fig. 9.2. With this technique, highly organized monolayers can be prepared at the air–water interface having their hydrophobic moieties, typically  $n$ -alkyl tails, in a 2D crystalline analog state. Such layers can be deposited onto a solid substrate by controlled dipping of the substrate through the interface. The major drawback of monomolecular films prepared in this manner is the limited chemical and physical stability of the monolayer caused by its lack of strong specific (covalent) interactions, and the relatively tedious preparation, which limits the shape, surface topography and dimension of the substrate. Despite these drawbacks, it has to be noted that the LB-technique is not obsolete but still a very valuable tool for the study of amphiphilic compounds and the preparation of two-dimensional arrangements.

Monomolecular layers of the same quality in terms of the degree of order can also be prepared by *self-assembly*. Molecules forming self-assembled monolayers (SAMs) are characterized by three features: (1) A surface active *head group*, able to specifically bind to the substrate, (2) a suitable *mesogenic unit* to ensure favorable lateral intramolecular interactions and (3), a *tail group* which ultimately defines the surface physics and chemistry of the resulting SAM (Fig. 9.2). Since it is *self-assembly* the preparation is rather simple: The molecules assemble themselves

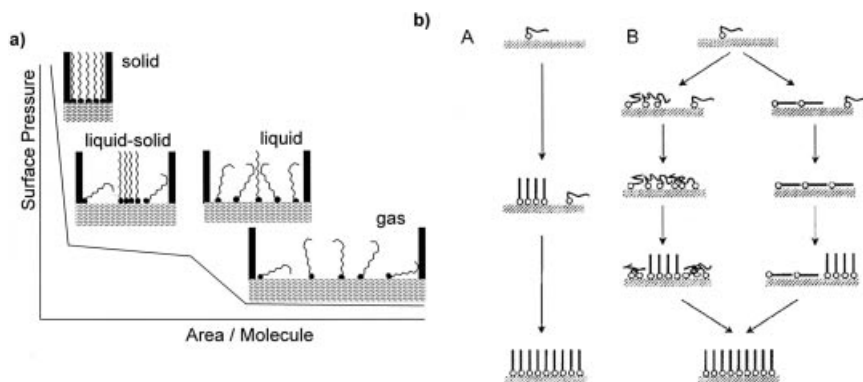


**Fig. 9.3** (a) Typical pressure-area ( $\Pi$ -A) isotherm with phase transition during compression of a monomolecular film of a surfactant along with a schematic depiction of the molecules. Depending on the mesogen, coexistence phases (e.g. liquid-solid coexistence phases) can be observed in form of a plateau in the  $\Pi$ -A isotherm. (b) Scheme of possible pathways of the formation of SAMs. Depend

ing on the concentration of surfactant molecules and the temperature, the growth proceeds via (A) first a 2D-vapor phase to a solid-vapor coexistence, to the final solid phase, or (B) through various intermediate coexistence phases (Reprinted with permission, from the Annual Review of Physical Chemistry, Volume 52 ©2001 by Annual Reviews www.AnnualReviews.org).

from the gas phase or from a solution onto the substrate. With the right choice of head group, mesogen and tail group well-defined monolayers can be prepared.

Interestingly, in both approaches the two-dimensional arrangement undergoes sooner or later similar 'phase transitions' as illustrated in Fig. 9.3.

While for LB-layers, the molecules have to be organized by means of compression prior to deposition of the monolayer at the air-water interface, the self-organization process into SAMs follows similar pathways by itself. This requires sufficient mobility of the molecules on the solid substrate before the formation of the final SAM. Ulman pointed out that the energy gain of the system during self-assembly (physisorption and especially chemisorption) can be compared with the pressure applied with the barrier of an LB-trough, to increase the order in the LB-monolayer at the air-water interface [5].

By now a broad range of SAMs on various substrates are available. For an overview on SAM systems several comprehensive reviews are available [1-4] as well as the reference book by A. Ulman [5]. In Tab. 9.1 a list of examples is given [5, 6, 33].

The process of formation of SAMs on the various substrates strongly depends on the nature of all three moieties of the surface active molecule. If a suitable mesogen is chosen, the affinity of the head group toward the substrate determines the kinetics of the physisorption and chemisorption as well as the stability of the resulting layer.

Among the SAM systems listed in Tab. 9.1, SAMs based on silanes on silica and thiols on (noble) metals represent the majority of the reported accounts. In the following some specific properties of these two systems will be outlined.

**Tab. 9.1** Selected examples of substrates and surface active molecules suitable for the formation of SAMs.

<i>Substrate</i>	<i>Ligand or Precursor</i>	<i>Binding</i>	<i>Reference</i>
Au	RSH, (aliphatic thiols)	RS–Au	2–4, 7
Au	ArSH (aromatic thiols)	ArS–Au	4, 8–12
Au	RSSR' (disulfides)	RS–Au	2–4, 13
Au	RSR' (sulfides)	RS–Au	2–4, 14
Au	RSO <sub>2</sub> H	RSO <sub>2</sub> –Au	15
Au	R <sub>3</sub> P	R <sub>3</sub> P–Au	16
Ag	RSH, ArSH	RS–Ag	2, 4, 17
Ag	ArSH	ArS–Ag	8, 11, 12
Cu	RSH, ArSH	RS–Cu	2, 18
Pd	RSH, ArSH	RS–Pd	2, 19
Pt	RNC	RNC–Pt	2, 20
Pt	ROH, amides	RO–Pt	21
GaAs	RSH	RS–GaAs	22
GaAs	RSSR; RCOOH	RS–GaAs; RCOO–//GaAs	23
InP	RSH	RS–InP	24
SiO <sub>2</sub> , glass	RSiCl <sub>3</sub> , RSi(OR') <sub>3</sub>	R–Si–O–Si	2, 3, 25, 46–48, 53, 59
Si/Si–H	(RCOO) <sub>2</sub> (neat)	R–Si	26
Si/Si–H	RCH=CH <sub>2</sub>	RCH <sub>2</sub> CH <sub>2</sub> –Si	27
Si/Si–Cl	RLi, RMgX	R–Si	28
Metal oxides	RCOOH	RCOO–//MO <sub>n</sub>	29
Metal oxides	RCONHOH	RCONHOH//MO <sub>n</sub>	30
ZrO <sub>2</sub>	RPO <sub>3</sub> H <sub>2</sub>	RPO <sub>3</sub> <sup>2-</sup> //Zr <sup>4+</sup>	31
In <sub>2</sub> O <sub>3</sub> /SnO <sub>2</sub> (ITO)	RPO <sub>3</sub> H <sub>2</sub>	RPO <sub>3</sub> <sup>2-</sup> //M <sup>n-</sup>	32

### 9.2.2

#### Self-assembled Monolayers of Alkanethiols

SAMs of alkanethiols on gold are the systems by far the most studied. For detailed descriptions of their growth and structural features, the recent reviews by F. Schreiber [4] and D.K. Schwarz [33] are highly recommended. It is believed that the thiol reacts with the gold substrate according to the following equation [5]:



Although the chemical reaction appears to be quite simple and the system have been studied for decades, the given reaction equation is still a working model. In particular, the fate of the hydrogen during and after the reaction is not fully understood. Because the final SAMs formed from thiols and disulfides are similar, it has been assumed that the chemisorption process follows a similar reaction pathway in both cases. Fig. 9.4 outlines some structural features of this system. The three aspects that determine the final molecular packing parameter of the SAM

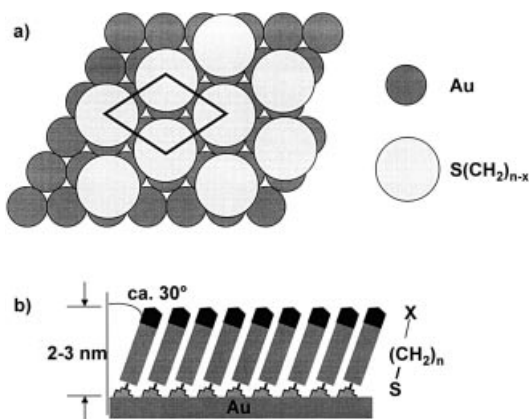


**Fig. 9.4** Structural features of a SAM of an alkanethiol formed on a Au(111) surface with a) a  $(\sqrt{3} \times \sqrt{3})R30^\circ$  structure in which the thiulates display a S–S distance of 4.99 Å. (modified from ref. 5) b) This results in a tilt of the alkanethiolate molecular axis of approx.  $30^\circ$  with respect to the surface normal to reestablish the vdW interchain interactions of the alkyl mesogen (modified from ref. [6]).

are first, the interaction between the thiolate and the crystalline Au(111) surface; second, the intramolecular forces in the two-dimensional assembly; and third, the interactions among the terminal functional groups [34–37]. The thiulates on Au(111) are tilted approx.  $34^\circ$  from the surface normal and the unit cells of the C–C–C planes are defined by two all-*trans* zig-zag chains twisted in different directions [38]. For further details on the monolayer structure on gold as depicted in Fig. 9.4 [39–42] and silver (Ag(111)) please refer to the original accounts [34, 43, 44] or the comprehensive review by Schreiber [4].

### 9.2.3

#### Self-assembled Monolayers of Silanes

In contrast to LB-monolayers, SAMs were from the very beginning of their development not only model systems for the study of interfacial phenomena but were readily used in technological applications. One example is the use of monomolecular coatings for chromatographic stationary phases. As mentioned, SAMs can be formed on substrates with various shapes or morphologies especially porous and nonporous amorphous silica. Silica gel is a common stationary phase in chromatography and its controlled modification using alkyl silanes were developed at an early date, for the preparation of reversed-phase (RP) stationary phases used in high performance liquid chromatography (HPLC). In this field, detailed knowledge of the surface chemistry of silica and the proper reaction conditions of the silanization procedure were soon developed. By the mid-1970s RP silica packings for HPLC became commercially available, which carried bonded *n*-octyl and *n*-octadecyl groups at the surface [45]. Protocols that were developed for the preparation of RP-stationary phases, are readily applicable to the preparation of SAMs on planar silica substrates. An RP-coating, especially RP-18, and a SAM of *n*-octadecyltrichlorosilane [46] are closely related, if, in many cases, not the very same thing.

For the surface modification of silica, the reactive surface group is the silanol group which can be reacted with a mono- or polyfunctional alkoxy- or chlorosilane:



The surface chemistry of SAMs of silanes on planar substrates such as oxidized silicon wafers is comparable to the chemistry of silica gel, with the absence of a porous structure [47].

The maximum surface density of the reactive silanol groups in a fully hydrated state is 8–9  $\mu\text{mol m}^{-2}$  (or  $\sim 5 \text{ SiOH nm}^{-2}$ ). This can be achieved by a hydrothermal activation of silica gel [48, 49] or, for planar substrates, a solution with hydrogen peroxide/sulfuric acid ('piranha') or ideally a modified cleaning procedure used for silicon/silicon dioxide wafers ('RCA-method') [50, 51]. The different treatments for planar silica surfaces and silica gel particles are necessary because of their different specific surface areas and practical issues of handling the 'substrate'. It was found that the RCA method yields highly active, homogeneous surfaces and most importantly, they are of reproducible quality without a significant change of the surface roughness. The hydrothermal treatment of (porous) silica gel was optimized in terms of reactivity and maintaining the specific pore structure (specific surface area) and particle morphology.

It is not easy to obtain SAMs of trifunctional silanes on planar silica or silica gel particles. During the development of (RP-) stationary phases, several protocols were established, including modifications in aqueous systems [52]. For polyfunctional silanes, a hydrolysis and polycondensation reaction easily results in the formation of undefined three-dimensional polysiloxanes bound to the silica surface [47]. For the modification of porous silica, it was found that the uncontrolled grafting of oligo- or polysiloxanes from aqueous solution altered the pore structure and accessible surface area by clogging the pores. On planar substrates, the adsorbed polysiloxanes increased the surface roughness, and irregular coatings were observed using scanning electron microscopy (SEM) or scanning probe microscopy (SPM). To form a defined two-dimensional SAM, great care should be taken to avoid polymerization of the silane compound in the solution and the consecutive physisorption/chemisorption of siloxane oligomers [53]. Besides thorough purification of the silane compound, anhydrous reaction conditions for the silanization are required. By this method, the hydrolysis and condensation reaction of the silane is confined to the interface because only the thin layer of surface water on the silica is used for the silanization reaction. For the most popular silane compounds, the different reactivity follows the trend:  $\equiv \text{SiCl}_2 >> \equiv \text{Si}(\text{OCH}_3)_2 > \equiv \text{Si}(\text{OC}_2\text{H}_5)_2$ . In the two-step process of hydrolysis of the silane to the silanol species and the condensation (silanols to siloxane), the reaction-determining step is the rate of hydrolysis [54]. However, for polyfunctional silanes, the hydrolysis and condensation overlap. Under defined reaction conditions, the reaction between the surface hydroxyl groups of the silica and the silane compound follows a distinct stoichiometry, which can be expressed by the number of surface hydroxyl groups that react with the organosilane. For monofunctional silanes this ratio is unity. For bifunctional and trifunctional reagents it varies between 1 and 2, depending on the cross-sectional area of the molecule. The stoichiometry is discussed in detail in Ref. [48]. Possible reaction pathways of mono- to trifunctional silane with

surface hydroxyl groups are outlined by E. Bayer *et al.* [55]. Grafting densities can be increased by using various amines as a catalyst and base [56]. Although Wirth *et al.* [57] defined the bonding of trifunctional silanes as self-assembly, only if the grafting density approaches  $8 \mu\text{mol m}^{-2}$  (equal to  $2.2 \text{ nm}^2$  per molecule), whereas the ligand density for conventional RP-packings are in the range of  $\sim 5 \mu\text{mol m}^{-2}$ , it is doubtful whether most of the reported silane-based SAMs satisfy this extremely high ligand density criterion. Complete stoichiometric saturation of all silanol groups with ligands is sterically impossible. In several studies it was pointed out that in the ordered SAMs of alkyl silanes, not all ligands are bonded to the surface but that a laterally cross-linked monomolecular layer covers the surface and chemical bonding occurs with 1 out of 5 silane molecules [58]. Studies from Silberzahn *et al.* [59] lead to the same view [47, 48], and it was argued that even full cross-linking is sterically hindered [60]. The structural features of silane-based SAMs are discussed in detail in Refs. [4, 5, 33]. Compared with the SAM formed by alkanethiols on gold, silane-based SAMs do not display the same degree of lateral long-range molecular order. This is because the SAM of silanes are a two-dimensional polysiloxane network with focal pinning points to the amorphous silica substrate, whereas in alkanethiol monolayers, the crystalline metal surface directs the epitaxial arrangement of the monolayer. The morphological picture that arises for SAMs of polyfunctional (trialkoxo- or trichloro-) silane compounds is depicted in Fig. 9.5.

This distinct difference between SAMs of silanes on silica and e.g. thiols on gold leads to the consequence that ordered SAMs of silanes require an effective mesogen for lateral intralayer interactions to overcome the steric difficulties of the polysiloxane network. The behavior of silanes at an air-water interface, studied by the LB-technique during compression and during formation of the two-dimensional polysiloxane network layer, is a helpful tool for the investigation of the morphology of a SAM formed by self-assembly on a silica surface using the surface water layer. Hence, reports of surface modifications using silane compounds with, for example, short *n*-alkyl moieties as the order-inducing unit do often not meet the criteria of a SAM in terms of the morphology, degree of order and, in consequence, behavior of a defined surface coating.

#### 9.2.4

#### **Self-assembled Monolayers for Surface Engineering**

The intriguing aspect of SAM systems is the direct control of surface properties by the choice of the distal (tail) group of the molecules forming the new interface. The surface properties can be tailored more or less independently from the original substrate since surface properties are dominated by the outermost 5–10 Å of the organic material [61]. A variety of surfaces with specific interactions can be produced with fine structural control [62]. Jarzebinska *et al.* [63] compared composite polymer coatings containing nickel catalyst for the catalytic reduction of carbon dioxide with surface coatings prepared by the Langmuir-Blodgett technique using glassy carbon electrodes, as well as self-assembly on metals. They found a



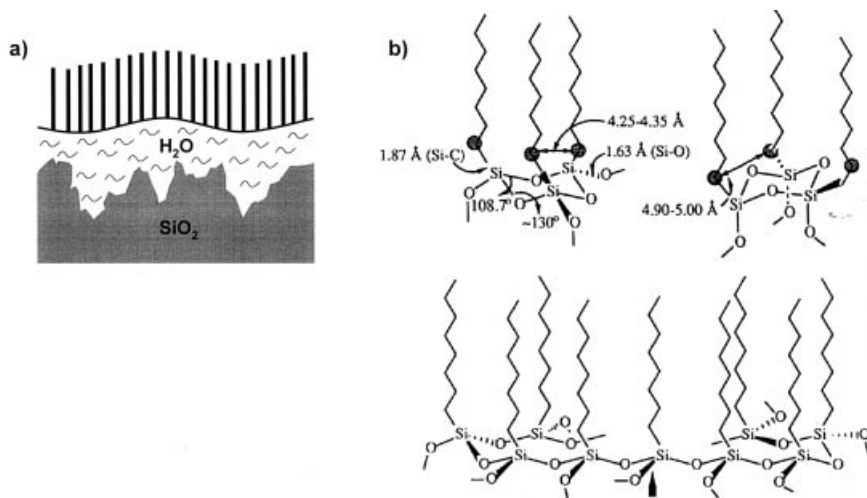


**Fig. 9.5** a) Schematic view of a SAM of trifunctional silanes on a silica surface according to Silberzahn *et al.* (modified from ref. [59]) along with b) A siloxane trimer with possible conformations of the alkyl chains in the equatorial (upper, left) and axial (upper, right) positions allowing a connection with a substrate. A schematic description of a polysiloxane at the monolayer-substrate surface (down). The arrow points to an equatorial Si-O bond that can be connected either to another polysiloxane chain or to the surface.

The dotted line on the left is a bond in a possible precursor trimer. X-ray data suggest an area of  $21 \pm 3 \text{ \AA}^2$  per alkyl chain, with a thickness of  $25 \pm 2 \text{ \AA}$ . FTIR spectroscopy suggest that the alkyl chains in *n*-octadecyltrichlorosilane SAMs are perpendicular to the surface (Reprinted with permission from: [5] A. Ulman, *Introduction to Thin Organic Films: From Langmuir-Blodgett to Self-Assembly*, Academic Press, Boston, 1991. p. 257 and 258. © Copyright 1991 Academic Press/Elsevier Science)

significantly higher catalytic activity of surfaces prepared by LB and especially with the organized self-assembled monolayers.

In addition, these thin films have been important in studies of electron transfer, relevant for catalytic systems [64], molecular recognition [65], biomaterial interfaces [66], cell growth [67], crystallization [68], adhesion [69], and many other aspects [70]. SAMs provide ideal model systems, because fine control of surface functional group concentration is possible by preparing mixed SAM systems of two or more compounds, evenly distributed over the surface [71, 72], as two- or three-dimensional gradients [73] or as patterned mixed monolayers as prepared by  $\mu$ CP [6].

$\omega$ -functionalized SAMs are frequently used for the controlled attachment onto a substrate surface of catalytic sites, which otherwise do not offer the proper chemistry or which have to be shielded from the catalyst in order to enable specific reactions. In biocatalysis, tailored SAM systems are especially useful as intermediate coatings to attach enzymes in a defined way [74–76].

Fig. 9.6 outlines the possibilities of using SAMs for the study and application of physical and chemical surface engineering on the molecular scale.

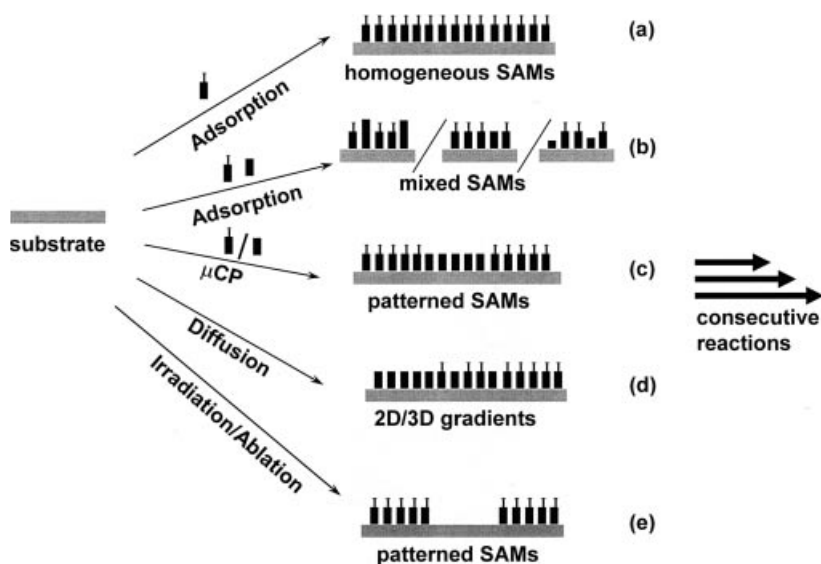


**Fig. 9.6** Tailored SAMs for surface engineering provides the control of the surface physical properties, chemical reactivity and heterogeneity on the molecular level. a) Self-assembly of one kind of surface active compound results in homogeneous monolayers. b) Adsorption of two components give rise to mixed SAMs, combining the physical and

chemical properties of both terminal functionalities into one layer, thus varying the reactivity by dilution or screening. c) Patterned two component SAM by, for example micro contact printing ( $\mu\text{CP}$ ) or post-deposition irradiation such as chemical lithography. d) Patterned SAMs prepared by partial photoablation.

In many supported catalytic systems, it is nearly impossible to determine either the specific species, responsible for the observed catalytic activity, or the mechanistic pathway of the reaction. Using a defined SAM system in which careful molecular design is followed by controlled deposition into a solid-supported catalyst of known morphology, surface coverage, mode of binding and molecular orientation, allows direct correlation of an observed catalytic activity with the structure on the molecular scale. SAM and LB-systems allow detailed and meaningful study of established surface bound catalysts to understand their behavior in heterogeneous environments. Recently, this approach was followed by Talham *et al.* [77]. They investigated the effect of a controlled surface immobilization of manganese tetraphenylporphyrin as an oxidation catalyst. A combination of LB and self-assembly was used for controlled binding of the catalytic active site. The metalloporphyrin monolayer showed enhanced catalytic activity, which could be attributed to the influence of a combination of enhanced catalytic lifetime and the altered conformation that the catalytic species adopts when confined to the defined surface. Similarly, Töllner *et al.* [78] used the LB-technique to assemble monolayers of amphiphilic rhodium bipyridine complexes. The LB-monolayers were found to have largely enhanced the catalytic efficiency with respect to an analog system in solution.

Besides the morphology, the free surface energy of a given surface determines the accessibility of catalytic active sites in heterogeneous catalysis (wettability). SAM surfaces can be produced to have free surface energies that span the range from “Teflon-like” surfaces (surface  $\text{CF}_3$  groups) to very high-energy surfaces (surface OH or COOH groups), e.g., surface tensions of 10–70 dyne  $\text{cm}^{-1}$ . For example, when the acidic protons in highly hydrophilic surfaces, such as  $-\text{OH}$ ,  $-\text{CONH}_2$ , and  $-\text{CO}_2\text{H}$  surfaces [79], are substituted by methyl groups [80], the surfaces become more hydrophobic, thus showing the sensitivity of wetting to the SAM surface functionality.

### 9.2.5

#### Surface Reconstruction: A Dynamic View of Self-assembled Monolayer Systems

Although SAMs of alkanethiols can in principle be described as well packed, quasi-crystalline assemblies, the shortcoming of the flexible  $n$ -alkyl mesogen is that for example an increase of temperature or change in the polarity at the interface results in surface-*gauche* defects, and thus surface disorder. Studies of sum-frequency vibration spectroscopy show that the structure of a surface is clearly perturbed when it interacts strongly with another condensed phase [81], hence structural perturbations need to be considered. This is especially serious for very polar surface groups, such as OH [82], where the disorder introduced may be significant [83] and not confined to the outermost surface [81]. Thus, one cannot neglect surface reorganization during exposure to environments of various polarity during wetting or adhesion experiments or during chemical conversion involving the  $\omega$ -functionality. Recalling our introductory Fig. 9.1, even in monomolecular films, the game of order and mobility is already on.

Ulman *et al.* discussed the static and dynamic wetting behavior of pure 11-hydroxyundecane-1-thiol (HUT) and mixed HUT  $n$ -dodecanethiol in great detail [72] and found significant surface reconstruction in such monolayers. The time evolution of the minimization of surface free energy related to exposure towards air and the water contact angle hysteresis is depicted in Fig. 9.7 along with a schematic drawing.

Siepmann *et al.* [84] carried out Monte Carlo simulations of  $\text{CH}_3$ -terminated SAMs under the influence of compressive stress. It was found that the monolayers relax almost elastically after the stress is removed. Their observation was that under pressure surface-*gauche* defects developed in 40% of the chains. These defects result in the exposure of  $\text{CH}_2$  groups at the surface, which, for  $\omega$ -substituted alkyl chains with polar groups, results in a significant decrease in surface free energy. In the case where stabilizing surface H-bonding interactions are enhanced by surface reorganization, the latter may not be reversible [81]. In consequence, especially polar  $\omega$ -functionalities are no longer accessible. This is a major limitation for the application of SAMs as reference or model systems for the study of interfacial phenomena or as intermediate binding systems for the immobilization of catalytic active sites.

Recently, Genzer and coworkers [85] presented an interesting new approach for the preparation of stable silane-based SAM systems. As a substrate, cross-linked

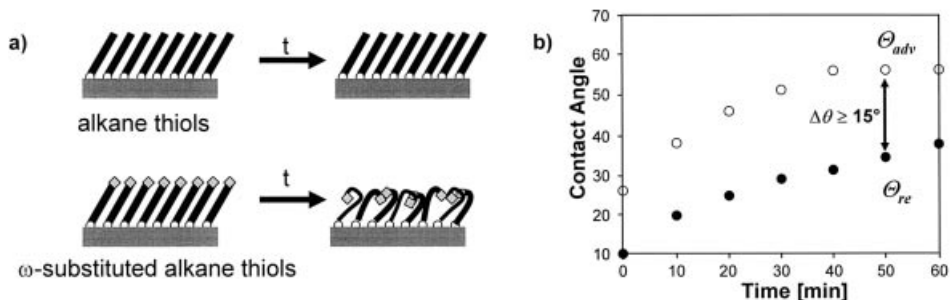


**Fig. 9.7** a) Highly polar surfaces of SAMs of *n*-alkylthiols undergo surface reconstruction when exposed to air to minimize the surface free energy. b) Advancing and receding water

contact angles on SAMs of HUT [HO(CH<sub>2</sub>)<sub>11</sub>SH] SAMs on Au(111) (modified from ref. [82]).

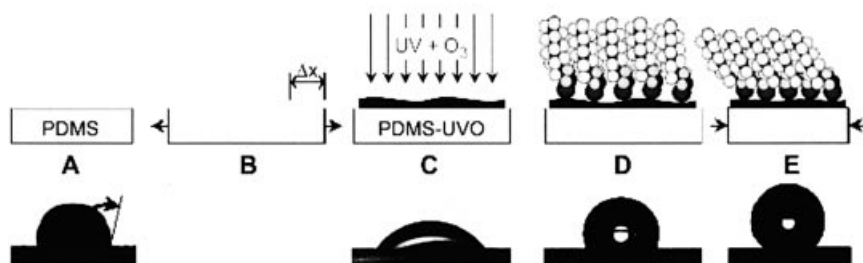


**Fig. 9.8** Schematic illustration of the preparation of mechanically assembled monolayers (MAMs). (A) A cross-linked PDMS film is (B) mechanically stretched by  $\Delta x$  (C), oxidized by UV/ozone treatment to yield a thin SiO<sub>2</sub> sur-

face layer which was used to assemble SAMs of fluorinated trichlorosilanes (D). Release of the strain of the PDMS substrate resulted in further increase of the molecules/surface area in a so-called MAM (E). (modified from [85 a]).

polydimethylsiloxane (PDMS) was oxidized by UV/ozone treatment to yield a thin silicon dioxide surface. The surface was then treated with fluorinated alkyltrichlorosilanes from the gas phase while being mechanically stretched by a certain length  $\Delta x$ . After modification the elastomer was allowed to relax resulting in a mechanically assembled monolayer (MAM) at the surface (Fig. 9.8).

The MAMs were found to be closely packed. NEXAFS and FTIR spectroscopy studies revealed that the molecular tilting angles relative to the surface normal varied from 4° to 21° as a function of  $\Delta x$ . In wetting studies it was found that the highest water contact angles (~131°) with the lowest contact angle hysteresis could be obtained at  $\Delta x \sim 70\%$  resulting in an optimal molecular dense packing. From hysteresis measurements and long-term stability studies it was concluded that the surface reconstruction in MAMs is significantly suppressed by the extremely high packing density. In principle, the MAM approach of Genzer *et al.* [85] can be viewed as an analog of the preparation of ordered LB films at the air-water interface subsequent to the self-assembly step.

## 9.2.6

## Self-assembled Monolayers of Rigid Mercaptobiphenyls

Another, more direct approach to overcome the problem of surface reconstruction, is the variation of the mesogenic unit of the surface active molecule. Instead of using flexible *n*-alkyl moieties with high conformational freedom, SAMs formed from molecules featuring a rigid mesogen in which conformational disorder has been eliminated as completely as possible should be suitable for the preparation of reference systems for the study of interfacial phenomena. Very early, systems were under study containing aromatic units.

Several groups investigated aromatic thiol systems for the formation of rigid, conjugated SAM systems [86–94] and it soon became clear that among the discussed systems, mercaptobiphenyls and 4'-substituted-4-mercaptobiphenyls are promising candidates and currently the most intensively studied thiol-based SAM systems.

Rubinstein and coworkers were the first to investigate SAMs made of 4,4'-methyl-mercaptobiphenyls (MMB) on gold [87]. In recent investigations of the structure and growth of the 4'-methyl substituted mercaptobiphenyls using grazing-incidence X-ray diffraction (GIXD) and low-energy atom diffraction (LEAD) [95], a low-coverage ('lying-down' or 'striped') phase and a high-coverage ('standing-up') phase was found (Fig. 9.9), similar to the phase evolution of a comparable *n*-decanethiol. In the standing-up phase a commensurate hexagonal

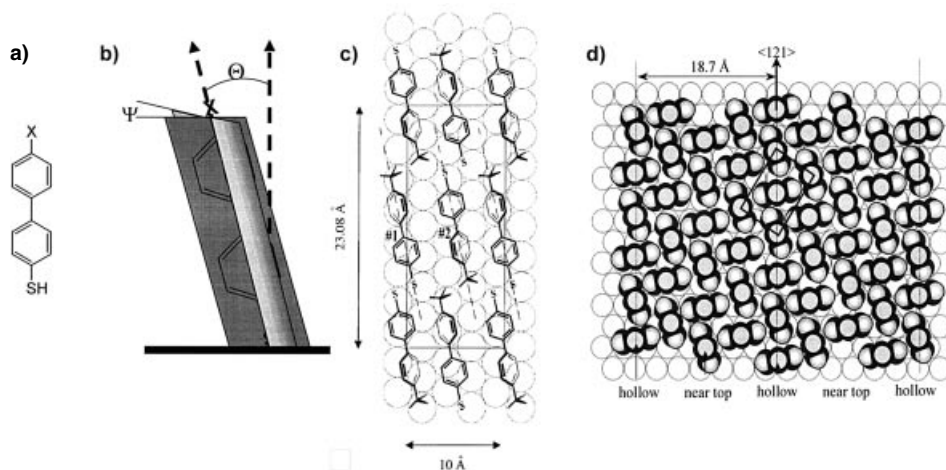


**Fig. 9.9** a) General molecular structure of 4-substituted-4'-mercaptobiphenyl. b) Eulerian angles defining the orientation of the molecule with respect to the surface normal. c) Proposed structure for the low coverage 'striped' phase of MMB (Reprinted with permission from: [4] F. Schreiber *Prog. Surf. Sci.*

**2000**, 65, 151–256 © Copyright 2000 Elsevier Science). d) Proposed structure of 4-chloro-4'-mercaptobiphenyl SAM (Reprinted with permission from: [10] J.F. Kang, A. Ulman, S. Liao, *et al.*, *Langmuir* **2001**, 17, 95–106. © Copyright 2001 American Chemical Society).

$(\sqrt{3} \times \sqrt{3})R30^\circ$  structure was found, analogous to alkane thiols. However, the tilt angle of about  $14^\circ$  of the molecular axis with respect to the surface normal was found to be significantly smaller than for alkanethiols. It was concluded that for biphenyls, it is not necessary to tilt as strongly as *n*-alkanes to maximize the lateral intermolecular (van der Waals or  $\pi$ - $\pi$ ) interactions. This results in the picture of a closely packed SAM of mercaptobiphenyls with the molecules standing almost normal to the substrate surface. The generally low tilt angles were also found in studies using ellipsometry and ER-FTIR spectroscopy performed on different 4'-substituted-4-mercaptobiphenyls [10–12, 96–99]. These findings were further corroborated by recently performed detailed studies using X-ray photoelectron spectroscopy (XPS) and near-edge X-ray absorption fine structure spectroscopy (NEXAFS) [100, 101]. By comparing the alkanethiols with aromatic thiols on gold and silver, it was found that in the aromatic SAMs, the balance between the head group/substrate interactions and the intermolecular forces is shifted towards the intermolecular forces [101].

In conclusion, the overall picture arises that a biphenyl is a suitable if not ideal mesogen for the formation of highly ordered SAM systems if compared with aliphatic thiols. This is also reflected by the significantly higher thermal stability (melting temperature,  $T_M \geq 140^\circ\text{C}$  for MMB as compared with  $T_M \sim 100^\circ\text{C}$  for *n*-decanethiol) of mercaptobiphenyl SAMs [95].

However, silane-based SAMs were found to be thermally stable up to a temperature of  $467^\circ\text{C}$  (C–C decomposition [102]). Detectable changes with surface probe microscopy and in terms of wetting behavior were reported to appear at around  $125^\circ\text{C}$  [103].

Besides the elimination of conformational freedom in the mesogen by switching from an aliphatic to an aromatic system, several other aspects have to be considered. First, the electronic nature of the molecule is entirely different. Because of the conjugation, the 4'-substitution has a strong influence upon the reactivity of the thiol head group. Electron donating or withdrawing substituents changes the acidity of the thiol. Second, asymmetric 4',4'-substituents induce a molecular dipole moment which should have a significant impact upon the formation as well as the stability of the corresponding SAM. Third, the polarity and polarizability of the molecule and the SAM is different, thus changing the surface potential as well as the optical properties of the SAM.

Kang *et al.* first studied the wetting properties of 4'-methyl- (MMB) and 4'-hydroxy-4-mercaptobiphenyls (HMB) as an analog system for the aliphatic HUT/DDT mixed monolayer [97]. In Fig. 9.10 the results of analog wetting experiments for the two systems are compared.

For both cases, mixed monolayers can be prepared without a significant preferential adsorption of one compound (Fig. 9.10a,b). The plot of  $\cos \theta$  against the surface OH concentration reveals an overall higher free surface energy of the biphenyl system, caused by the polar/polarizable biphenyl group. For example, the advancing contact angle of an HMB SAM is  $30^\circ$ , while that of HUT is about  $15^\circ$ . Although both surfaces feature OH terminal groups, the impact of the mesogen is significant. Both systems follow more or less the Cassie equation [104]. How-

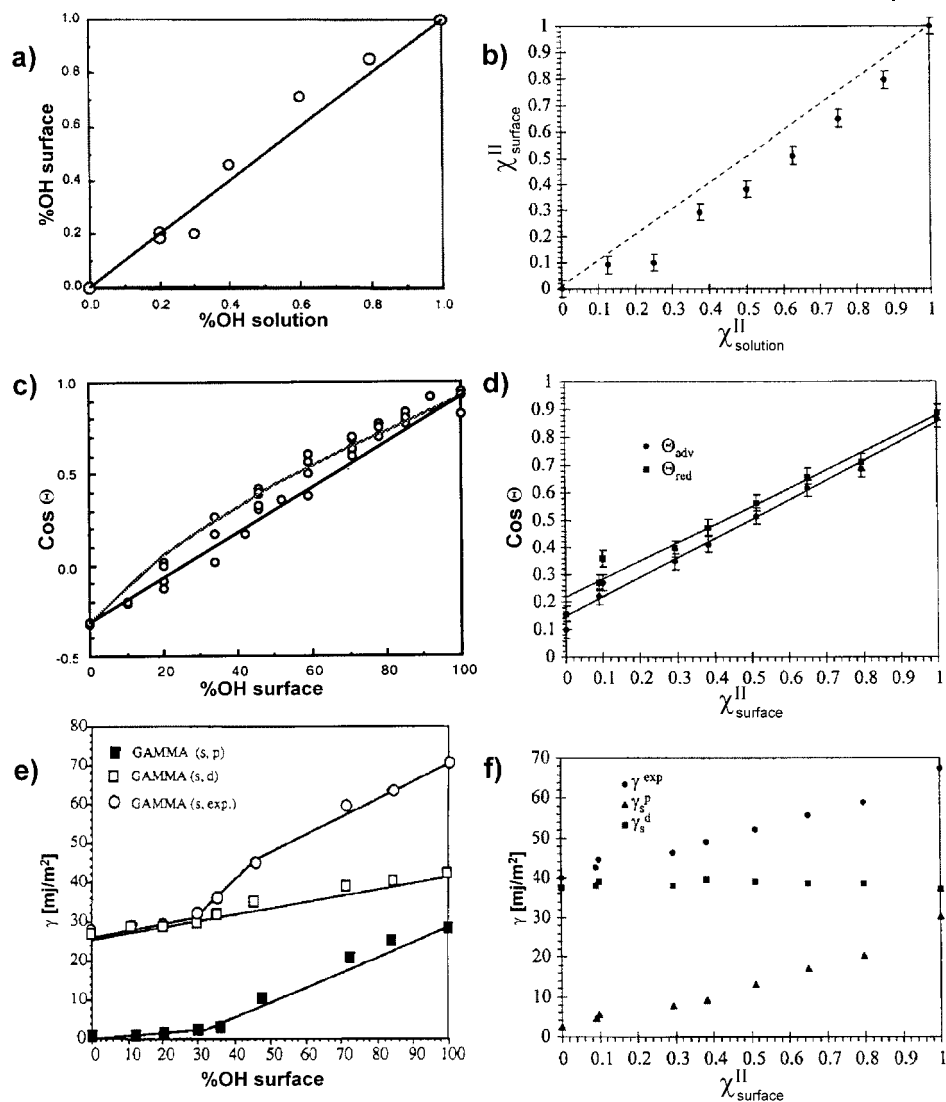


**Fig. 9.10** Comparison of the formation and wetting behavior of the aliphatic HUT/DDT (a, c, e) and the aromatic HMB/MMB (b, d, f) mixed monolayer system on Au(111). (a, b) Composition of the solution and surface composition of the resulting SAM. (c, d) Plot of the  $\cos \theta = (\gamma_{\text{sv}} - \gamma_{\text{sl}}) / \gamma_{\text{lv}}$  of the advancing (and additionally in d) receding) water contact angle as a function of the surface OH concentration. The straight line represents the Cassie equation [104], in c) the grey line is calculated after the equation from Israelachvili [105] describing the contact angle on heterogeneous surfaces. (e, f)

Plots of the total surface free energy ( $\gamma_s^{\text{exp}}$ ), polar ( $\gamma_s^{\text{p}}$ ) and dispersive component ( $\gamma_s^{\text{d}}$ ) of both systems as a function of the surface composition. (b, d modified from ref. [97]); (a, c, e Reprinted with permission from: [62] A. Ulman, S. D. Evans, Y. Shnidman, *et al.*, *J. Am. Chem. Soc.* **1991**, *113*, 1499–1506. © Copyright 1991 American Chemical Society; [72] A. Ulman, S. D. Evans, Y. Shnidman, *et al.*, *Adv. Coll. Interf. Sci* **1992**, *39*, 175–224. © Copyright 1992 Elsevier Science; [97] J. F. Kang, R. Jordan, A. Ulman, *Langmuir* **1998**, *14*, 3983–3985. © Copyright 1998 American Chemical Society).

ever, the water contact angle hysteresis for the HMB/MMB system, at  $5^\circ$ , is unusually small. Referring to the plot in Fig. 9.7 in aliphatic systems (pure HUT monolayer) a hysteresis of about  $15^\circ$  is usually observed. Additionally, while the aliphatic system undergoes dramatic changes with time of exposure to ambient air, the HMB/MMB system was found to show constant water contact angles for at least 1 month storage under nitrogen. This difference accounts for the fact that in the biphenyl system, the surface reconstruction is eliminated.

By the geometric-mean method [106] the total surface free energy ( $\gamma_s^{\text{exp}}$ ), the polar ( $\gamma_s^{\text{p}}$ ) and dispersive component ( $\gamma_s^{\text{d}}$ ) of both systems were calculated (Fig. 9.10 e, f). While the aliphatic HUT/DDT system displays an abrupt change in the polar surface free energy component at about 30% OH and a wetting transition onset occurs at about the same concentration, for the biphenyl system,  $\gamma_s^{\text{p}}$  grows almost linearly and the dispersive component remains constant with increasing surface OH concentration and no wetting transition is observable.

The outlined properties make the biphenyl system ideal for the study of interfacial phenomena and applications as stable intermediate binding sites for catalytic systems.

#### 9.2.6.1 Self-Assembly of Dipoles

The impact of the dipole moment in mercaptobiphenyls induced by the 4'-substitution and the polarity of the solvent upon adsorption kinetics, formation and stability was found to be much more significant than for analog aliphatic thiols [10, 96, 98]. For example, the formation of pure and mixed SAMs of MMB and 4'-trifluoromethyl-4-mercaptobiphenyl (TFMB) from different solvents were studied by means of ellipsometry, ER-FTIR spectroscopy and wetting experiments [96]. Varying the polarity of the solvent (ethanol and toluene) it was found that the stabilization of the polar SAM of TFMB leads either to an increasing tilt angle of the biphenyls to reduce the total dipole moment of the layer or to a SAM of upright standing TFMB which is stabilized by dipolar interactions with polar solvent molecules (Fig. 9.11). The study of mixed SAMs of TFMB and MMB of various solution compositions in the less polar toluene indicated a driving force to reach an equally mixed SAM. This could be explained by the fact that the two components have molecular dipoles in the opposite direction when assembled on the surface. In fact, the experiment where pure SAMs of either MMB or TFMB were submerged in a solution of the other component resulted in mixed SAMs of MMB/TFMB of approximately the same composition (Fig. 9.11).

The above-mentioned experiments clearly show that the molecular dipoles of the assembling units direct the morphology and composition of the resulting assembly. The driving force for the mixing should therefore increase with increasing difference of the molecular dipole moments of the two components. This was demonstrated in the study of pure and mixed monolayers of the highly polar 4'-nitro-4-mercaptobiphenyl (NMB) and 4'-dimethylamino-4-mercaptobiphenyl (DMAMB) [98].

When mixed SAMs of NMB and DMAMB were prepared in toluene, the surface  $\text{NO}_2$  concentration, as determined by external reflection FTIR spectroscopy,



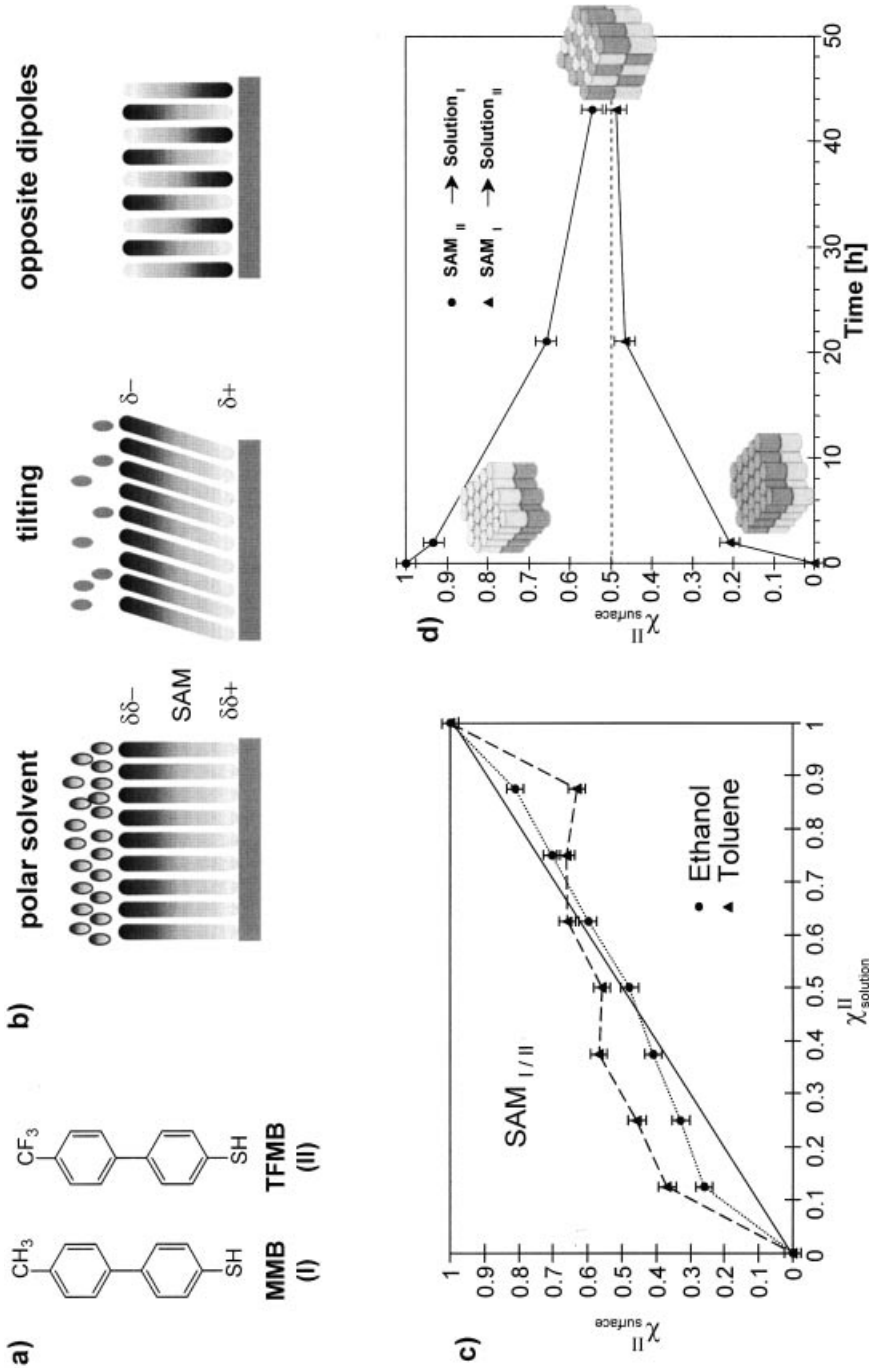


**Fig. 9.11** a) Chemical structures of MMB and TFMB. b) Possibilities to reduce the total dipole moment in a SAM of mercaptophenyls by interactions with a polar solvent, tilt or assembly of opposite dipoles in mixed monolayers. c) Surface versus solution composition found for MMB and TFMB mixed systems in polar (ethanol) and less polar (toluene) solutions illustrating the effect of the assembling dipoles. d) The opposite molecular dipoles of MMB and TFMB proved to be sufficient to induce ligand exchange in order to reach an equilibrium situation in the surface composition (modified from ref. [96]).

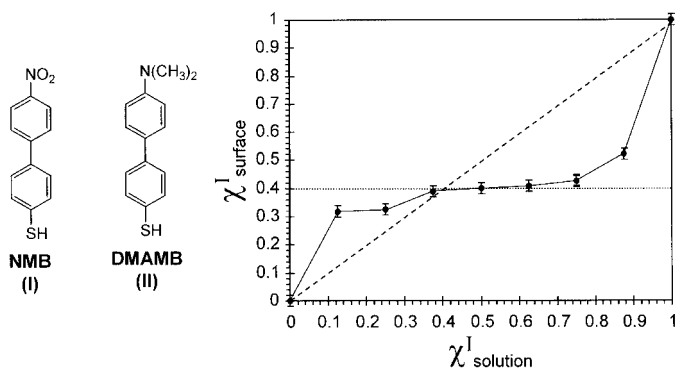


**Fig. 9.12** Chemical structure of NMB (I) and DMAMB (II). Composition of mixed monolayers of I and II versus the composition of the solution (modified from ref. [98]).

displays a plateau at about 40%. If one assumes that the equilibrium concentration of the two components in the mixed SAM, in a nonpolar solvent, is driven by the formation of a two-dimensional assembly with zero net dipole moment, the results can be explained by using the Hammett equation.

Such control of surface functionalities, surface chemical potential, and surface dipole is not possible in mixed SAMs of  $\omega$ -functionalized saturated *n*-alkanethiols, since dipolar interaction of surface functionalities will result in surface reorganization [95, 99–101].

As already indicated in Fig. 9.9 and 9.12, the induced molecular dipole by 4'-substituent should have a significant impact upon the tilt angle of the bonded molecule. This was examined in great detail using ER-FTIR spectroscopy of SAMs of several 4'-substituted-4-mercaptobiphenyls on Au(111) and Ag(111) [10].

The impact of the choice of the substrate to be either gold or silver upon a different molecular orientation of rigid moieties within a SAM was recently demonstrated by Somashekarappa and Sampath [107]. They studied the impact of the different orientation of 2,9,6,23-tetraamino cobalt phthalocyanine bound as a SAM onto silver or gold upon their behavior in electrocatalysis. It was found that the different tilt of the phthalocyanine macrocycles and the consequently different accessibility of the metal surfaces and catalytic center results in a different reaction pathway and oxidation products.

### 9.2.7

#### Patterned Self-assembled Monolayers

The formation of mixed SAMs composed of two components provides unique possibilities in the control of the physical and chemical surface properties. Besides homogeneously mixed SAMs, a directed deposition of the components results in surfaces of controlled heterogeneity. One example reported by Liedberg *et al.*, forming SAM gradients (Fig. 9.6d) by controlled diffusion has already been mentioned [73].

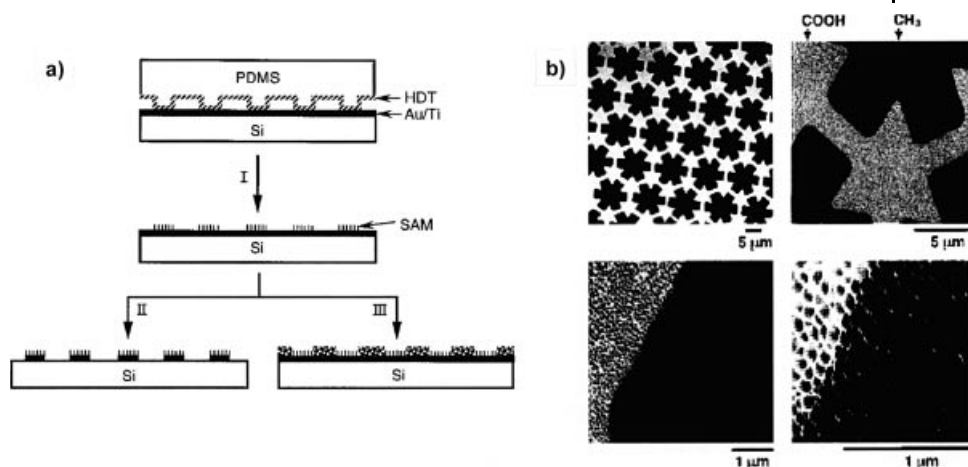
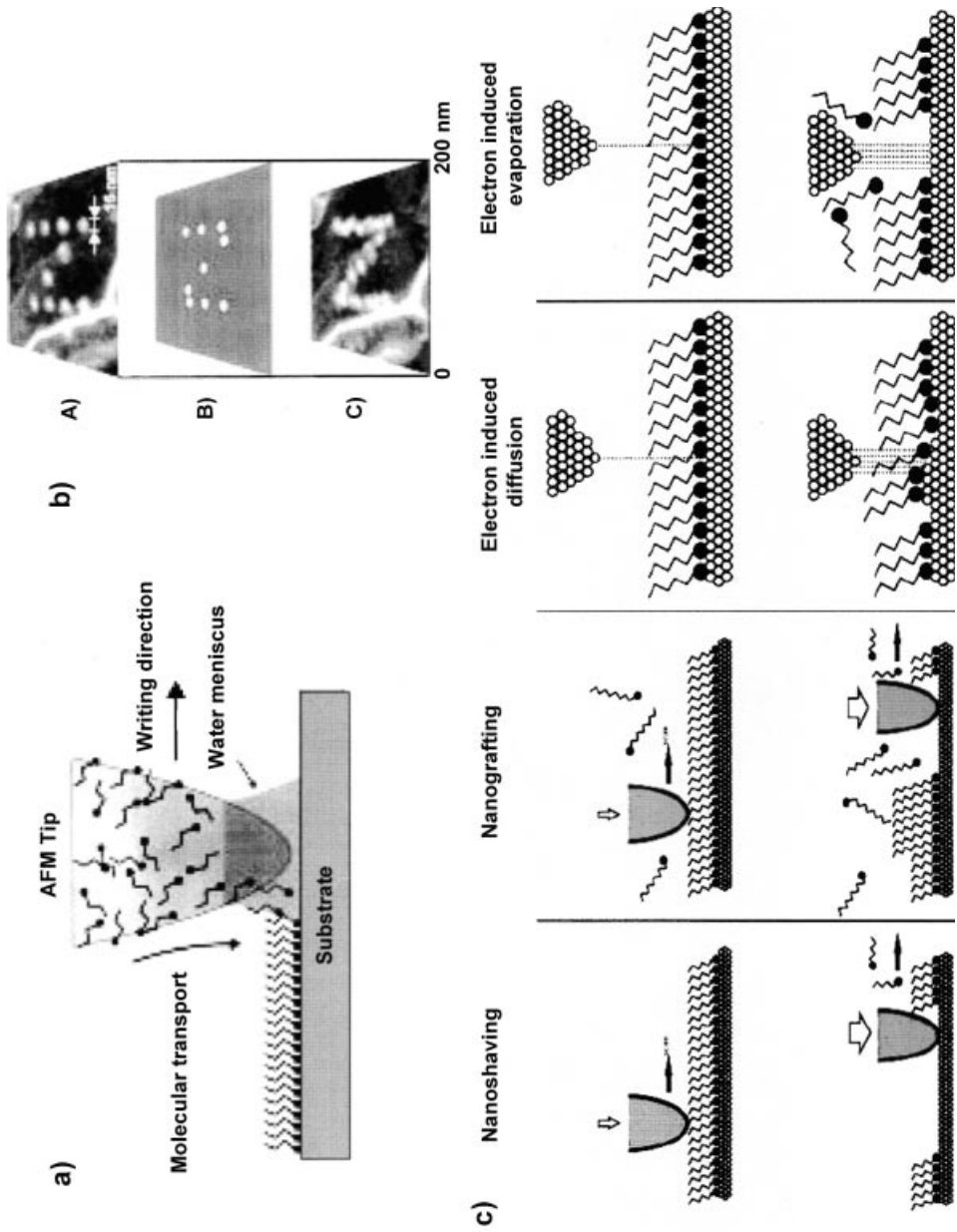


**Fig. 9.13** a) Preparation of laterally structured SAMs by the microcontact printing ( $\mu$ CP) technique. A structured PDMS stamp is 'inked' with self-assembling molecules (hexadecanethiols; HDT) and placed onto a planar substrate (gold). SAM formation occurs within seconds at the areas of contact (I). The structure can be further processed by etching (II) or deposition of a second SAM (III) onto

the remaining free substrate surface. b) Example of a structured SAM of HDT (dark) and HS-(CH<sub>2</sub>)<sub>15</sub>-COOH (bright) at for different magnifications, visualized by lateral force microscopy (LFM). (Reprinted with permission from: [6] Y. Xia, G. M. Whitesides, *Angew. Chem.* **1998**, *110*, 568–594; *Angew. Chem. Int. Ed.* **1998**, *37*, 550–575. © Copyright 1998 Wiley-VCH).

In Fig. 9.6c) and e), patterned SAM systems are schematically outlined. They can be prepared by lithographic tools using UV, electron beam, scanning probe and focused ion beam lithography, by simply decomposing or desorbing a SAM formed in selected areas using a mask or focused beams [108]. Although these techniques are limited by the wavelength of the irradiation used, significantly smaller features can be prepared because the thickness of the resist material is significantly reduced to the thickness of a monomolecular layer and hence, broadening of the inscribed structures during irradiation and development of the patterns as known in common polymeric photoresist materials is negligible.

An alternative way to a partial decomposition of a SAM is the laterally *directed* deposition of a SAM at desired loci. Whitesides and coworkers developed the so-called soft lithography or microcontact printing ( $\mu$ CP) technique [6]. From elastomeric PDMS, a stamp with a defined relief is formed by casting and cross-linking PDMS on a master, 'inked' with a thin layer of surface active molecules (thiols or silanes) and placed on an appropriate substrate (gold, silicon dioxide etc.). At the areas of mechanical contact, a SAM is formed and the original structure of the stamp is positively transferred onto the substrate. The SAM has restricted formation because of the rapid physisorption/chemisorption of the thiol with the gold substrate, with locally high concentrations and the 'autophobicity' of the resulting SAM [109]. The remaining uncovered areas of the substrate can either be modi-



fied by deposition of another SAM from solution or further manipulated (for example etched). The procedure is outlined in Fig. 9.13. It was found that the quality of Au/thiolate SAMs formed by  $\mu$ CP is comparable to SAMs prepared by solution deposition [110].

The feature sizes that can be realized by  $\mu$ CP are typically within the range of several micrometers whereas recently, Michel *et al.* reported a resolution of approx. 100 nm [111].

For direct patterning on the nanometer scale, scanning probe microscopy (SPM) based techniques such as ‘dip-pen-nanolithography’ (DPN), [112–114] ‘nanografting’, ‘nanoshaving’ or scanning tunneling microscopy (STM) based techniques such as electron induced diffusion or evaporation have recently been developed [115, 116]. The SPM based methods, allows the deposition of assemblies into restricted areas with 15 nm linewidths and 5 nm spatial resolution. Current capabilities and future applications of DPN are discussed in Ref. [117].

Patterned SAMs with feature sizes of comparable dimension can also be obtained by using electron beam irradiation. The smallest structures that have been generated with this technique into SAMs of *n*-octadecylsilane had a size of 5–6 nm [118]. Grunze and Götzhäuser applied e-beam nanolithography and proximity printing on aliphatic and aromatic thiol SAMs on gold [119]. While irradiation of SAMs of aliphatic thiols results in partial decomposition and cross-linking, inducing high disorder by *gauche*-defects within the irradiated areas, irradiation of SAMs of mercaptobiphenyls (MB) yielded an intact and most interestingly highly cross-linked monolayer. The observed cross-linking of mercaptobiphenyls SAMs in the irradiated areas improved the mechanical and chemical stability of the SAM which was found to resist a consecutive wet-etching procedure much better than the original MB SAM.

Based on this system an intriguing twist of nanolithography was developed by the same group, the so-called *chemical (nano)lithography* [120, 121]. The name was chosen, since electron irradiation of SAMs of 4-nitro-4'-mercaptobiphenyl (NMB) results in selective and quantitative reduction of the nitro functionalities to amino groups [122], while the aromatic biphenyl layer is dehydrogenated and cross-linked (Fig. 9.15 a). Hence, local irradiation of SAMs can be used for the chemically selective binding of functional entities using the terminal amino group. In contrast to the above-mentioned techniques based on SPM and mechanical inter-

←

**Fig. 9.14** a) Principle of dip-pen nanolithography (DPN) and b) example of direct writing and positioning precision using DPN. b) Schematic diagram with lateral force microscopy (LFM) images of patterning and aligning multiple nanostructures via DPN. A) A pattern of 15 nm diameter 16-mercaptohexadecanoic acid (MHA) dots on Au(111) B) Projected second set of dots. C) Image after a second pattern of MHA nanodots. (Reprinted with permission from: [117] C.A. Mirkin, S. Hong, L. Demers, *CHEMPHYSICHEM* **2001**, 2, 37–39. © Copyright 2001 Wiley-VCH). c) Schematic outline of SPM and STM based nanolithography techniques. The imaging (top) and manipulation modes (bottom) are illustrated. (Reprinted with permission from: [115] G.Y. Liu, S. Xu, Y. Qian, *Acc. Chem. Res.* **2000**, 33, 457–466. © Copyright 2000 American Chemical Society).

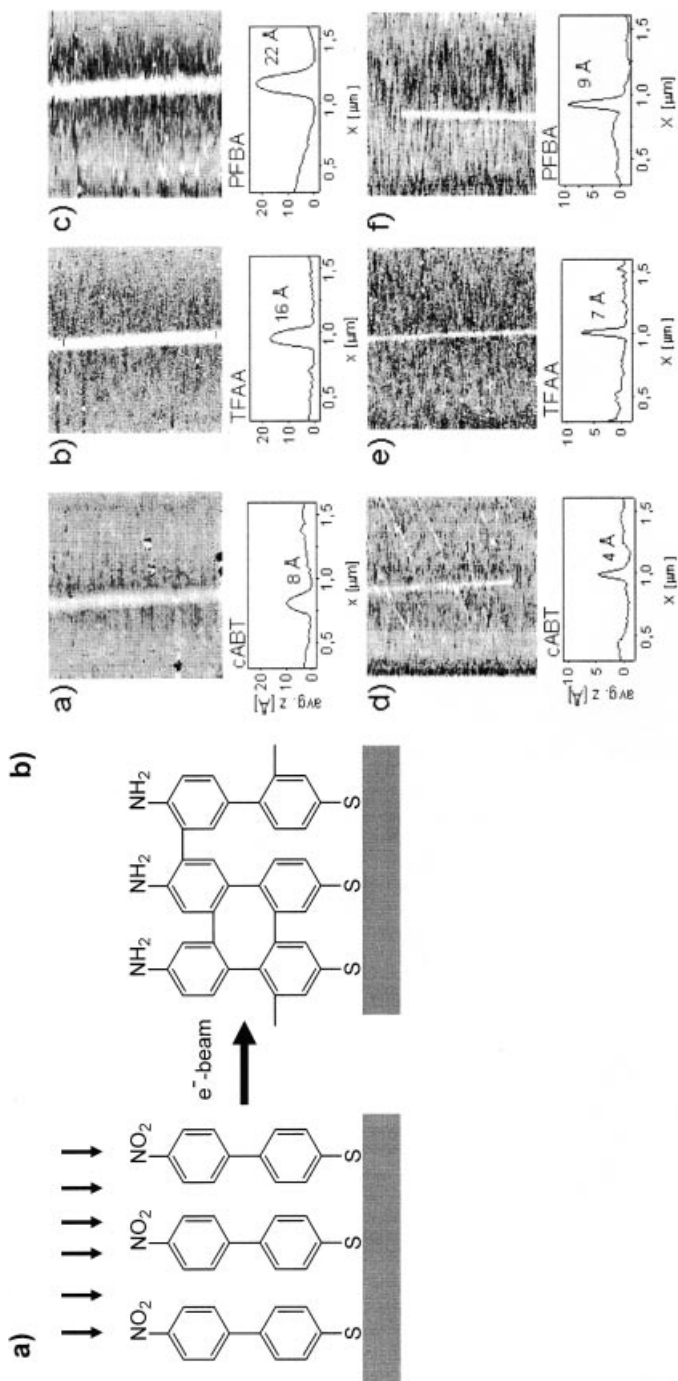


**Fig. 9.15** a) Principle of chemical nanolithography. Exposure of NMB results in the conversion to a cross-linked SAM of AMB (= cross-linked aminophenylthiol; cABT). b) AFM images and averaged height profiles of lines that were written with a focused electron beam into a NMB monolayer. a–c) 100 nm lines after electron exposure (a) and immobilization of trifluoro acetic acid anhydride (TFAA) (b) and perfluoro butyric acid anhydride (PFBA) (c). d–f) 20 nm lines after electron exposure (d) and immobilization of TFAA (e) and PFBA (f) (Reprinted with permission from: [120] A. Götzhäuser, W. Eck, W. Geyer, et al., *Adv. Mater.* **2001**, 13, 806–809. © Copyright 2001 Wiley-VCH).

actions, chemical lithography is not restricted to any length scale since the use of electron flood guns in combination with adequate stencil masks allows an efficient patterning of large areas. For high resolution patterning, electron beams can be focused to nanometer sized spots, and the resolution is only limited by secondary electrons that are generated during irradiation. The smallest chemical nanostructures so far had lateral dimensions of  $\sim 20$  nm (Fig. 9.15 b) [120, 121].

The preparation and application of SAM systems patterned by STM and their use in catalysis was demonstrated by Wittstock and Schuhmann [123]. The patterning (local desorption) of SAMs from alkane thiols on gold was performed by scanning electrochemical microscopy (SECM), followed by the assembly of an amino-derivatized disulfide and coupling of glucose oxidase to form a catalytically active pattern of the enzyme. The enzymatic activity could be monitored/imaged by SECM.

A different approach was followed by Blackledge *et al.* [124]. They used the catalytic activity of a palladium coated SPM-tip to selectively generate a pattern into different  $\omega$ -functionalized SAMs.

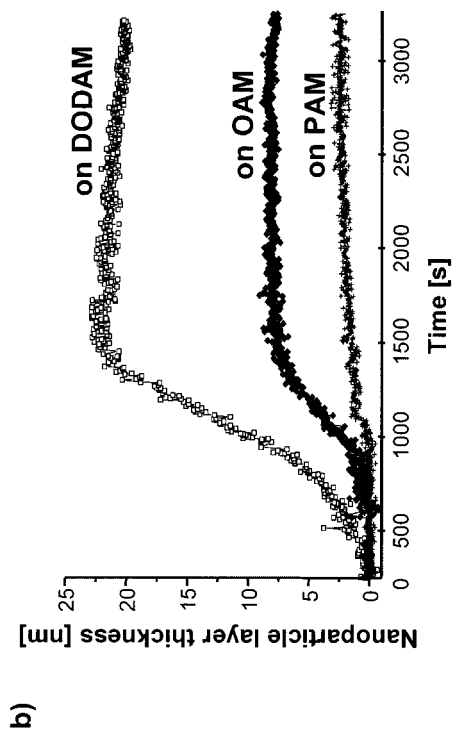
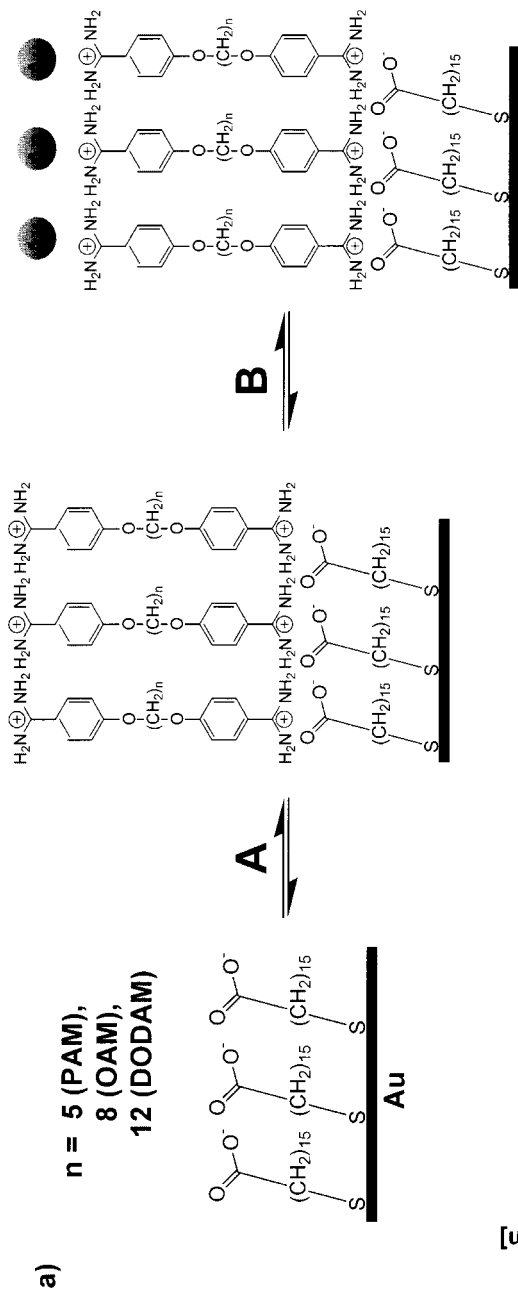
### 9.2.8

#### Self-assembled Monolayers as Tailored Functional Surfaces in Two and Three Dimensions

Since virtually any functional group can be introduced in SAMs as the tail group, SAM systems became a working platform for the study of surface confined reactions involving specific chemical reactions of small molecules [125], synthetic oligomers and polymers (see for example [6] as well as following paragraphs), peptides, proteins [126] and DNA [127], controlled deposition of functionalized nanoparticles [128–130], formation of surface confined heterostructures [4, 6] and control of cell adhesion [131, 132]. The combination of laterally structured SAMs with two or more different surface functionalities, the steric control of surface confined reactions and the broad range of characterization and detection methods of thin films resulted in numerous studies of SAM systems for directed (hierarchical) self-assembly of molecules and small objects as well as applications in sensor technology [133].

Specific, surface confined reactions not only directly involve catalysis but also the built-up of *self-assembled multilayers* (see Fig. 9.1 (3)) with  $\omega$ -functionalities for more complex (bio-) catalytic systems such as proteins or the directed deposition of active metals. Furthermore, SAM on flat substrates can be used for the study and development of, e.g. catalytic systems, but are not useful for large scale applications because they have very limited specific surface. Here, nanoparticle systems covered with 3D-SAMs are the ideal solution of combining the advantages of high surface area, defined surface composition and accessibility of proximal active catalytic centers.

Auer *et al.* [134] presented an example for multilayer formation and controlled deposition of functionalized nanoparticles on SAM of mercaptohexadecanoic acid (MHA) using electrostatic interactions. As a pH-sensitive switchable linker between the SAM of MHA and negatively charged gold nanoparticles, bis-benzami-





dine bolaamphiphiles having different alkyl spacers were used [135]. This strategy resulted in a potentially tunable and switchable property of the entire assembly. For example, the kinetics of adsorption as well as the final particle layer thickness can be controlled by the kind of bis-benzamidine used as the linker (Fig. 9.16).

Nanoparticles bearing a so-called three-dimensional self-assembled monolayer (3D-SAM) [136] coating or shell are ideal construction units for programmed, hierarchical self-assembly of larger objects [137]. Several research groups have successfully assembled functionalized nanoparticles into large nanocrystalline arrays using hydrophobic or electrostatic interactions, as well as chemical bridging [138] or even biologically inspired specific interactions using the biotin-streptavidin system [139] (see Fig. 9.17).

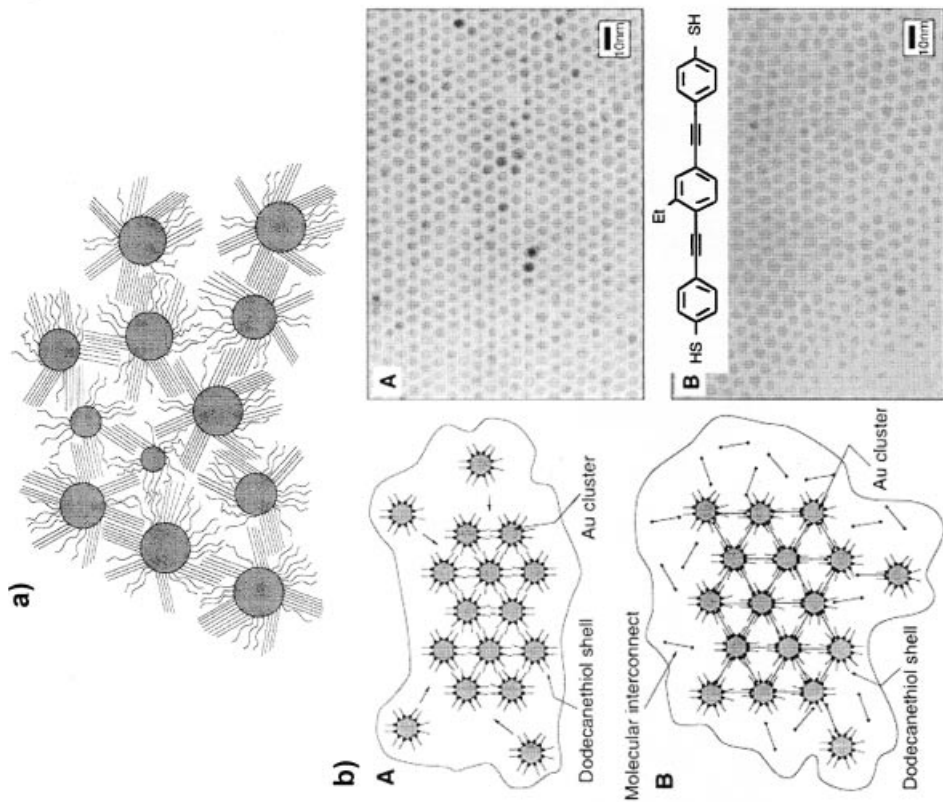
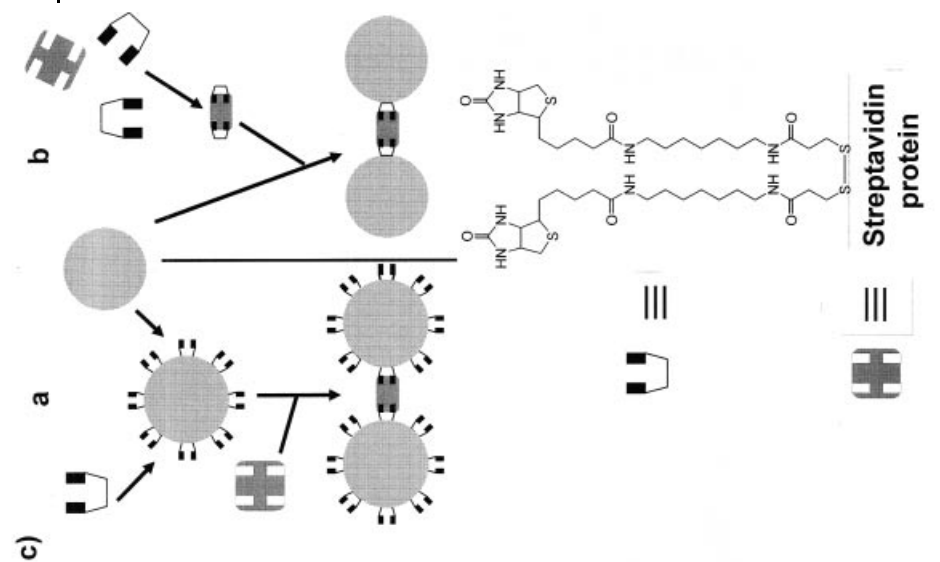
The preparation and study of nanoparticles has attracted a remarkable academic and industrial effort of research because of their potential applications, ranging from fundamental studies in quantum physics, fabrication of composite materials, information storage/optoelectronics, immunoassays, to catalysts. The precise control of size and chemical behavior (stability *and* reactivity) by means of the synthesis itself is still one of the main targets because the direct correlation of the new intriguing properties with the particle size is just between a molecule and a bulk material [140].

Considerable research effort was focused on systems of colloidal gold of which a broad variety of synthetic procedures were reported [140b,f]. While native colloidal gold solutions are only stable for a restricted time, Brust *et al.* [141] were able to overcome this problem by developing a simple method for the *in situ* preparation of alkyl thiol-stabilized gold nanoparticles. This synthetic route yields air-stable and easy to handle passivated nanoparticles of moderate polydispersity, and is now commonly employed for the preparation of inorganic-organic core-shell composites. Such composites are used as catalytic systems with principally two different functions of the protective 3D-SAM layer. Either the metal nanoparticle core can be used as the catalytically active center and the thiol layer is only used to stabilize the system [142], or the 3D-SAM is used as a linker system to chemically attach further catalytic functions [143].

While the method by Brust *et al.* is well-suited for the passivation of the gold colloids with simple *n*-alkanethiols, excessive purification of the decorated particles is required in the case of  $\omega$ -substituted thiols, forming polar surfaces. In this case, a second layer of the ammonium surfactant covers the nanoparticles and the purification process is long, and rarely successful. A solution to this problem was a one-phase synthesis in methanol as reported by the same group. Yee *et al.* [144]

**Fig. 9.16** a) Schematic outline of the consecutive built-up of SAM/nanoparticle composites by means of charge interactions. Three different bis-benzamidines were used to serve as a linking layer, varying their alkyl chain length:  $n = 5$  pentamidine (PAM),  $n = 8$  octa-

midine (OAM) and  $n = 12$  dodecamidine (DODAM). b) Real time change in layer thickness during the adsorption of MUA-modified gold nanoparticles on bis-benzamidine-MHA modified gold surfaces as measured by *in situ* ellipsometry (modified from ref. [134]).



reported a simple one-phase preparation of thiol-functionalized gold, palladium, and iridium nanoparticles, using surfactant-free conditions in THF as the solvent and lithium triethylborohydride as the reducing agent. An alternative route to introduce chemical functionalities into a 3D-SAM is a post-synthesis exchange reaction, successfully employed by several research groups [145].

The main difference between a 2D-SAM on a flat surface and a 3D-SAM on a nanoparticle is their high 'surface curvature'. The entire size of the substrate is within the similar dimension as the thickness of the SAM. This does not allow the formation of a uniform crystalline SAM but can rather be pictured as a SAM on a substrate with a considerable number of surface defect sites. This is also expressed by the significantly higher total amount of bonded alkanethiols on a given specific surface area on gold nanoparticles. For early in-depth investigation on 3D-SAM of alkanethiols on gold nanoparticles as well as their assembly/crystallization and order/disorder ratio as a function of the particle size and chain length of the alkanethiol shell please refer to Refs. [145–149].

### 9.3 Polymers on Surfaces

In the second part of this Chapter the thickness of the organic layer under discussion is slightly increased and a closer look at recent developments of more complex surface-bonded systems involving polymers is outlined. Despite the introduction of flexible polymer chains, the surface coating should still be defined and uncontrolled heterogeneities minimized. Here, especially, polymer brush-type layers where self-assembled monolayers (SAMs) are used as two-dimensional template systems for the preparation of well-defined surface coatings will be subject of a more detailed discussion.

For many applications such as catalysis and possible functional devices, SAMs are simply too thin, the organized structure not flexible enough or the sterical situation within the layer too confined in order to incorporate a desired function or

**Fig. 9.17** Examples of self-assembly of nanoparticles by a) hydrophobic interactions via a shell of unfunctionalized *n*-alkanes. Depicted is a Schematic 2D Representation of the RS/Au nanoparticle packing structure in the solid state. Domains or bundles of ordered alkylthiolate chains on Au particles interdigitate into the chain domains of adjacent particles in order to compensate the free volume of the outer region of the alkyl shell (Reprinted with permission from: [146] A. Badia, L. Cuccia, L. Demers, *et al.*, *J. Am. Chem. Soc.* **1997**, *119*, 2682–2692. © Copyright 1997 American Chemical Society). b) Direct comparison of hydrophobic interactions and chemical brid-

ing. TEM micrographs of monolayer films of 3.7 nm gold nanoparticles supported on MoS<sub>2</sub>. (A) Unlinked array encapsulated by dodecanethiol. (B) Cluster network linked by a 2.0 nm-long aryl dithiol (reprinted with permission from: [138 d] R. P. Andres, J. D. Bielefeld, J. I. Henderson *et al.*, *Science* **1996**, *273*, 1690–1693. © Copyright 2000 American Association for the Advancement of Science). c) Example for the self-assembly of nanoparticles using specific interactions: Two routes for aggregation of gold nanoparticles using streptavidin and a disulfide-biotin analogue (modified from ref. [139]).

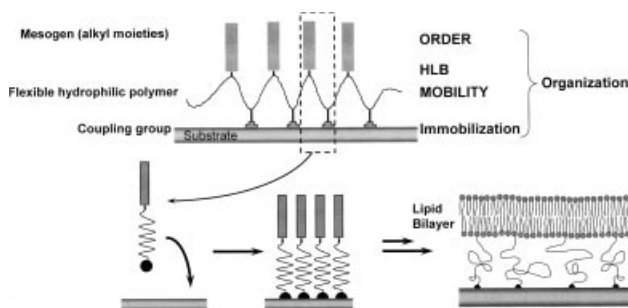


**Fig. 9.18** The *polymer spacer* concept for the construction of a biomimetic cell membrane on solids. Mesogenic units, coupling groups and the flexible polymer can be combined either in form of a statistical terpolymer (above). Variation of the ratio of the three monomers allows an easy tuning of the system. In an alternative system, an end-functionalized linear hydrophilic polymer chain bearing a coupling group at the proximal and the mesogen at the distal end was employed. After grafting the polymers onto a substrate, a polymer-tethered lipid bilayer can be pre-

pared by e.g. vesicle fusion (modified from ref. [51, 150]). A polymer-tethered fluid lipid membrane can function as the optimal host matrix for membrane associated proteins. Such constructs would enable the detailed study of cell membrane associated processes such as cell-cell recognition, transport phenomena and biocatalysis. However, despite many promising approaches and candidates, a robust functional biomimetic membrane system for technological applications has not yet been developed.

respond to changes in the environment in a dynamic and reversible way. One approach to increase the layer thickness of well-ordered self-assembled structures of up to 100 nm is the formation of SAM and LB multilayers by means of consecutive preparation steps (Fig. 9.1 (3)) [5, 108]. This strategy was successfully applied by several research groups, but requires the constant intervention of the experimenter to put one type of monomolecular layer on top of the other. The dynamic behavior of the layer is limited by the crystal-like organization of the system and the extreme confinement of all surface-bonded molecules. Hence, surface defects such as interfacial roughness or chemical heterogeneity become augmented with each additional layer deposited. This can be overcome by introducing some flexibility into the system.

In 1991, Ringsdorf and coworkers [150] introduced the *polymer spacer* concept into the field of ultrathin organic layers that combines the intrinsic organization of small amphiphilic moieties and the flexibility and dynamic behavior of polymers (Fig. 9.1 (4)). Successive publications [151, 152] demonstrated the potential of this approach to overcome substrate defects, provide an 'inner compartment' with water and ion storage capabilities for water, ions (buffer) or other analytes, enable the fluidity of the layer (diffusivity of the lipids within the bilayer) and improve the elasticity of the lipid bilayer membrane. This resulted in a second-generation system to mimic a cell membrane surface as outlined by Sackmann [153]. Based on this idea, Jordan *et al.* [51, 154–156] synthesized a system based on amphiphilic end-functionalized poly(2-ethyl-2-oxazoline)s and demonstrated the impact of the delicate ratio between a flexible polymer part and the organizing lipid end group in the surface-bound li-

popolymers upon the formation of a defined layer morphology, the total film thickness as well as on the stimuli responds of the amphiphilic layer.

While in neither system did the total film thickness exceed several nanometers, swelling and contact angle measurements displayed dynamic behavior of the amphiphilic surface, and the reversibility of the ordering-disordering process.

To prepare thicker polymer films, one can easily spin-coat or adsorb polymers onto a planar substrate from concentrated solutions using, for example, coulomb interactions. Layered structures can be obtained by consecutive procedures or by deposition of segregating block-copolymers. These techniques result in layered structures suitable for a variety of applications. One of the few examples demonstrating the consecutive deposition of polymers by means of a self-assembling technique was developed by Decher *et al.* [157]. He used strong coulomb-interactions to create multilayers of oppositely charged polyelectrolytes (Fig. 9.1 (7)).

However, polymer layers deposited by the techniques mentioned are in most cases subject to irreversible rearrangements because no specific, or only relatively weak, interlayer interactions are present. For stabilization, high molar mass polymers with high melting or transition temperatures are used or consecutive cross-linking reactions are applied. Within the layer, the polymers adopt random coil morphology and chemical functionalities are isotropically distributed and oriented with respect to the surface. Anisotropic orientation or enrichment of polymer bond functional groups can only be expected within the thin interfacial regions. Upon relaxation, an introduced layered structure typically dissolves [158].

By studying the properties of polymer layers on solid surfaces it soon became obvious that not only is the chemical composition of the immobilized polymer crucial for the performance of the material, but so is its morphology. This has been recognized in various fields of applications e.g. stabilization of small particles suspensions by attached polymer brush-type layers [159, 160], control of adhesion [161] or friction [162] and tailored stationary phases for chromatography [163–165].

The use of polymeric coatings in catalysis is mainly restricted to the physical and sometime chemical immobilization of molecular catalysts into the bulk polymer [166, 167]. The catalytic efficiency is often impaired by the local reorganization of polymer attached catalytic sites or the swelling/shrinking of the entire polymer matrix. This results in problems of restricted mass transport and consequently low efficiency of the polymer-supported catalysts. An alternative could be a defined polymer coating on a solid substrate with equally accessible catalytic sites attached to the polymer (side chain) and uniform behavior of the polymer layer upon changes in the environment, such as *polymer brushes*.

The unique behavior of polymer brushes at an interface results from the fact that they consist of end-grafted, strictly linear chains [168] of the same length [169]. The grafting density has to be sufficiently high with respect to the free radius of gyration ( $R_g$ ) of the macromolecules. In order to avoid crowding, the chains are forced to stretch away from the interface, resulting in a brush height ( $h$ ) significantly larger than the typical chain dimension ( $R_g$ ) of a free chain.

In consequence, a significantly larger uniform structure is obtained for a given molecular weight. This is important for the 'reaction time' for a responding sys-

tem such as a polymer brush. Entanglement and high molecular weight, broaden the relaxation time window of the response to reach a new thermodynamic equilibrium upon a change in the environment. In brush systems, entanglement is already minimized by the confinement and consequent alignment of the brushes. High molecular weight polymers are principally not necessary to obtain layer thicknesses at the nm– $\mu\text{m}$  scale for a stretched brush system (Fig. 9.1 (6)).

The layer thickness or brush height  $h$  in a good solvent scales linearly with the degree of polymerization  $N$ , as well as with the grafting density  $\sigma$  as  $h \propto N \sigma^{1/3}$ . This can be written as [170]:

$$h = (12/\pi)^{1/3} N \sigma^{1/3} (\omega/\nu)^{1/3} \quad (3)$$

Because of its confinement and uniform polymer constitution, the *preorganized* polymer brush reacts *collectively* to environmental stimuli such as changes of the pH or ion strength [171–173], temperature [174], solvent quality or mechanical forces [175, 176], irradiation [177] or redox reactions [178].

Polymer brushes were found to minimize adsorption of proteins by the ‘soft’ or ‘steric’ repulsion of the flexible yet immobilized macromolecules [179], although a generally valid explanation of the protein resistant properties of some hydrophilic brushes is not available. A similar explanation can be formulated for the improvement of the colloidal stability of particle suspensions, when polymer ‘brush-type’ layers are bound to small particles. This and other intriguing features of polymer brushes prompted a remarkable experimental and theoretical research activity in order to understand and exploit the unique properties of polymer brushes.

A successful theoretical description of polymer brushes has now been established, explaining the morphology and most of the brush behavior, based on scaling laws as developed by Alexander [180] and de Gennes [181]. More sophisticated theoretical models (self-consistent field methods [182], statistical mechanical models [183], numerical simulations [184] and recently developed approaches [185]) refined the view of brush-type systems and broadened the application of the theoretical models onto more complex systems, although basically confirming the original predictions [186]. A comprehensive overview of theoretical models and experimental evidence of polymer brushes was recently compiled by Zhao and Brittain [187] and a more detailed survey by Netz and Adelman [188].

The properties mentioned make polymer brushes ideal systems for the preparation of preorganized ‘intelligent’ materials to serve as functional devices on significantly larger length scales [189, 190].

### 9.3.1

#### Polymer Brushes by Surface-initiated Polymerizations

Traditionally, polymer brushes have been prepared by: (a) selective physisorption of block-copolymers from bulk or solution onto a solid surface, where a shorter ‘anchor’ block adsorbs strongly onto the surface, leaving the remaining ‘buoy’ block tethered to the interface [191] or by (b) chemical grafting or chemisorption

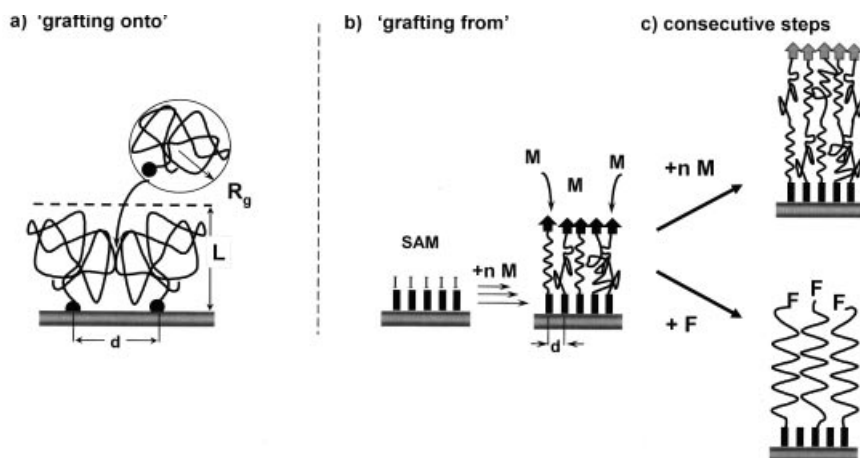


**Fig. 9.19** Preparation of polymer brushes on solid surfaces by a) chemical grafting of end-functionalized linear polymers or selective adsorption of asymmetric block copolymers and b) by surface-initiated polymerization (SIP) using initiator functions on the solid surface. The depicted SAM bearing  $\omega$ -functionalities

as initiators or initiator precursors are especially suitable for the design and control of surface-bonded initiator sites. c) Preparation of block copolymer and end-functionalized brushes via surface-initiated controlled or living polymerization techniques (modified from ref. [194]).

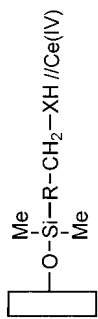
of polymer chains onto a reactive surface via a terminal coupling group [192]. However, both techniques have their limitation in terms of the maximum grafting density that can be obtained. It is easy to picture that chains that are already adsorbed, screen grafting sites still available in their vicinity, because a tethered polymer chain tries to maintain its random coil conformation (Fig. 9.19a). As the grafting density increases, the chains have to increasingly stretch to allow further grafting, which results in a decrease of the rate of grafting kinetics [193]. At some point, a limiting situation is reached that is dominated by the free energies of stretching, chain–chain interactions, and solvation. Hence, the grafting density of a brush, formed by the traditional ‘transplanting’ methods, is self-limiting [194]. Indeed, although brushes have been theoretically successfully modeled using scaling arguments, effective synthetic routes for defined polymer brushes on solid surfaces, where the average distance between grafted polymers  $d$  is significantly smaller than  $R_g$ , have only recently been developed. The limitation by the impairing adsorption process of large polymers was overcome by the ‘grafting from’ method.

In this method, a reactive group on the surface initiates the polymerization, and the propagating polymer chain grows from the surface (Fig. 9.19b). In principle, it can be employed with all polymerization types, and a number of papers have reported high amounts of immobilized polymer using surface-initiated polymerization with various initiator/monomer systems. If controlled or living polymerization techniques are used, block copolymer or end-functionalized polymer brush systems can be prepared in consecutive reaction steps (Fig. 9.19c).

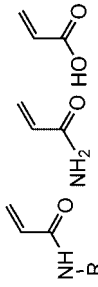
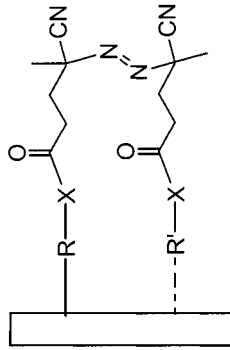
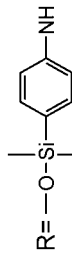
**Tab. 9.2** Specific surface modifications and SAM systems of particles or planar substrates for the surface-initiated free radical polymerization of vinyl monomers.

Substrate	Intermediate Layer//Initiator	Monomer(s)	Reference
Carbon black		Various vinyl monomers	196–201
SiO <sub>2</sub> , TiO <sub>2</sub>	<p data-bbox="1079 1106 1125 1434">X = -S-Ar, -SO<sub>2</sub>-Ar, -SO<sub>3</sub>-Ar, -NH-Ar, -C(CN)<sub>2</sub>R, -C(CN)(COOR)R</p>		202–207

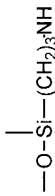
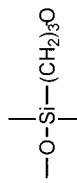
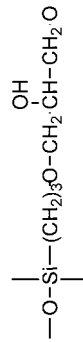
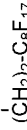
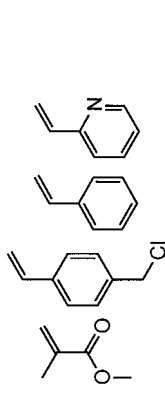
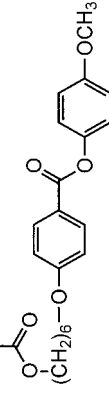


SiO<sub>2</sub>XH= OH, NH<sub>2</sub>, SHr

208-211

R= —(CH<sub>2</sub>)<sub>2</sub>-N(CH<sub>3</sub>)<sub>2</sub>—(CH<sub>2</sub>)<sub>2</sub>-N(C<sub>2</sub>H<sub>5</sub>)<sub>2</sub>—(CH<sub>2</sub>)<sub>2</sub>-N(CH<sub>3</sub>)<sub>3</sub><sup>⊕</sup>—C(CH<sub>3</sub>)<sub>2</sub>CH<sub>2</sub>-SO<sub>3</sub><sup>⊖</sup>SiO<sub>2</sub>, Au

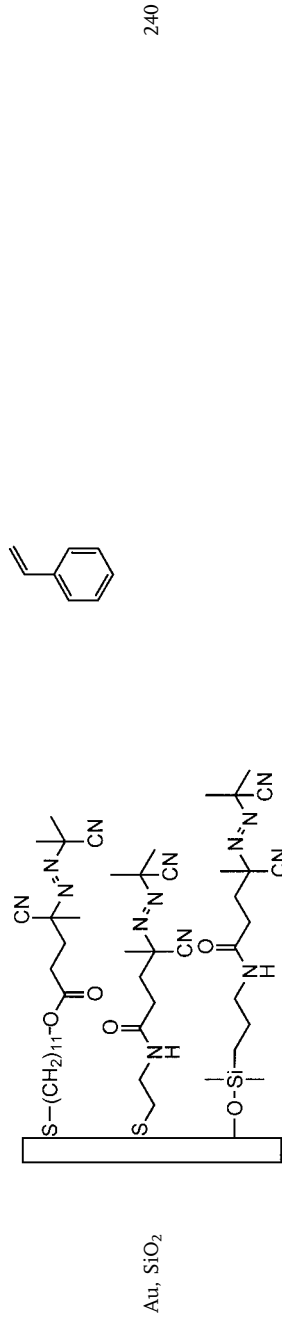
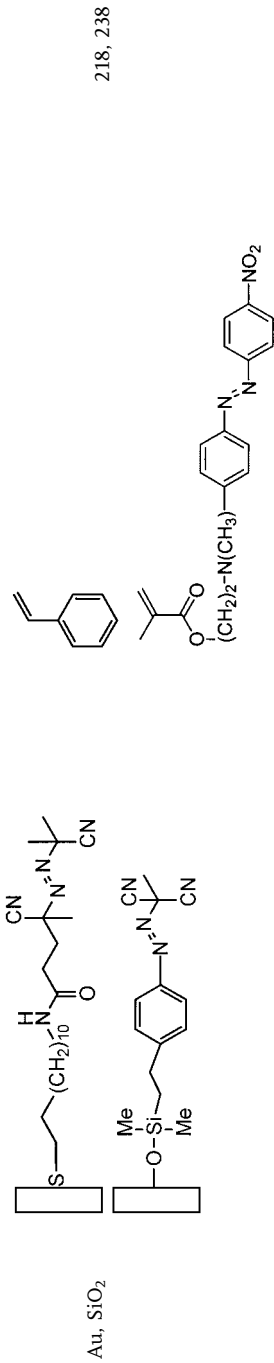
R=

—O-Si-(CH<sub>2</sub>)<sub>3</sub>NH—O-Si-(CH<sub>2</sub>)<sub>3</sub>O—O-Si-(CH<sub>2</sub>)<sub>3</sub>O-CH<sub>2</sub>-CH(OH)-CH<sub>2</sub>O—S-(CH<sub>2</sub>)<sub>10</sub>S(CH<sub>2</sub>)<sub>2</sub>-C<sub>8</sub>F<sub>17</sub>

212-218

Tab. 9.2 (continued)

Substrate	Intermediate Layer//Initiator	Monomer(s)	Reference
Au			219, 220
Mica			221–225
SiO <sub>2</sub>			218, 226–237



To realize surface-bonded initiating sites or their precursors, a variety of methods are applicable. Either organic (polymer) surfaces are irradiated or plasma treated to yield suitable functional groups [187, 195] or inorganic supports are covered with an interlayer of functional polymers bearing the desired groups. However, to gain control over the quantity of surface reaction sites and define the surface chemistry, interlayers of low molar mass  $\alpha,\omega$ -functionalized surface active compounds are suitable. For the latter, the advantages of SAM systems of  $\omega$ -functionalized silanes on oxide surfaces or thiols on metals already outlined, are especially intriguing (see again Fig. 9.6). Hence, in the following, the focus is trained on these systems.

### 9.3.2

#### Surface-initiated Polymerization Using Free Radical Polymerization

To initiate free radical polymerization on a surface, the common initiators as used in solution polymerization are employed. This includes peroxides, symmetric and asymmetric azo-compounds, as well as redox systems. The initiator/monomer systems immobilized on different substrate types along with the monomers used have been compiled in Tab. 9.2. By the early 1970s, Hamann and Laible *et al.* [202–207] had reported on the preparation of polymer layers on silica and titanium dioxide particles prepared by SIP. Extensive work is reported, on a variety of azo-initiators based on 1,4-substituted aryl compounds directly bond to the oxide surface. The azo function was varied in the terminal substitution and the SIP behavior studied for most of the common vinyl monomers. Tsubokawa and Sone *et al.* [196–201] grafted polymers onto carbon black particles by SIP using azo-initiators, peroxides and redox systems with were bond via the surface phenol groups to carbon black. Since at that time elaborate characterization techniques had not yet been developed, the main criterion was the pure amount of polymer bound to the colloidal particles, taking full advantage of the high surface area of the supports and therefore the high total amount of initiator. However, the principle was demonstrated and the main initiator types of free radical SIP screened. Based on the work of these two groups, several other researchers developed SIP using more sophisticated initiator systems such as symmetric azo compounds (supposedly) bound on both sides to the substrate surface [212–218] via a thiol group on gold surfaces, a silanization reaction onto silica or glass or employing another coupling reaction on prefunctionalized surfaces using, for example  $\alpha,\omega$ -amino silanes. The decomposition of a surface-bound azo initiator results in one free and one immobilized radical. Since the initiator preparation is performed in most cases directly on the surface and the question of the number of bonds formed by one or both of the groups can only be estimated, this initiator is in principle suitable for SIP, although no defined SAM system of initiators can be formed. Especially, when thiol terminal groups are used for attachment onto gold [215], desorbed thiols can impair the SIP by acting as a chain transfer agent. Therefore, Dryer *et al.* recently addressed this point and presented a detailed study of a corresponding system using contact angle measurements, ellipsometry, ER-FTIR spectroscopy and XPS. They found that even with a relatively long  $n$ -alkyl spacer between the azo func-

tion and the thiol, the initiator forms an unorganized surface layer with the initiator bonded only by one surface-active group. The remaining thiol group is most likely oxidized by air [215 a]. The poorly-defined surface morphology of the initiator is explained by the lack of a suitable mesogen as discussed in the previous part of this chapter on SAMs. The problem of poorly-defined surface chemistry during immobilization or *in situ* generation of the initiator was tackled by R uhe *et al.* using a preformed AIBN analog equipped with a monofunctional silane group [e.g. 226, 227] or thiol [238]. Additionally, the initiator featured a cleavable group to detach the resulting polymer brushes and analyze the amount, molecular weights and polydispersities of the polymer formed by SIP. They presented detailed studies of, for example, the effect of the polymerization temperature and surface concentration of the initiators ranging from a monolayer to submonolayer coverage upon the standard polymer analytical values. High grafting densities ( $\sigma \sim 3$  nm), high molecular weights and thick polymer brush layers have been reported. Besides the polymerization of styrene as the reference monomer to investigate SIP, functional monomers bearing a mesogen for the preparation of liquid crystalline polymer brushes [216], methacrylates bearing a dye label [238] or perfluoroalkyl chains for the preparation of low surface free energy polymer brushes [217] were polymerized. Despite the fact that free radical polymerization suffers from termination and transfer reactions, which results in a typical polydispersity index ( $PDI = M_w/M_n$ ) of 1.5 to 2, a linear relationship between the polymerization time and film thickness was found. In general, surface-initiated free radical polymerization proved to be an effective method of immobilizing polymer brushes with high molecular weights on a variety of surfaces. The polymer brush layer becomes dense so that, for example, the original support, such as colloidal silica particles, can no longer be dissolved in a solution of concentrated HF [213 b, 226]. Free radical SIP seems to have much in common with bulk polymerization. This was observed by Schouten and coworkers, who reported on a pronounced Tommsdorff effect in the surface confined free radical polymerization [212].

M uller *et al.* [209–211] reported extremely thick polymer (brush) layers of poly(acrylamide) formed by SIP with redox initiators of primary alcohols and Ce(IV) which can be easily visualized by light microscopy [211]. With this initiator system, as originally developed by Mino and Kaizermann [249, 250] for the SIP of vinyl monomers from cellulose and also applied by Tsubokawa *et al.* [200, 201] for carbon black, M uller and coworkers prepared a row of polymer brush type electrolyte layers on porous silica as high capacitance ion-exchange stationary phases (there called ‘tentacle-type’) for the separation of biopolymers. Polyelectrolyte brushes can also be formed by polymer analog quaternization of poly(4-vinylpyridine) brushes as reported by Biesalski *et al.* [230, 231]. Polyelectrolyte brushes are of special interest because their morphology and physical behavior are dominated by the strong electrostatic interactions along the grafted chain and within the polymer layer [242]. As an alternative to covalent attachment of the initiator molecules, ionic groups can be used to prepare permanently grafted brushes by SIP. In fact, in the 1950s Dekking *et al.* [221, 222] used 2,2'-azobisisobutyramidine as the very first initiator systems for the free radical SIP. This class of surface initiator is relatively

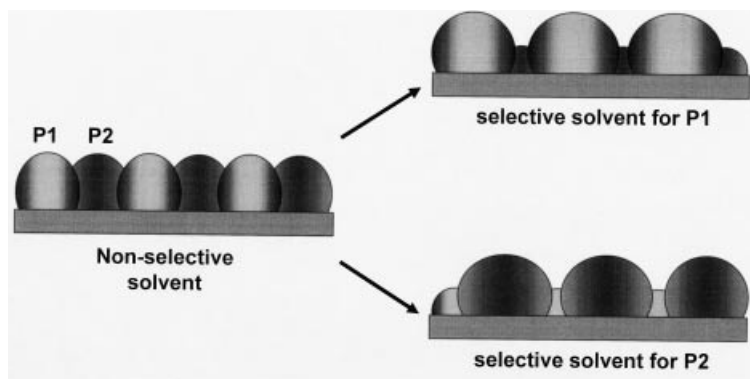


**Fig. 9.20** Grafted heterogeneous polymer brushes in different environments and principle of switching : (a) Structure in a nonselective solvent, (b) in a selective solvent for polymer P1 (e.g. PS), and (c) in a selective solvent for polymer P2 (e.g. P4VP) (modified from ref. [214]).

simple to prepare from commercially available compounds and was later revisited by other groups to form responsive polymer brushes of poly(*N*-isopropylacrylamide) (PNIPAM) on planar substrates to control bacteria attachment and detachment [220] or to form patterned polymer brushes by  $\mu$ CP of SAMs and enhancement of the patterns by SIP [219]. Suter and coworkers found that using this initiator on mica, initiation from the surface plays a minor role in the formation of the surface-bound polymer but instead, a ‘grafting onto’ mechanism dominates, in which active chain ends react with the decomposition product of the initiator [223]. The same group [224, 225] alternatively used quaternary amino groups to attach peroxide initiators for the SIP of styrene on high surface area mica.

The development of surface analytical techniques enabled detailed investigations of polymer brush dynamic behavior or morphology. Today, SIP is frequently carried out on flat surfaces and studied in detail regarding these aspects. Especially, the dynamic swelling behavior of brush systems as a collectively and fast-responding functional system was studied by e.g. SPM [228], ellipsometry [194, 233, 243] or scattering methods [244, 245]. Although the preparative possibilities of free radical polymerization is limited to homopolymers or statistical copolymers, heterogeneous polymer brushes could be created. Minko and Stamm [214] successively polymerized styrene and 2-vinylpyridine on surfaces functionalized with azo initiators. They demonstrated a controlled change in the layer morphology by selective swelling (Fig. 9.20).

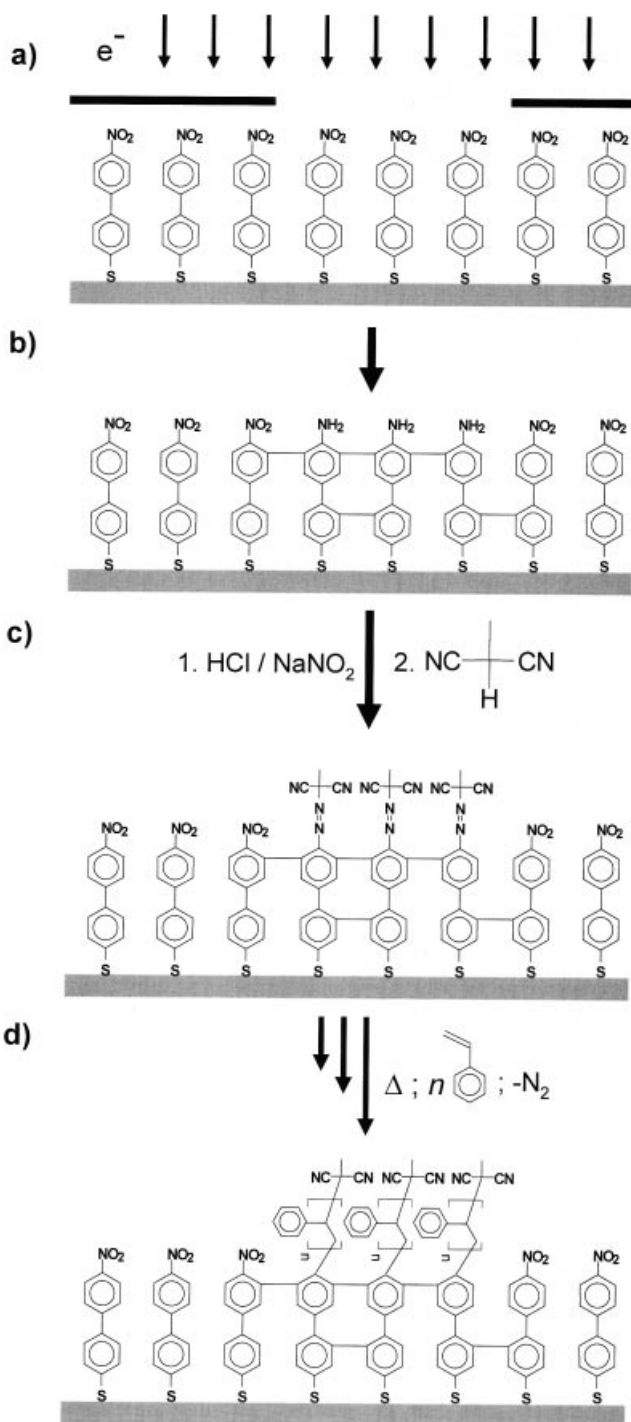
Laterally-defined heterogeneous polymer surfaces can be created by using a homogeneous layer of an azo initiator. UV irradiation through a mask in the presence of monomer leads to the locally confined photopolymerization [234]. A second polymerization using the remaining initiators results in patterned surfaces composed of two types of polymer brushes [238]. However, the lateral resolution of obtainable patterns is limited by the irradiation used and type of mask (in this case polymer brush patterns of 260  $\mu\text{m}$  spaced by  $\sim 40 \mu\text{m}$  were formed).

Chilkoti *et al.* took advantage of the  $\mu$ CP method to prepare patterned SAM of mercaptoundecanoic acid (MUA) for the binding of 2,2'-azobisisobutyramidine. Thermal SIP resulted in the topographical enhancement of the originally printed SAM structure with feature size of about 40  $\mu\text{m}$  [219]. Also, the selective binding of thiols onto gold can be used for spatio-selective SIP. Dryer *et al.* [215] used gold patches on silicon wafers, bonded a SAM onto the gold and used the functionalized SAM/Au patches ( $\sim 90 \times 90 \mu\text{m}^2$ ) for photopolymerization of styrene.

In recent examples, the morphology of the initiator layer was mainly that of a surface modification and not that of an organized SAM. As an alternative, one can also use a cross-linked or otherwise immobilized macromolecular interlayer containing azo or peroxide initiators [246–248], or redox systems ( $-\text{OH}/\text{Ce(IV)}$ ) [249–251]. In most of the reported work, the choice of the linker between the surface coupling group and the actual initiator is mainly determined by the chemistry of the synthesis of the initiator rather than to ensure the formation of a well-ordered SAM. For alkyl derivatives it appears that the bulky azo function inhibits the formation of a crystalline-analog SAM on gold when the entire initiator is immobilized. Surface analog reactions on SAMs may circumvent this problem but the surface chemistry has to be tailored to the steric situation at the interface (Fig. 9.6). Additionally, the problems of detached thiols as potential chain transfer agents are discussed in the corresponding reports since SAM of thiols are limited in their thermal stability or during UV irradiation.

Recently, Schmelmer *et al.* combined the chemical lithography of well-defined SAMs of 4,4'-substituted mercaptobiphenyls (see Fig. 9.15) and enhancement of surface patterns by means of SIP to create patterned polymer brushes on the micrometer and nanometer scale [241]. The selectivity, flexibility, high throughput and superior resolution of chemical lithography make it an ideal technological platform for the preparation of SAM patterns amplified by SIP. The preparation of initiator sites and a consecutive polymerization was first carried out without structuring: a SAM of 4,4'-nitromercaptobiphenyl (NMB) on Au(111) was converted to cross-linked 4,4'-aminomercaptobiphenyl (AMB) SAM by irradiation with e-beams. The terminal amino groups were then diazotized and reacted with methyl malonodinitrile to give a surface-bound monolayer of the 4-substituted mercaptobiphenyl azomethylmalonodinitrile (cMBA) (see Fig. 9.21).

Phenylazoalkyl malonodinitriles and their derivatives are known as second generation initiators for the radical polymerization of a broad variety of vinyl compounds to prepare graft copolymers in solution [252] as well as for SIP [203–207, 238]. In contrast to commonly used symmetrical azo initiators, thermal or photo-initiated decomposition yields one (in our case bound) phenyl radical of high reactivity and one (free) malonodinitrile radical which is not capable of initiating radical polymerization because of its resonance stabilization. In other words, by decomposition of the surface-bound asymmetric phenylazoalkyl initiator, the polymerization is only initiated at the surface and not by a cleaved free radical in solution, as with dialkylazo initiators. Furthermore, previous results indicate that the radical polymerization initiated by phenylazomethyl malonodinitrile follows a controlled polymerization mechanism, since in 'grafting from' reactions the degree of polymerization of the side chains





can be varied with the reaction time and the typical polydispersity index is significantly lower ( $M_w/M_n \sim 1.4$ ) than in free radical polymerization. It is suspected that the methyl malonodinitrile radical acts as a reversible termination agent [253].

The monolayer of cMBA was then exposed to a solution of styrene in toluene at 80 °C.

Inspection of the substrates with ER-FTIR spectroscopy, AFM and ellipsometry revealed that the surfaces were homogeneously covered by a polystyrene (PS) brush layer with a typical polymer layer thickness of 6.3 nm after a polymerization time of 6 h. The surface modification proved to be surprisingly stable at elevated temperatures and good solvent environments (soxhlet extraction) because of the cross-linked SAM support and the known stabilization effect of the polymer brush itself. Inspection of the AFM scans of the polymer brush in comparison with the native polycrystalline gold substrate showed the rendering of the single gold crystals, decreasing the step height of individual crystals from  $\sim 2.5$  nm to approximately 1 nm and a small decrease of the root mean square roughness value of 0.7 nm in contrast to the original surface roughness of the gold substrate of 0.9 nm.

The preparation of structured polystyrene brushes was carried out following the same procedures, only the irradiation was performed through a stencil mask with circular openings of 800 nm radius that was placed on the NBT covered substrate. Fig. 9.22 shows an SEM micrograph.

The dark dots represent areas where the NMB SAM was converted to AMB by irradiation, reacted further to cMBA and the SIP of styrene took place with good selectivity and uniformity. SPM scans revealed typical heights of the PS dots of 6 nm, a width of 1.6  $\mu\text{m}$  spaced with a periodicity of 2.5  $\mu\text{m}$  which is a one-to-one translation of the feature size of the mask. Investigation of different areas by AFM showed almost no variation of the structures.

Using a stencil mask with slits varied between 300 and 70 nm nanometer size structured polymer brushes were created following the same procedure, resulting in a one-to-one translation of the mask patterns.

The structures obtained created by the combination of chemical lithography and SIP are significantly smaller than features reported with comparable techniques. The advantage of this approach is not only the free choice of surface structures which can be created, the material contrast which can be realized by the combination of chemical lithography and amplification with SIP, but also the potential to bridge the gap in structural feature sizes ranging from the microscopic to the nanoscopic scale. Since the feature sizes reported are still limited to the features of the



**Fig. 9.21** Reaction and preparation scheme starting from SAMs of NBT on Au(111) (a). By exposure to electron beams, intralayer cross-linking and conversion of the terminal nitro group to the amino group occurs, resulting in cABT (b). Diazotization and coupling of malonodinitrile gives a SAM bearing an asymmetric azo-initiator: cMBA (c). Finally, by

exposure to a vinyl monomer (styrene) and heating to 80 °C, the radical polymerization results in a polymer brush layer at the irradiated areas (d) (Reprinted with permission from: [241] U. Schmelmer, R. Jordan, W. Geyer, *et al.*, *Angew. Chem.* **2003**, *115*, 577–581. © Copyright 2003 Wiley-VCH).

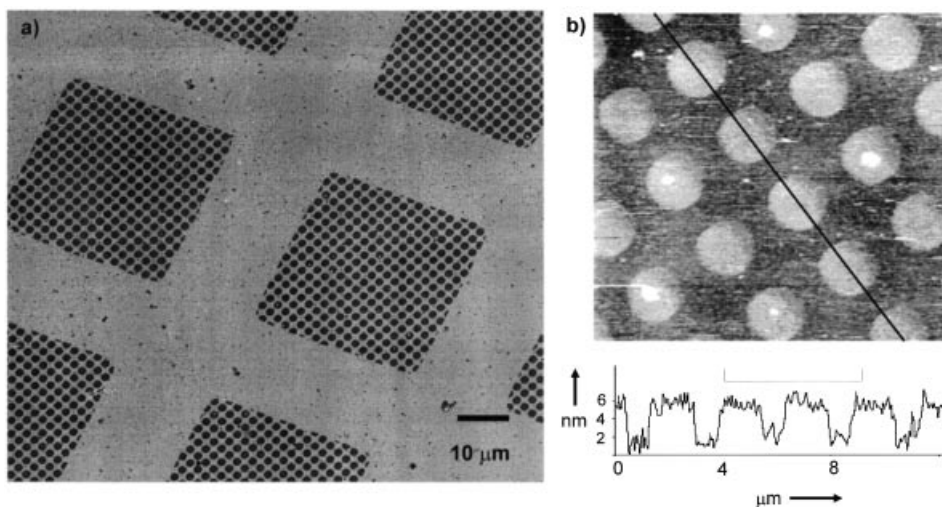


**Fig. 9.22** a) SEM micrograph of polystyrene brushes generated via SIP on a substrate that was irradiated through a stencil mask with a coarse grid with 60  $\mu\text{m}$  periodicity. Each square contains an array of circular holes of 1.6  $\mu\text{m}$  dots (2.5  $\mu\text{m}$  periodicity). b) AFM im

age of a small region of a similar substrate along with a height profile along the line indicated. (Reprinted with permission from: [241] U. Schmelmer, R. Jordan, W. Geyer, *et al.*, *Angew. Chem.* **2003**, *115*, 577–581. © Copyright 2003 Wiley-VCH).

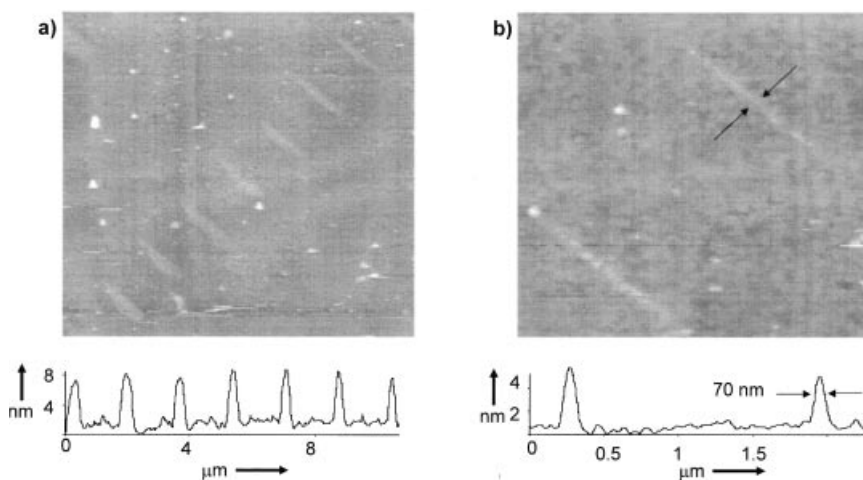


**Fig. 9.23** AFM micrographs of PS brushes generated by SIP on a chemical nanolithography substrate prepared by a stencil mask with a slit pattern. The height profiles below the images show an average profile along the

a)  $\sim 200$  nm, b)  $\sim 70$  nm wide lines (Reprinted with permission from: [241] U. Schmelmer, R. Jordan, W. Geyer, *et al.*, *Angew. Chem.* **2003**, *115*, 577–581. © Copyright 2003 Wiley-VCH).

mask used, direct writing with a focused e-beam should result in patterned polymer brushes of features matching the size of the immobilized macromolecule.

### 9.3.3

#### Surface-initiated Polymerization Using Living Ionic Polymerization

In comparison to the numerous accounts that are reported for free radical SIP, reports on living cationic or anionic SIP are scarce. This is mainly because the nature of the polymerization is sensitive, and the amount of initiator is tiny, and hence, the resulting total numbers of propagating polymer chains within the reactor is also small. Even amounts of impurities forming a sub-monolayer concentration on the reaction flask would strongly interfere with the living polymerization. One solution to this problem is to increase the specific surface area of the substrate by using small or porous particles and thus increasing the total number of surface-bonded initiators in the reaction. Another possibility is to initiate ionic polymerization on the surface *and* in the solution to use the free propagating species as scavengers for undesired termination. In any case, the living ionic polymerization and especially anionic SIP is experimentally rather difficult to perform, especially on flat substrates with just a couple of square centimeters surface area to cover. Despite these experimental difficulties, it is worthwhile to look into living ionic SIP. The synthetic possibilities of living SIP reactions are unique, such as the formation of homopolymers with low polydispersities, synthesis of defined block copolymers and the introduction of functional end groups results in polymer brushes of uniform length, (multi)layered polymer brushes which may not be obtainable by the 'grafting onto' approach, as well as polymer brushes with defined terminal end groups (Fig. 9.19). Additionally, the uniform growth of the polymer brush during polymerization and the absence of cross-linking, chain transfer and combination guarantee the formation of a well-defined brush of strictly linear chains of uniform length. In free radical polymerization the propagating species are confined within a thin surface layer which enhances the probability of side reactions such as combination and cross-linking by chain transfer. Furthermore, the decomposition of the initiator to the reactive radical species occurs throughout the propagation reaction of the polymerization. At advanced reaction time, this will lead to problems in mass transfer of the monomer through the increasingly denser polymer brush layer. Schouten [254] already pointed out that in the case of living ionic SIP where the initiation is much faster than the propagation reaction ( $k_i \gg k_p$ ) no grafting sites (propagating chain ends) are screened.

On the other hand, the observed polydispersities of polymer brushes prepared by SIP are still within the range of polymerization in solution. This may also be because the impact of transfer and other side reactions only partially shows up in the final surface-bonded brush since the fraction of created polymers which is not bonded on the surface, is simply washed away. In general, for most of the polymerization reactions employed, cross-linking, competitive side and termination reactions are augmented in surface-initiated polymerizations because of the extremely small total number of reactive chain ends, as well as their high concentration, confined in a thin layer. Recalling the characteristics of a brush, as a layer of

linear chains of uniform length, controlled/living polymerization reactions are most suitable for their formation.

### 9.3.3.1 Surface-initiated Polymerization Using Living Anionic Polymerization

Recalling the demands on the polymer architecture of a polymer brush and the projected properties in terms of swelling, wetting and friction, as described in the theoretical work, the brush has to consist of linear polymer chains of the same length at high grafting densities. The closest approximation to this can be obtained by the living anionic SIP (LASIP). The experimental difficulties outlined mean that only relatively few examples of LASIP are documented in the literature.

For example, Ohkita *et al.* [255] reported that OLi surface groups created by the treatment of carbon black with *n*-BuLi are reactive enough to start LASIP of MMA and acrylonitrile (AN) but not styrene or *o*-methylstyrene. These monomers were only polymerizable in the presence of crown ethers [256, 257].

Braun *et al.* [258] used a combination of *tert*-butyllithium (*t*-BuLi) and tetramethylethylenediamine to create initiator sites at the surface of carbon black for the LASIP of styrene. Schomaker *et al.* [259] first immobilized a methyl methacrylate derivative on colloidal silica and after activation by a Grignard reagent polymerized MMA.

Based on this approach Schouten *et al.* [254] attached a silane-functionalized styrene derivative (4-trichlorosilylstyrene) on colloidal silica as well as on flat glass substrates and silicon wafers and added a five-fold excess BuLi to create the active surface sites of LASIP in toluene as the solvent. With THF as the reaction medium, the BuLi was found to react not only with the vinyl groups of the styrene derivative but also with the siloxane groups of the substrate. It was found that even under optimized reaction conditions, LASIP from silica and especially from flat surfaces could not be performed in a reproducible manner. Free silanol groups at the surface as well as the ever-present impurities adsorbed on silica, impaired the anionic polymerization. However, living anionic polymerization behavior was found and the polymer load increased linearly with the polymerization time. Polystyrene homopolymer brushes as well as block copolymers of poly(styrene-*block*-MMA) and poly(styrene-*block*-isoprene) could be prepared.

Because of the difficulty in investigating polymer layers on small particles, the characterization of the obtained materials was mainly restricted to accounts of the total amount of grafted polymer, and to estimations of the grafting density based on the remaining initiation sites. Hence, no detailed information on layer and polymer morphology or brush characteristics could be provided.

Till now, only three reports on the preparation of polymer brushes by means of surface-initiated anionic polymerization on planar substrates with accounts on the morphology and special properties can be found.

Jordan *et al.* [194] presented the only report of LASIP on planar substrates using a well-defined SAM as the initiator system.

In an all-glass reactor, a SAM of 4',4-bromo-mercaptobiphenyls on Au(111) surfaces was converted to biphenyllithium moieties by treatment with *sec*-BuLi to initiate anionic polymerization of styrene on gold substrates (Fig. 9.24).

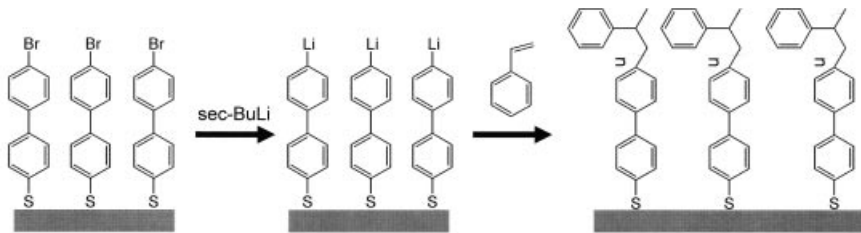


Fig. 9.24 Reaction scheme for the surface-initiated living anionic polymerization using the

rigid self-assembled monolayer of 4'-lithio-4-mercaptobiphenyl [194].

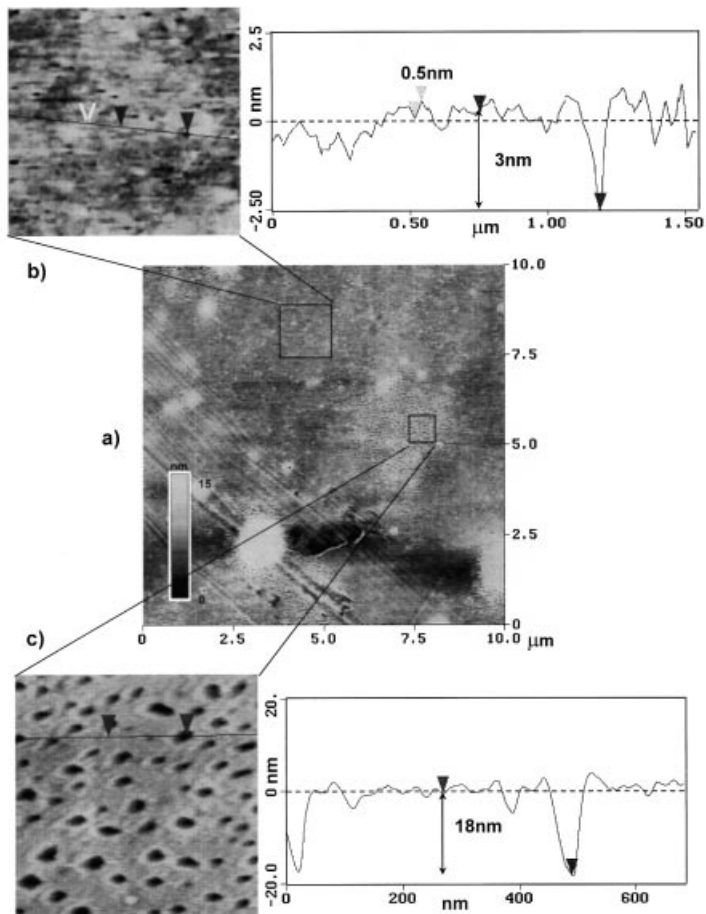


Fig. 9.25 Surface topography of grafted polystyrene brushes layer after soxhlet extraction as probed by SPM. a) Typical scan ( $10 \times 10 \mu\text{m}^2$ ) with detailed scans as marked in the overview along with the dept profile analysis along the indicated lines (Reprinted with permission from: [194] R. Jordan, A. Ullman, J.F. Kang, *et al.*, *J. Am. Chem. Soc.* **1999**, *121*, 1016–1022. © Copyright 1999 American Chemical Society.

It is noteworthy that the choice of the SAM system of rigid mercaptobiphenyls thiols avoided the effect of surface reconstruction discussed previously. Analog SAMs made of longer alkanethiols (Fig. 9.7 and 9.10) may most probably not be suitable when the polymerization medium (in this case benzene/cyclohexane) is nonpolar. This would first reduce the number of initiator sites and secondly lead to an unfavorable  $k_i/k_p$  ratio. The thickness of the resulting polystyrene brush in the dry (collapsed) state, as estimated by ellipsometry and atomic force microscopy (Fig. 9.25), was  $18 \pm 0.2$  nm. These techniques also reveal a smooth homogeneous polymer surface throughout the substrate on the macroscopic, as well as on the microscopic scale, with a roughness of 0.3–0.5 nm (rms). However, treatment of the substrate with BuLi and the complications of transferring planar substrates in and out of an all-glass reactor also gave rise to microscopic and macroscopic defects. The extremely dense polymer brush around such defect sites were partly desorbed or originally of lower grafting density because the lithiated SAM shows incomplete formation.

A polymerization degree of  $N=382$ , and grafting density of approx. 7–8 chains per  $R_g^2$ , or 3.2–3.6 nm<sup>2</sup> per chain was calculated using mean-field theory [170, 260], based on results from swelling experiments. In numerous experiments it was observed that LASIP was only possible when simultaneously, living anionic polymerization was performed in solution by the presence of small amounts of unreacted BuLi. The molecular weight of polymer created by LASIP was about  $34 \times 10^3$  g mol<sup>-1</sup>, the simultaneous polymerization in solution yielded a molecular weight of  $1.6 \times 10^6$  g mol<sup>-1</sup>. This is in agreement with observations of other groups that the SIP of controlled polymerization reactions proceeds significantly slower than in solution, because they are confined.

Polarized ER-FTIR spectra of the PS brush layer indicated strongly stretched and preferentially oriented polystyrene chains. Upon closer inspection of the  $\nu\text{CH}_x$  region (3000–2800 cm<sup>-1</sup>) of the spectra of a deposited bulk PS film and of the PS brush, the relative intensities are significantly different for both spectra. For example, while the ratio  $\nu\text{CH}_2(\text{as})/\nu\text{CH}_2(\text{s})$  is approx. 4.5 in the 'bulk' spectrum,  $\geq 10$  was found in the spectrum of the extracted polymer brush. Differences in ratios of CH-aromatic stretching modes are also noticeable. This indicates an apparent difference in the average chain orientation between bulk and tethered polystyrene chains. Such an orientation can only be explained if the chains are considerably stretched by the high grafting density.

One of the unusual properties of dense polymer brushes is their wetting behavior towards identical polymers [261]. In contrast to a simple liquid, which always spreads on a free surface of identical surface tension, a homopolymer may de-wet a substrate of identical chemical composition. If the interfacial macromolecules are confined in some way, i.e. tethered at one end so that they form a dense brush, an entropic barrier is established to interpenetration. Indeed, the wetting behavior of the polystyrene brush showed this effect. A 20 nm-thick layer of polystyrene was spin-coated directly onto the brush surface. After annealing of the sample above the glass transition temperature, AFM and scanning near-field optical microscopy confirms that the spin-coated polystyrene layer completely de-wets the polystyrene brush surface. The observed average contact angle of 3° is somewhat smaller

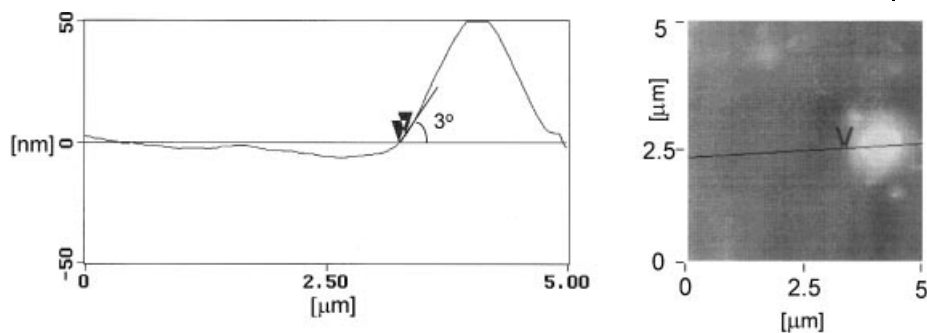


**Fig. 9.26** AFM scan of a single droplet of polystyrene on top of the polystyrene brush along with its dept profile and contact angle. (Reprinted with permission from: [194]

R. Jordan, A. Ulman, J. F. Kang, *et al.*, *J. Am. Chem. Soc.* **1999**, 121, 1016–1022. © Copyright 1999 American Chemical Society).

than predicted by Leibler [262] in the absence of substrate deformation. In contrast to a hard surface, a brush surface can deform at the contact line in response to the vertical component of the droplet surface tension. The entropic penalty of chain stretching is balanced by minimizing the contact angle (Fig. 9.26).

Similarly, Ingall *et al.* [263] lithiated monolayers of short 3-bromopropylsilane on planar silica substrates to perform LASIP with AN. They obtained up to 245 nm thick PAN films within eight days of polymerization time.

Recently, Quirk and Mathers [264] performed LASIP of isoprene on silicon wafers. A chlorodimethylsilane-functionalized diphenylethene (DPE) was coupled onto the surface and lithiated with *n*-BuLi to form the initiating species. The living poly(isoprene) (PI) was end-functionalized with ethylene oxide. A brush thickness of 5 nm after two days of polymerization (9.5 nm after four days) was obtained in contrast to a polymer layer thickness of 1.9 nm by the ‘grafting onto’ method using a telechelic silane functionalized PI.

Advincula *et al.* used the same initiator type (DPE activated with *n*-BuLi) to perform LASIP from colloidal silica [265] or clay [266, 267]. The spacer between the DPE unit and the surface active group (quaternized amine for clay and chlorodimethylsilane for silica) was a long *n*-alkyl chain. In all cases, a relatively broad polydispersity for the prepared polystyrene brush (PDI=1.2–2) was observed.

### 9.3.3.2 Surface-initiated Polymerization Using Living Carbocationic Polymerization (LCSIP)

The first report on living carbocationic surface-initiated polymerization (LCSIP) using a defined surface modification is by Vidal and Kennedy [268–270]. They prepared poly(isobutene) (PIB) brushes from silica surfaces using a silane functionalized benzylchloride activated by a Lewis acid.

In a recent review, Spange *et al.* [271] compiled LCSIP systems on inorganic substrates as well as ‘grafting onto’ methods involving carbocations in the grafting

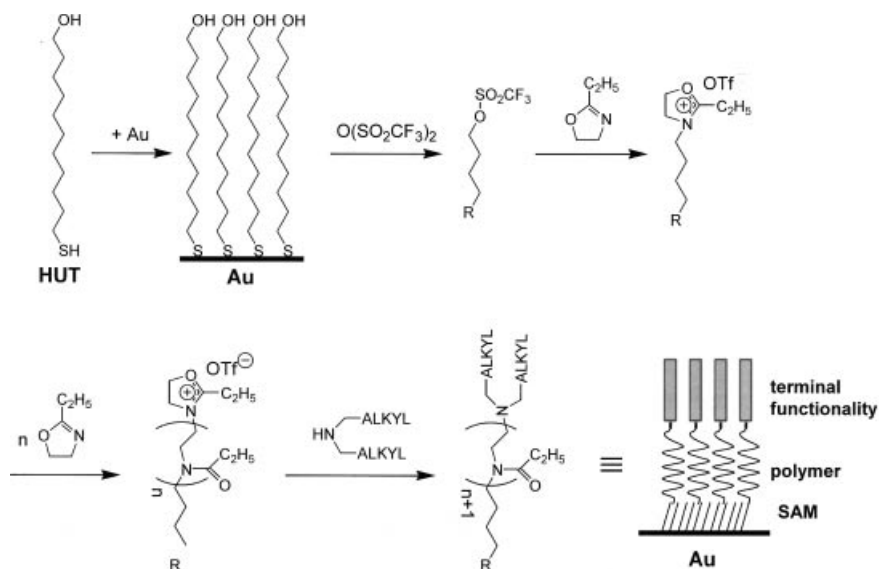


**Fig. 9.27** Reaction scheme for the preparation of amphiphilic poly(2-ethyl-2-oxazoline) brushes by means of LCSIP [272].

reaction and gave a detailed account on the extensive work of his group in the field of LCSIP employed directly on the silica surface.

Jordan *et al.* [272] performed LCSIP using SAMs of 11-hydroxyundecane thiol (HUT) on planar Au(111) substrates as well as on gold nanoparticles functionalized with mixed 3D-SAMs of [273]. The primary hydroxyl groups were converted by a gas phase reaction using trifluoromethanesulfonic anhydride to trifluoromethylsulfonates (triflates) as a good leaving group to initiate cationic living polymerization of 2-alkyl- and 2-phenyl-2-oxazolines. One crucial aspect of LCSIP is the choice of the surface-bond initiator for the start of the living polymerization. Since surface-confined reactions are relatively slow, LASIP or LCSIP should be initiated fast compared with the propagation reaction to ensure homogeneous growth of the polymer brush from the surface. This enables a stoichiometric polymerization on the surface and consequently results in low polydispersities. Triflates as fast initiators were introduced by Kobayashi *et al.* [274] and were found to be ideal candidates for the defined start of the living cationic polymerization of 2-oxazolines involving large initiators [51, 154–156]. The living ends of the polymer brushes were terminated with piperidine or further functionalized with *N,N*-dioctadecylamine to yield amphiphilic polymer brushes of a defined hydrophilic lipophilic balance. The reaction is outlined in Fig. 9.27.

The brush layer thickness (dry collapsed state) obtained after seven days of polymerization time and successive soxhlet extraction was found to be approx. 10 nm and very uniform ( $\pm 0.3$  nm). The uniform thickness values are provided by the homogeneous initiation, polymerization and termination reaction. Meanwhile



poly(2-oxazoline) homopolymers brushes with layer thicknesses of 20 to 30 nm can be obtained [275].

The amphiphilic brush displayed dynamic wetting behavior towards selective solvents such as water. If the substrate was immersed in water and then air-dried, an initial contact angle (sessile drop) of 80–75° was found, because of selective swelling of the intermediate hydrophilic polymer brush layer and segregation of the hydrophobic moieties towards the gas-phase [51, 156, 243]. This value decreased rapidly to a stable value of 60–62° because of the reorganization of the amphiphilic lipopolymer layer in the presence of water. Advancing and receding contact angles showed a pronounced hysteresis of approx. 30°. This has been observed earlier with similar surfaces prepared by the grafting of silane functionalized lipopolymers onto silica substrates and appears to be characteristic for polymer supported alkyl monolayers [276]. The introduction of a flexible polymer interlayer enables a pronounced surface reconstruction process (compare to Section 9.2.5). One drawback of the SIP is the analysis of the polymer brush formed. Here the end-functionalization was confirmed by the wetting behavior as well as by ER-FTIR spectroscopy. To estimate the efficiency of the termination reaction, the CH<sub>x</sub>-stretching area of both spectra was analyzed (Fig. 9.28). Subtraction of the HUT monolayer spectrum from the

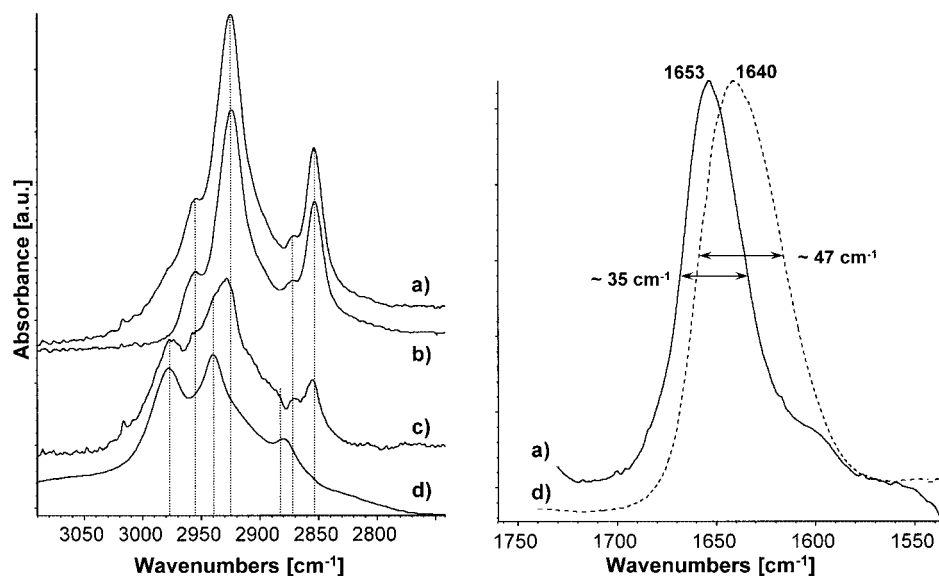
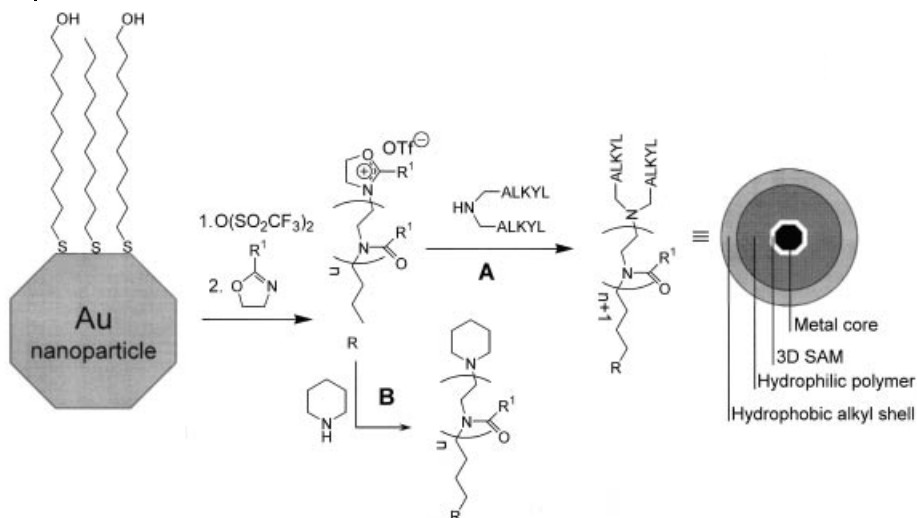


**Fig. 9.28** Analysis of the CH-stretching region (3000–2800 cm<sup>-1</sup>) and the amide I band around 1650 cm<sup>-1</sup>. (a) ER-FTIR spectrum of poly(2-ethyl-2-oxazoline) (PEOx) as grown on the triflate functionalized HUT SAM. (b) ER-FTIR spectrum of HUT SAM. (c) Subtraction result of (a)–(b). (d) Bulk spectrum of PEOx. In the spectrum to the left, a significant shift

of the amide I band to higher wavenumbers and decrease of the half width in the ER-FTIR spectrum of the grafted PEOx (a) can be observed. This can be explained by a different conformational freedom and/or intra- and intermolecular interactions between polymer chains in the grafted polymer when compared with the bulk phase (modified from ref. [272]).



**A** (amphiphilic core-shell):  $R^1 = C_2H_5^-$ ; Terminating agent: *N,N*-di-*n*-octadecylamine; polymerization : 72h  
**B** (*ex situ* kinetics):  $R^1 = C_6H_5^-$ ; Terminating agent: piperidine; polymerization : 2, 8, 24, 79h

**Fig. 9.29** Reaction scheme of the LCSIP of 2-oxazolines on gold nanoparticles: For the preparation of the amphiphilic nanocomposite 2-ethyl-2-oxazoline and *N,N*-di-*n*-octadecylamine were used as monomer and terminat-

ing agent, respectively (pathway A). The kinetic studies were performed with 2-phenyl-2-oxazoline and piperidine. A schematic representation of the core-shell morphology of the amphiphilic metal-polymer composite [273].

grafted PPEI spectrum (Fig. 9.28a) reveals an overall higher integral adsorption for the complete CH<sub>x</sub>-stretching area (Fig. 9.28c). The characteristic bands for the CH<sub>3</sub>/CH<sub>2</sub>-stretching modes of the propionyl side group, appearing at 2978, 2940 and 2880 cm<sup>-1</sup>, could be unambiguously identified by comparison with the PPEI bulk spectrum (Fig. 9.28d). Furthermore, stronger adsorption at 2926 and 2854 cm<sup>-1</sup> indicate the presence of additional long *n*-alkyl chains. This suggests a successful termination reaction of the polymerization by the *N,N*-dioctadecylamine.

However, quantitative analysis of the brush composition or extraction of standard polymer analytical values is difficult if not impossible because an extremely small total amount of polymer is immobilized on flat substrates. Therefore, Jordan *et al.* [273] performed analog LCSIP experiments were performed on gold nanoparticles using a mixed 3D-SAM consisting of HUT and *n*-decanethiol. The triflation of the primary OH groups of HUT and subsequent analog polymerization reaction yields core-shell amphiphilic polymer-metal nanocomposites (Fig. 9.29) whose amphiphilic nature was studied by means of LB-experiments. *Ex situ* kinetic studies of the polymerization of 2-phenyl-2-oxazoline using FTIR spectroscopy and MALDI/TOF mass spectrometry, resulted in a linear relationship between the reaction time and degree of polymerization of the grafted polymer (Fig. 9.30). This, as well as the successful end-functionalization by termination with secondary amines, confirmed the initial view of a well-defined living polymerization mechanism of 2-oxazolines using LCSIP.

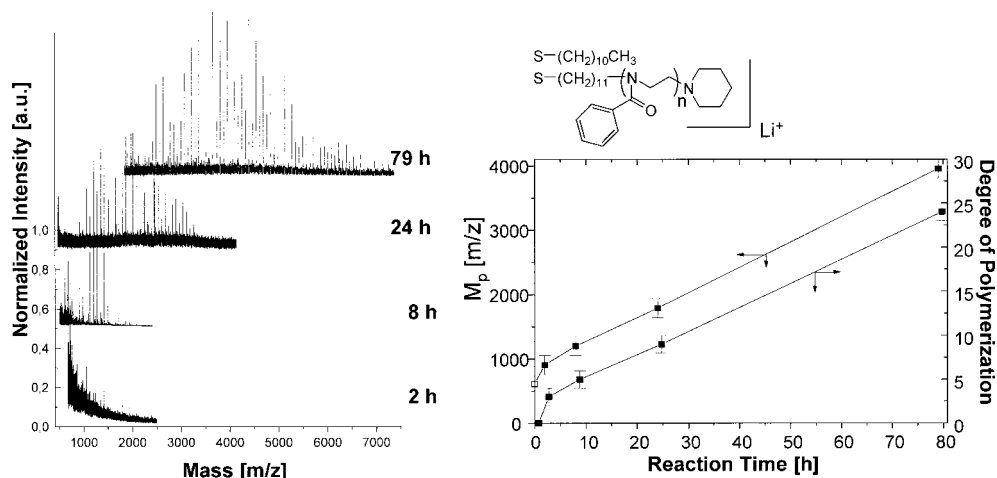


**Fig. 9.30** a) Normalized MALDI TOF mass spectrum of all fractions (taken after 2 h to 72 h of polymerization time) of poly(2-phenyl-2-oxazoline) freed by dissolving the gold core with NaCN solution and collection of the polymer. The calculated mass of the monomer unit (147.17) is in good agreement with the spacing of the mass signals ( $\Delta M = 146.93$ ) of the most prominent peaks. Based on ear-

lier findings by Tempelton *et al.* [277], the species of the isolated polymer is assumed to have an asymmetric dialkyl disulfide structure. Spectra are shifted along the y-axis for clarity. b) Plot of the most intensive mass signal ( $M_p$ ) vs. reaction time. The corresponding degree of polymerization was calculated based on the identified species as depicted (modified from ref. [273]).

In Fig. 9.30 a broadening of the molecular weight distribution at increasing time of polymerization is observable which is typical for the polymerization of 2-oxazolines. Plotting the  $m/z$  value of the most intensive mass signal versus the reaction time, a strictly linear relationship is obtained (Fig. 9.30). These results are consistent with recent experimental and theoretical studies of surface-initiated atom transfer radical polymerization (ATRP) by Matyjaszewski and coworkers [278]. The initiation reaction by the alkyltriflate seems to be much faster than the propagation reaction, which is indicated by the significantly steeper slope between  $t=0$  and 2 h. This means that the induction period of the polymerization is not noticeably hindered by the surface confinement of the initiator.

In a similar approach Ruhe *et al.* [279] reported the preparation of poly(2-oxazoline) brushes by the 'grafting onto' as well as 'grafting from' method. For LCSIP of 2-ethyl-2-oxazolines silane functionalized undecane tosylate was first prepared and then immobilized on the substrate surface. SIP resulted in PEOx layers with thickness close to 30 nm. PEOx brushes were prepared by chemisorption of PEOx disulfides onto gold substrates. Preliminary static and dynamic swelling experiments are reported for these brushes. However, later observations [243] contradicted these findings.

Zhao and Brittain [280–282] reported the LCSIP of styrene on planar silicon wafers using surface modifications of 2-(4-(11-triethoxysilylundecyl)phenyl)-2-methoxypropane or 2-(4-trichlorosilylphenyl)-2-methoxy- $d_3$ -propane respectively. Growth of PS brushes from these SAMs has been successfully achieved; factors that influ-

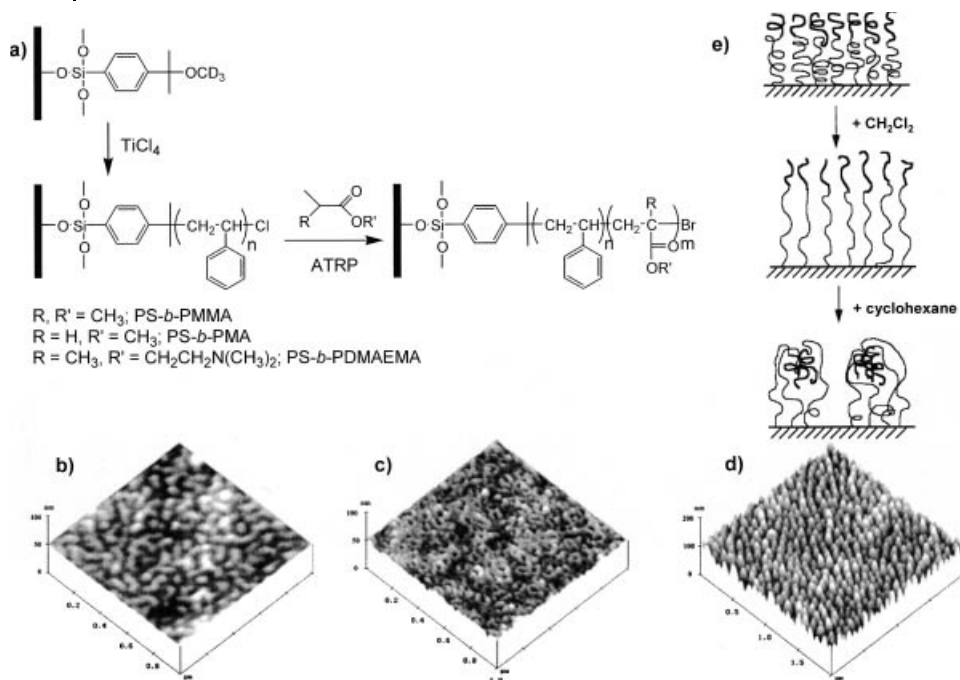


**Fig. 9.31** a) Synthesis of PS-*b*-polyacrylate brushes by LCSIP and consecutive ATRSIP [282]. AFM images of the tethered PS-*b*-PMMA brushes with 23 nm thick PS layer and 14 nm thick PMMA layer b) after treatment with  $\text{CH}_2\text{Cl}_2$ , c) with cyclohexane and d) after solvent exchange from  $\text{CH}_2\text{Cl}_2$  to cyclohexane. e) Cartoon proposing a model for the regular nanopattern morphology ('pinned micelles')

after solvent exchange. (Reprinted with permission from: [282] B. Zhao, W.J. Brittain, *Macromolecules* **2000**, *33*, 8813–8820. [283] B. Zhao, W.J. Brittain, W. Zhou, *et al.*, *J. Am. Chem. Soc.* **2000**, *122*, 2407–2408. [284] B. Zhao, W.J. Brittain, W. Zhou, *et al.*, *Macromolecules* **2000**, *33*, 8821–8827. All © Copyright 2000 American Chemical Society).

ence PS thickness included solvent polarity, additives and  $\text{TiCl}_4$  concentration. Sequential polymerization by monomer addition to the same silicate substrate bearing the living polymer chains resulted in thicker PS films. FTIR-ATR studies using a deuterated initiator indicated that the initiator efficiency is low, and the second carbocationic polymerization on the same sample involved initiation from both PS chain ends and unconsumed surface-immobilized initiators. SPM investigations revealed a uniform and smooth PS brush surface with a roughness value of 0.3 nm (rms) for a 30 nm thick PS layer. Additionally they succeeded in sequential LASIP and surface-initiated atom transfer radical polymerization (ATRSIP) of MMA, MA or (*N,N*-dimethylamino)ethyl methacrylate) (PDMAEMA) using the terminal halogen of the polystyrene chains [280].

Surface reconstruction of the PS-PMMA brush in selective solvents gave rise to pattern formation which was investigated by SPM, wetting experiments and XPS. The obtained morphologies depended on the thickness of the brush and its composition [283, 284] (Fig. 9.31).

## 9.3.4

**Surface-initiated Polymerization Using Controlled Radical Polymerization**

While in most of the reports on SIP free radical polymerization is utilized, the restricted synthetic possibilities and lack of control of the polymerization in terms of the achievable variation of the polymer brush architecture limited its use. The alternatives for the preparation of well-defined brush systems were living ionic polymerizations. Recently, controlled radical polymerization techniques has been developed and almost immediately applied in SIP to prepare structurally well-defined brush systems. This includes, living radical polymerization using nitroxide species such as 2,2,6,6-tetramethyl-4-piperidin-1-oxyl (TEMPO) [285], reversible addition fragmentation chain transfer (RAFT) polymerization mainly utilizing dithiocarbamates as iniferters (iniferter describes a molecule that functions as an initiator, chain transfer agent and terminator during polymerization) [286], as well as atom transfer radical polymerization (ATRP) where the free radical is formed by a reversible reduction-oxidation process of added metal complexes [287]. All techniques rely on the principle to drastically reduce the number of free radicals by the formation of a dormant species in equilibrium to an active free radical. By this the characteristic side reactions of free radicals are effectively suppressed.

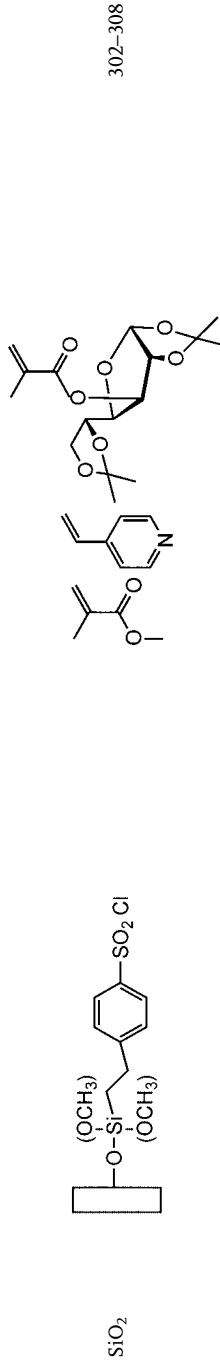
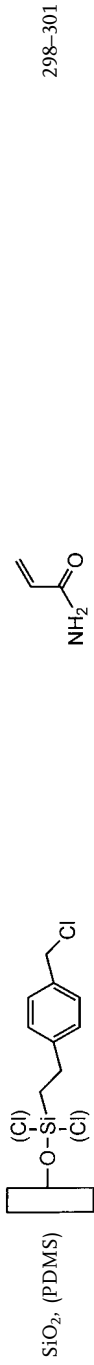
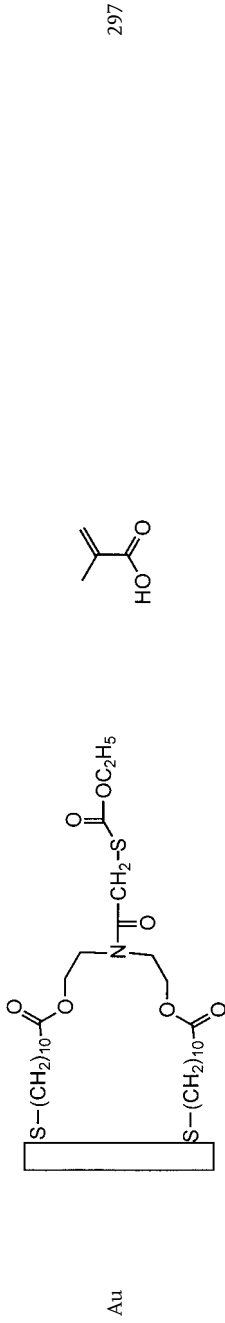
The initiator/monomer system applied in controlled radical (CR) SIP are compiled in Tab. 9.3.

Sogah *et al.* [288] immobilized a TEMPO-functionalized ionic surfactant on the surface of mica-type layered silicate and successfully polymerized styrene to give an organic-inorganic nanocomposite. Although the layered silicate delaminated when PS was incorporated within the layers, the polydispersities of the PS formed was relatively high. Hawker *et al.* [289] employed a TEMPO functionalized SAM on silica and employed besides the common styrene, the polymerization of acrylates, acrylamides and acrylonitrile. SIP with a linear increase of the brush film thickness and low polydispersities could only be obtained, when free alkoxyamine was added. A comparison of the polymer fraction as created in solution and via SIP gave almost identical molecular weights and low polydispersities of 1.14. The potential of CRSIP was demonstrated by preparing block as well as random copolymer brushes of styrene and 2-hydroxyethyl methacrylate. Laterally patterned polymer brush surfaces of poly(acrylic acid) (PAA) and poly(*t*-butylacrylate) with a resolution of approx. 25  $\mu\text{m}$  were also created, using a photoresist [290].

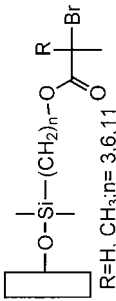
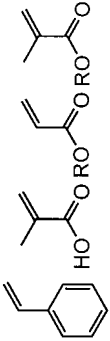
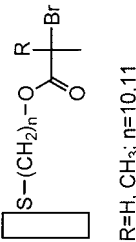
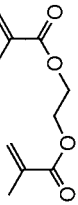
In a series of papers, Matsuda *et al.* [291–295] employed RAFT-SIP with immobilized benzyl *N,N*-diethyldithiocarbamate to form polymer brushes from styrene, methacrylamides, acrylamides and acrylates, NIPAM and *N*-vinyl-2-pyrrolidone on various surfaces. The SIP is initiated by UV irradiation of the surface-bonded dithiocarbamates. Thermoresponsive polymer brushes were prepared by the polymerization of NIPAM and investigated by XPS, wetting experiments and mainly SPM [294]. Patterned polymer brush layers were also prepared. When chloromethyl styrene was used as a comonomer, RAFT-SIP results in branching. By control of the branching, spatio-resolved hyperbranching of a controllable stem/branch design can be realized (Fig. 9.32) [293, 295].

**Tab. 9.3** Specific surface modifications and SAM systems of particles or planar substrates for the surface-initiated controlled radical polymerization (CRSIP) of vinyl monomers.

Substrate	Intermediate Layer//Initiator	Monomer(s)	Reference
Silicate			288
SiO <sub>2</sub>			289, 290
PS, SiO <sub>2</sub> ,			291–296



Tab. 9.3 (continued)

Substrate	Intermediate Layer//Initiator	Monomer(s)	Reference
SiO <sub>2</sub>	 <p>R=H, CH<sub>3</sub>; n= 3,6,11</p>		278, 310–318
Au	 <p>R=H, CH<sub>3</sub>; n=10,11</p>		319–325



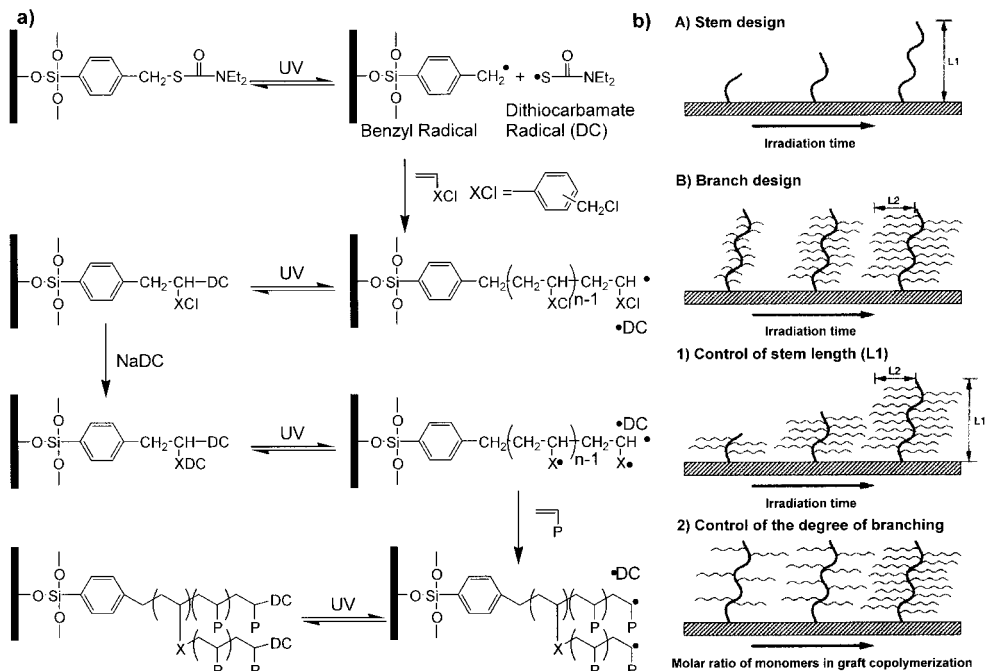


**Fig. 9.32** a) Reaction scheme for the preparation of the design of stem and branches in RAFT-SIP using dithiocarbamates [293]. b) Schematic representation of the various

(Reprinted with permission from: [293] H.J. Lee, Y. Nakayama, T. Matsuda, *Macromolecules* **1999**, 32, 6989–6995. © Copyright 1999 American Chemical Society).

Hadziioannou *et al.* [296] employed an analog surface-bond initiator for RAFT-SIP on silica substrates to prepare homogeneous block copolymers of styrene and methyl methacrylate. A patterned substrate was prepared by selective deposition of the initiator.

Niwa *et al.* [297] prepared a mixed SAM from dithiols on gold which partly bears a dithiocarbamate group. The RAFT-SIP of methacrylic acid was monitored by in situ quartz crystal microbalance. The polymerization rate depended strongly on the composition of the SAM.

The mechanism and kinetics of RAFT-SIP were studied by Fukuda *et al.* [326]. Besides the expected linear increase of the molecular weight of the surface grafted polymer with the monomer conversion, they observed the appearance of a prominent low molar mass fraction which was attributed to a combination reaction of the propagating active chains.

Using a SAM of an asymmetric azo compounds Baum and Brittain [327] homo- and block copolymerized styrene, MMA and *N,N'*-dimethylacrylamide under RAFT conditions in the presence of 2-phenylprop-2-yl dithiobenzoate as the chain transfer agent.

Within the short period of time since its discovery, ATRP has developed remarkably fast to become the most employed controlled radical polymerization technique

for SIP. In the first account, Wirth *et al.* [298–300] used a monolayer of silane functionalized benzyl chloride and  $\text{Cu}(\text{bpy})_2\text{Cl}$  to form polymer brushes of acrylamide as stationary phases in HPLC and in capillary electrophoresis. The polydispersity index of the grafted brush was typically between 1.15 and 1.3. Genzer *et al.* [301] immobilized this initiator onto oxidized PDMS substrates while under stress. Analogous to the preparation of MAMs, polymer brushes were produced by surface modification of the PDMS elastomer under stress and final relaxation (see Fig. 9.8). Giopireddy and Husson used an analog initiator function for ATRSIP of acrylamide featuring an undecane as a longer, effective mesogen to ensure SAM formation of the thiol on gold [309]. A similar surface initiator function was recently used by Zheng and Stöver [328] to prepare polystyrene homopolymer and poly(styrene-*b*-4-methylstyrene) on polymer resins. Fukuda *et al.* [302–308] employed a monolayer of 2-(4-chlorosulfonylphenyl)ethyl trimethoxysilane on planar and substrates and silica particles as an effective initiator group to start ATRP at the surface. Extremely high grafting densities between 0.07–0.7 chains  $\text{nm}^{-2}$  were obtained, similar to results obtained by LASIP. The group investigated the brush systems in terms of the impact of grafting density [305] and chain length [304] upon the surface interaction forces. Besides MMA and 4-vinylpyridine, MMA derivatives bearing sugar moieties could be polymerized in a controlled manner [303].

Brittain *et al.* [329] used a SAM on planar silica substrates, which were again functionalized with an asymmetric azo group to start the polymerization as a free radical polymerization. However, similar to the addition of dithiocarbamates, they added copper chloride and a suitable ligand to the polymerization reaction to control the free radical concentration during propagation (reverse ATRP). Secondary and tertiary *α*-bromoesters bearing various alkyl chains as mesogens for the formation of defined SAMs and equipped with mono- or trifunctional silanes [311–314, 316–318] or thiol [319–325] groups for chemisorption onto silica or gold surfaces became especially popular. Again, in the presence of copper complexes with various ligands, this type of surface initiator is well suited to effectively initiate ATRSIP. Especially for the SIP from SAM initiator systems of limited stability, the conditions of ATRP employing *α*-bromoesters are comparatively mild in terms of temperature [309, 320] and tolerance towards moisture. Baker *et al.* [323] and Huck *et al.* [325] performed ATRSIP with 2-hydroxyethyl methacrylate (HEMA) or MMA as well as glycidyl methacrylate in the presence of water or even in water as the solvent. Recently, a preliminary study from Rühle *et al.* [317] investigated the role of the added copper compounds for the surface-confined ATRP.

Beside planar surfaces, Patten *et al.* [310–312] and Hallensleben *et al.* [313, 314, 322] prepared well-defined nanocomposites by ATRSIP of from silica and gold nanoparticles. After spin-coating a solution of the polymer decorated particles onto mica, Hallensleben was able to image the single particles with the individual grafted polymer chains (Fig. 9.33).

Although controlled or living SIP techniques are mainly used to prepare strictly linear polymer brush layers, defined structural variations of the polymer layer give rise to new properties of the coating. Especially ATRP is useful to prepare such novel coatings. Using inimers (monomers bearing initiator functions) or bifunctional

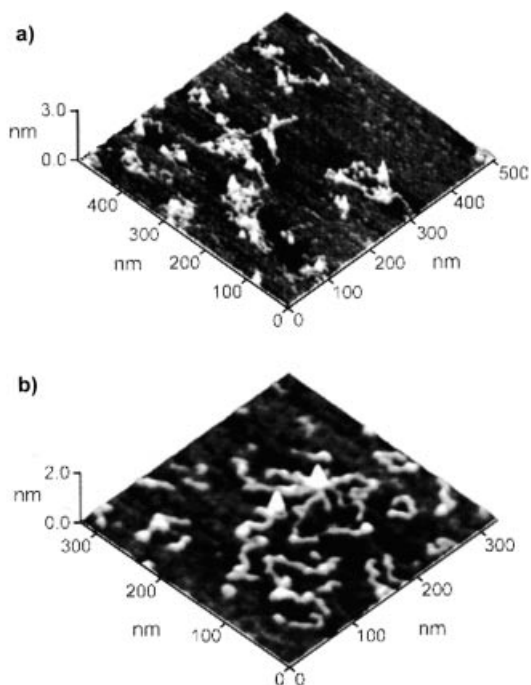


**Fig. 9.33** SPM micrograph of gold nanoparticles decorated with grafted chains of poly(*n*-butylacrylate) spin-coated onto mica. a) Deposition from chloroform and b) from THF solution. The gold cores are depicted by the white protrusions in the SPM images; the polymer chains are shown in gray. The micrographs clearly demonstrate that the polymer chains are bound to the gold cores, which

confirms the success of the ATRSIP. Figure 9.33 b) also shows that different numbers of chains of various lengths are attached to the gold particles (Reprinted with permission from: [322] S. Nuß, H. Böttcher, H. Wurm, M. L. Hallensleben, *Angew. Chem.* **2001**, *113*, 4137–4139; *Angew. Chem. Int. Ed.* **2001**, *40*, 4016–4018. © Copyright 2001 Wiley-VCH).

monomers, cross-linked or hyperbranched surface coatings can be prepared in a defined fashion. Figures 9.34 and 9.35 depicting two recent examples from Müller *et al.* [315] and Bruening *et al.* [321] using functional monomers for the preparation of branched or cross-linked polymer coating by means of ATRSIP on gold substrates.

ATRSIP is probably the most suitable SIP technique to prepare defined di- or triblock copolymers by successive monomer addition. This has been demonstrated in a very early paper by Matyjaszewski *et al.* [278]. Analog to the already mentioned work from Brittain *et al.*, forming diblocks by cross-over LCSIP and ATRSIP, di- [316, 330] and ABA- [318] and ABC [324] triblock copolymers could be prepared by ATRSIP alone. Again the dynamic responds (segregation, surface reconstruction) upon treatments with selective solvents in terms of surface topography and wetting behavior was investigated using various techniques including SPM.

ATRSIP was also used to amplify surface patterns, created by the  $\mu$ CP of SAMs. Shah *et al.* [319] stamped *n*-hexadecane thiol (HDT) onto planar gold substrates

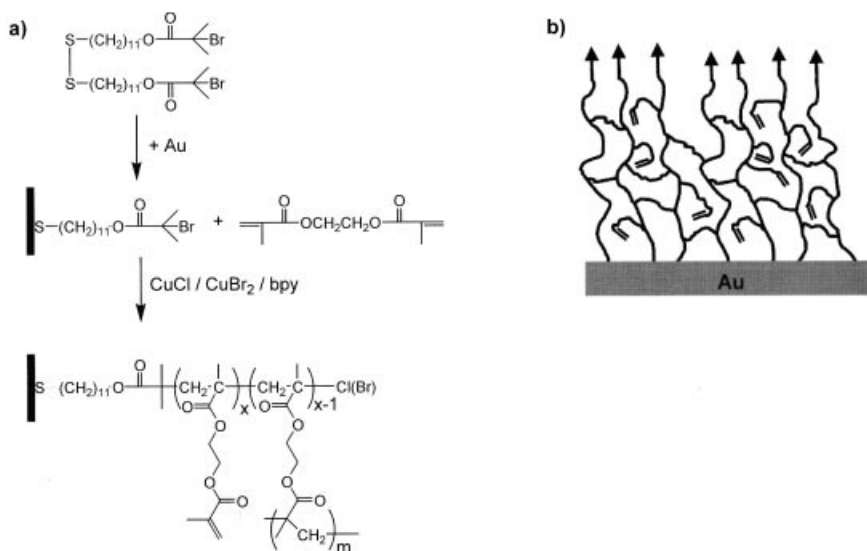


**Fig. 9.34** a) Synthetic outline for the preparation of cross-linked, ultrathin poly(ethylene glycol dimethacrylate) films on gold surfaces.

b) Schematic illustration of a cross-linked film growing from a gold substrate (modified from ref. [321]).

and filled the remaining bare surface with a SAM bearing a tertiary  $\alpha$ -bromoester function. Locally confined ATRISIP of five different monomers resulted in patterned polymer brushes as depicted in Fig. 9.36. The additional polymer brush layer enhanced the etch resistance of the covered areas. The amplified structures were investigated by XPS, wetting experiments and SPM.

### 9.3.5

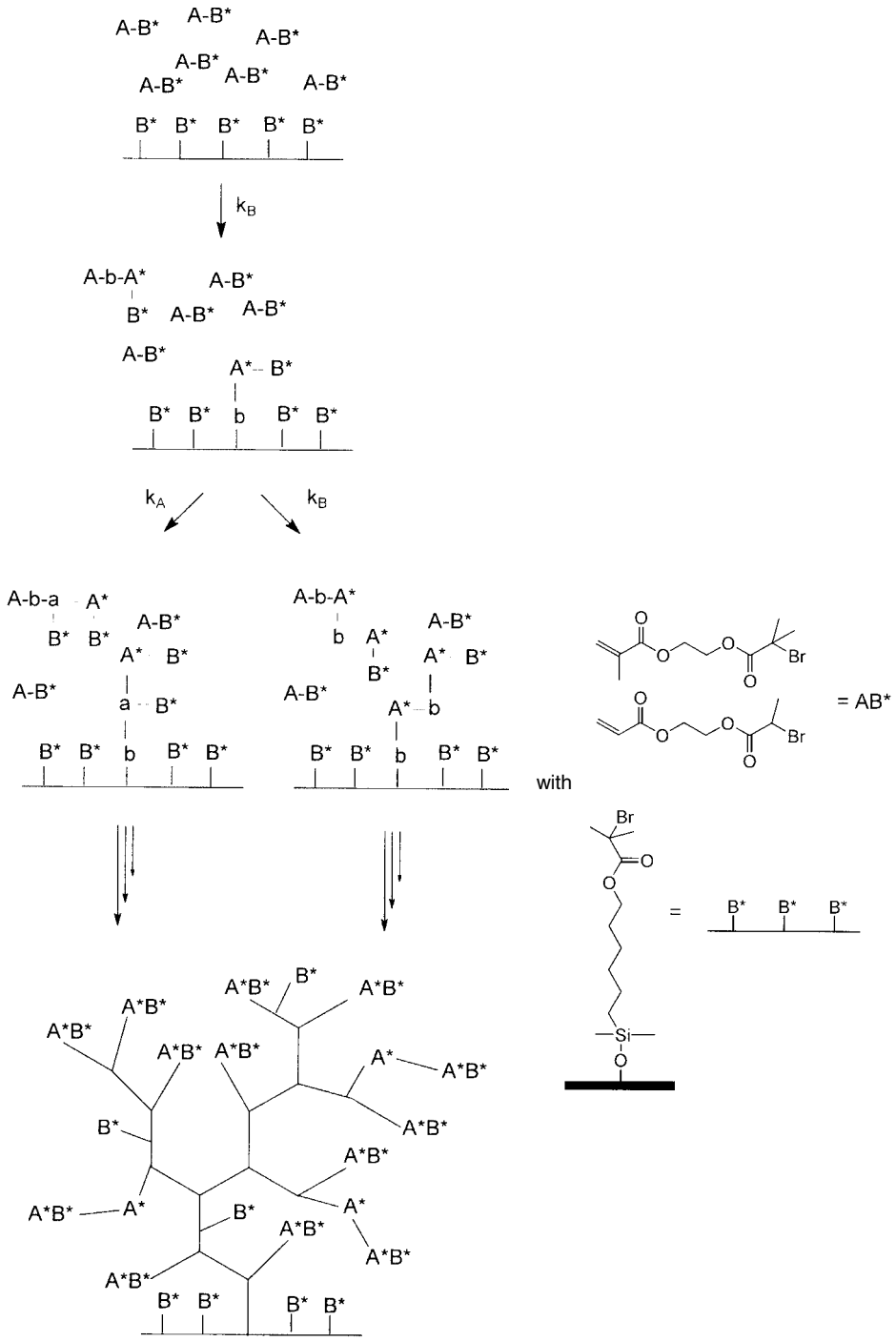
#### Surface-initiated Polymerization by Miscellaneous Techniques

Besides the polymerization techniques discussed above, other polymerization methods have been used for the preparation of surface grafts. Recently, ring-opening metathesis polymerization (ROMP) became popular. This polymerization type will be discussed by Buchmeiser in Chapter 8. Recently, interesting accounts have appeared on solventless polymerization techniques applying (living) ROMP on surfaces to prepare structured brush surfaces of conjugated polymers [331, 332].

Tsubokawa *et al.* [196, 333] and Hamann *et al.* [207, 334, 335] pioneered the SIP of *N*-carboxyanhydrides (NCA) on carbon black and colloidal silica and Schouten *et al.*

**Fig. 9.35** Schematic illustration of the 'self-condensing vinyl polymerization' ATRISIP on planar silica substrates resulting in hyperbranched surface-bonded polymer layers.

(Reprinted with permission from: [315] H. Mori, A. Böker, G. Krausch, *et al.*, *Macromolecules* **2001**, *34*, 6871–6882. © Copyright 2001 American Chemical Society).



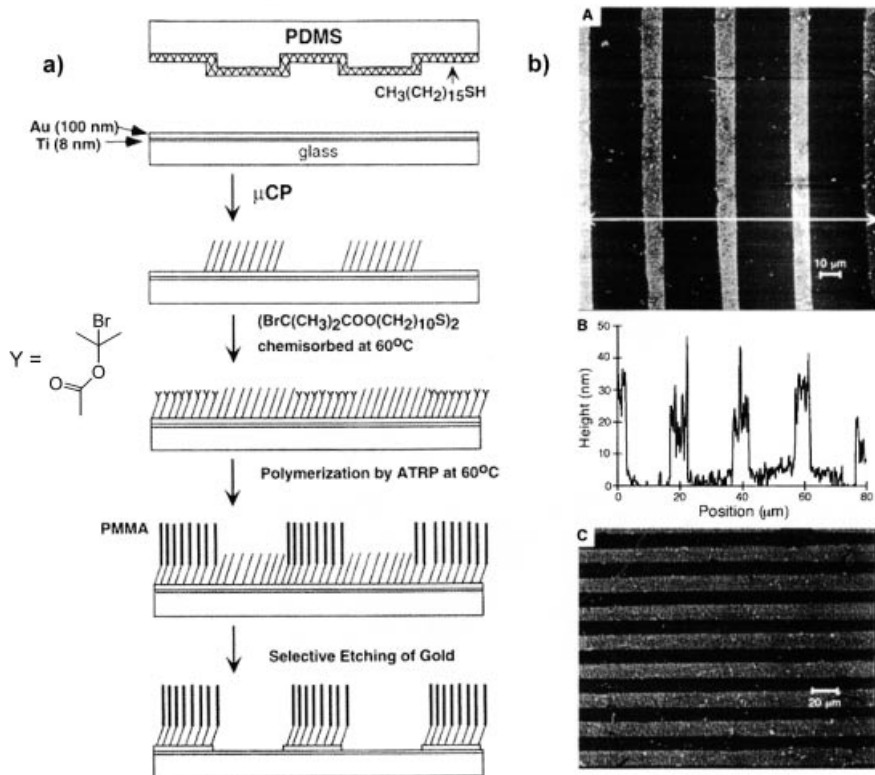


**Fig. 9.36** a) Procedure of the preparation steps starting with the  $\mu\text{CP}$  of an inert SAM, self-assembly of a monolayer of initiator sites, ATRP and selective wet etching. b) (A) AFM image of a patterned brush of PMMA formed by this procedure. The bright areas correspond to the patterned areas of SAMs formed from HDT. (B) Cross-sectional profile of the patterned PMMA brush shown in (A). The location of the cross-sectional pro-

file is marked in (A) by the double-headed arrow. (C) Optical image of a patterned brush of PMMA after immersion into aqueous  $\text{KI}/\text{I}_2$  for 60 s. The dark areas of the image are gold protected by the PMMA brush, and the light regions correspond to the supporting glass substrate. (Reprinted with permission from: [319] R.R. Shah, D. Merreceyes, M. Husemann, *et al.*, *Macromolecules* **2000**, *33*, 597–605. © Copyright 2000 American Chemical Society).

[336–338] successfully performed SIP of NCA on planar glass surfaces. The polymerization of NCA is initiated by surface-bonded primary amino groups and results in polypeptides (polyglutamates, polyasparates). The intriguing aspect of the surface-bonded polypeptides is the expected biocompatibility of such surfaces and potential control in biomineralization. Additionally, the predefined ( $\alpha$ )-helical conformation stabilized by hydrogen bonding makes the polymers rather rigid. A terminal attachment of the polymer results in rigid polymer 'brushes' with a high total dipole moment oriented along the axis of the  $\alpha$ -helix of the polypeptide chain. The impact of the molecular orientation of the rigid polypeptides upon the total dipole moment of

the entire polymer layer as a function of the grafting density and hence, the average orientation of the helices with respect to the surface has been investigated by Frank *et al.* [339, 340], using different deposition techniques including SIP.

Braun *et al.* [341] investigated the molecular dynamics of the rigid polypeptide brush by means of dielectric spectroscopy and prepared patterned brushes by SIP from  $\mu$ CP SAM initiators [342].

Whitesell and coworkers reported the preparation of highly organized helical peptide layers of thickness up to 200 nm [343, 344]. The major drawback of this system is a relatively high surface roughness and considerably broad molecular weight distribution. Solutions to this problem, like enzymatic digestion of the exposed helices were demonstrated [345], but it appears that the high rigidity of the brush and the polymerization mechanism itself offer no readily available options for improvement. Indeed, results regarding the grafting densities or layer thickness as reported by Whitesell *et al.* could not be reproduced by other researchers.

Surface-initiated ring-opening polymerization of  $\epsilon$ -caprolactone on  $\mu$ CP SAM initiators equipped with an oligo-ethylenoxide function is reported by Hawker *et al.* [346]. Choi and Langer used a similar SAM initiator system to polymerize L-lactide [347].

Group transfer polymerization was employed by Hertler and coworkers [348] as well as Huber *et al.* [349].

With the development of enzymatic polymerization in solution, also first accounts for SIP appeared. Loos *et al.* [350] reported on enzymatic surface polymerization of glucose-1-phosphate with potato phosphorylase as the catalyst resulting in oligo- or poly-( $\alpha$ ,1 $\rightarrow$ 4)-D-glucopyranose. As 'initiator' sites, immobilized maltoheptaose was used. Enzymatic grafting of hexyloxyphenol onto chitosan is reported by Payne and coworkers [351].

Finally, hyperbranched polymer layers by surface-initiated step polymerization was intensively studied mainly by Bergbreiter *et al.* and Crooks *et al.* Patterned surfaces were prepared on the micrometer scale and a variety of functional groups introduced interesting optical, electrochemical, biological, and mechanical properties into the films. For a recent review on surface-initiated step polymerization resulting in branched polymer layers see [352].

## 9.4

### Summary and Outlook

The preparation and properties of well-defined surface coatings, self-assembled monolayers and polymer brushes have been discussed. The approach in coating technology developed from a mere addition of surface functionalities, to the programmed assembly of molecules to form organic layers with controlled morphology on the molecular level and with designed functionality. Such layers are now used as a technology platform in all areas of surface science including catalysis. One serious drawback of SAMs, the stability, could be improved by the introduction of new SAM/substrate systems as well as the introduction of suitable mesogens. This makes the use of SAMs for the study of technologically relevant catalytic systems realistic.

The same applies to polymer brushes. The use of SAMs as initiator systems for surface-initiated polymerization results in defined polymer brushes of known composition and morphology. The different polymerization techniques, from free radical to living ionic polymerizations and especially the recently developed controlled radical polymerization allows reproducible synthesis of strictly linear, hyperbranched, dendritic or cross-linked polymer layer structures on solids. The added flexibility and functionality results in robust grafted supports with higher capacity and improved accessibility of surface functions. The collective and fast response of such layers could be used for the design of polymer-bonded catalytic systems with controllable activity.

Besides homogeneous and uniform SAMs or polymer brushes, systems of tailored heterogeneity such as mixed monolayers of two or more compounds, gradients, block copolymer brushes etc. are now under investigation. Especially, the development of patterned surfaces offers the exciting possibility to perform multiple parallel experiments on a single substrate or cascade reactions.

Presently, specific immobilization of various enzymes is studied under the aspect of the orientation and the local surface environments. The deeper understanding of biocatalytic systems together with suitable surface coating techniques may lead to biologically inspired and more complex catalytic systems grafted on solid supports.

## 9.5

### References

- 1 A. ULMAN, *Chem. Rev.* **1996**, *96*, 1533–1554.
- 2 General reviews on SAMs see: a) C. D. BAIN, G. M. WHITESIDES, *Angew. Chem.* **1989**, *101*, 522–528; *Angew. Chem. Int. Ed.* **1989**, *28*, 506–512. b) G. M. WHITESIDES, P. E. LAIBINIS, *Langmuir* **1990**, *6*, 87–96. c) J. D. SWALEN, *Annu. Rev. Mater. Sci.* **1991**, *21*, 373–408. d) L. H. DUBOIS, R. G. NUZZO, *Annu. Rev. Phys. Chem.* **1992**, *43*, 437–463.
- 3 Recent reviews on SAMs: a) J. XU, H.-L. LI, *J. Colloid Interface Sci.* **1995**, *176*, 138–149. b) A. ULMAN, *MRS Bull.* **1995**, *30*, 46–49. c) A. R. BISHOP, R. G. NUZZO, *Curr. Opin. Colloid Interface Sci.* **1996**, *1*, 127–136. d) E. DELAMARCHE, B. MICHEL, H. A. BIEBUYCK, *et al.*, *Adv. Mater.* **1996**, *8*, 719–729.
- 4 F. SCHREIBER, *Prog. Surf. Sci.* **2000**, *65*, 151–256.
- 5 A. ULMAN, *Introduction to Thin Organic Films: From Langmuir-Blodgett to Self-Assembly*, Academic Press, Boston, **1991**.
- 6 Y. XIA, G. M. WHITESIDES, *Angew. Chem.* **1998**, *110*, 568–594; *Angew. Chem. Int. Ed.* **1998**, *37*, 550–575.
- 7 a) P. FENTER, A. EBERHARDT, P. EISENBERGER, *Science* **1994**, *266*, 1216–1218. b) E. DELAMARCHE, B. MICHEL, H. KANG, *et al.*, *Langmuir* **1994**, *10*, 4103–4108. c) S. V. ATRE, B. LIEBERG, D. L. ALLARA, *Langmuir* **1995**, *11*, 3882–3893. d) P. WAGNER, M. HEGNER, H.-J. GÜNTHERODT, *et al.*, *Langmuir* **1995**, *11*, 3867–3875.
- 8 E. SABATINI, J. COHEN-BOULAKIA, M. BRUENING, *et al.*, *Langmuir* **1993**, *9*, 2974–2981.
- 9 J. M. TOUR, L. JONES II, D. L. PEARSON, *J. Am. Chem. Soc.* **1995**, *117*, 9529–9534.
- 10 J. F. KANG, A. ULMAN, S. LIAO, *et al.*, *Langmuir* **2001**, *17*, 95–106.
- 11 A. ULMAN, J. F. KANG, Y. SHNIDMAN, *et al.*, *Reviews in Molecular Biotechnology* **2000**, *74*, 175–188.
- 12 A. ULMAN, *Acc. Chem. Res.* **2001**, *34*, 855–863.



- 13 a) H. A. BIEBUYCK, G. M. WHITESIDES, *Langmuir* **1994**, *10*, 1825–1831. b) H. SCHÖNHERR, H. RINGSDORF, *Langmuir* **1996**, *12*, 3891–3897.
- 14 E. B. THROUGHTON, C. D. BAIN, G. M. WHITESIDES, *et al.*, *Langmuir* **1988**, *4*, 365–385.
- 15 J. E. CHADWICK, D. C. MYLES, R. L. GARRELL, *J. Am. Chem. Soc.* **1993**, *115*, 10364–10365.
- 16 K. UVDAL, I. PERSSON, B. LIEDBERG, *Langmuir* **1995**, *11*, 1252–1256.
- 17 a) P. FENTER, P. EISENBERGER, J. LI, *et al.*, *Langmuir* **1991**, *7*, 2013–2016. b) A. DHIRANI, M. A. HINES, A. J. FISHER, *et al.*, *Langmuir* **1995**, *11*, 2609–2614.
- 18 a) H. KELLER, P. SIMAK, W. SCHREPP, *et al.*, *Thin Solid Films* **1994**, *244*, 799–805. b) M. Itoh, K. Nishihara, K. Aramaki, *J. Electrochem. Soc.* **1995**, *142*, 3696–3703. c) J. B. SCHLENOFF, M. LI, H. LY, *J. Am. Chem. Soc.* **1995**, *117*, 12528–12536.
- 19 T. R. LEE, P. E. LAIBINIS, J. P. FOLKERS, *et al.*, *Pure Appl. Chem.* **1991**, *63*, 821–828.
- 20 J. J. HICKMAN, P. E. LAIBINIS, D. I. AUERBACH, *et al.*, *Langmuir* **1992**, *8*, 357–359.
- 21 B. BASSETTI, V. BENZA, P. JONA, *J. Phys. (France)* **1990**, 259–275.
- 22 See for example: a) C. W. SHEEN, J.-X. SHI, J. MAARTENSSON, *et al.*, *J. Am. Chem. Soc.* **1992**, *114*, 1514–1515. b) C. D. BAIN, *Adv. Mater.* **1992**, *4*, 591–594. c) J. F. DORSTEN, J. E. MASLAR, P. W. BOHN, *Appl. Phys. Lett.* **1995**, *66*, 1755–1757. d) K. ADELKOFER, M. TANAKA, *Langmuir* **2001**, *17*, 4267–4273. e) C. KIRCHNER, M. GEORGE, B. STEIN, *et al.*, *Adv. Funct. Mater.* **2002**, *12*, 266–276.
- 23 G. ASHKENASY, D. CAHEN, R. COHEN, *et al.*, *Acc. Chem. Res.* **2002**, *35*, 121–128.
- 24 Y. GU, Z. LIN, R. A. BUTERA, *et al.*, *Langmuir* **1995**, *11*, 1849–1851.
- 25 a) M. J. WIRTH, R. W. P. FAIRBANK, H. O. FATUNMBI, *Science* **1997**, *275*, 44–47. b) J. B. BRZOSKA, I. B. AZOUZ, F. RONDELEZ, *Langmuir* **1994**, *10*, 4367–4373. c) D. L. ALLARA, A. N. PARIKH, F. RONDELEZ, *Langmuir* **1995**, *11*, 2357–2360.
- 26 M. R. LINFORD, C. E. D. CHIDSEY, *J. Am. Chem. Soc.* **1993**, *115*, 12631–12632.
- 27 a) ref. 26. b) M. R. LINFORD, P. FENTER, P. M. EISENBERGER, *et al.*, *J. Am. Chem. Soc.* **1995**, *117*, 3145–3155. c) J. TERRY, M. R. LINFORD, C. WIGREN, *et al.*, *Appl. Phys. Lett.* **1997**, *71*, 1056–1058.
- 28 A. BANSAL, X. LI, I. LAUERMANN, *et al.*, *J. Am. Chem. Soc.* **1996**, *118*, 7225–7226.
- 29 a) D. L. ALLARA, R. G. NUZZO, *Langmuir* **1985**, *1*, 52–66. b) P. E. LAIBINIS, J. J. HICKINAN, M. S. WRIGHTON, *et al.*, *Science* **1989**, *245*, 845–847. c) Y.-T. TAO, M.-T. LEE, S.-C. CHANG, *J. Am. Chem. Soc.* **1993**, *115*, 9547–9555.
- 30 J. P. FOLKERS, C. B. GORMAN, P. E. LAIBINIS, *et al.*, *Langmuir* **1995**, *11*, 813–824.
- 31 a) G. CAO, H.-G. HONG, T. E. MALLOUK, *Acc. Chem. Res.* **1992**, *25*, 420–427. b) M. E. THOMPSON, *Chem. Mater.* **1994**, *6*, 1168–1175. c) H. E. KATZ, *Chem. Mater.* **1994**, *6*, 2227–2232. d) H. LEE, L. J. KEPPEY, H.-G. HONG, *et al.*, *J. Am. Chem. Soc.* **1988**, *110*, 618–620. e) M. L. SCHILLING, H. E. KATZ, S. M. STEIN, *et al.*, *Langmuir* **1993**, *9*, 2156–2160. f) H. E. KATZ, M. L. SCHILLING, S. B. UNGASHSE, *et al.* in: *Supermolecular Architecture*; (T. BEIN, ed.); ACS Symposium Series 499; American Chemical Society: Washington, DC, **1992**, 24. g) H. E. KATZ, M. L. SCHILLING, C. E. D. CHIDSEY, *et al.*, *Chem. Mater.* **1991**, *3*, 699–703. h) S. B. UNGASHSE, W. L. WILSON, H. E. KATZ, *et al.*, *J. Am. Chem. Soc.* **1992**, *114*, 8717–8719. i) H. E. KATZ, G. SCHELLER, T. M. PUTVINSKI, *et al.*, *Science* **1991**, *254*, 1485–1487.
- 32 T. J. GARDNER, C. D. FRISBIE, M. S. WRIGHTON, *J. Am. Chem. Soc.* **1995**, *117*, 6927–6933.
- 33 D. K. SCHWARZ, *Annu. Rev. Phys. Chem.* **2001**, *52*, 107–137.
- 34 H. SELLERS, A. ULMAN, Y. SHNIDMAN, *et al.*, *J. Am. Chem. Soc.* **1993**, *115*, 9389–9401.
- 35 C. A. WIDRIG, C. A. ALVES, M. D. PORTER, *J. Am. Chem. Soc.* **1991**, *113*, 2805–2810.
- 36 L. STRONG, G. M. WHITESIDES, *Langmuir* **1988**, *4*, 546–558.
- 37 C. E. D. CHIDSEY, D. N. LOIACONO, *Langmuir* **1990**, *6*, 682–691.
- 38 R. G. NUZZO, E. M. KORENIC, L. H. DUBOIS, *J. Chem. Phys.* **1990**, *93*, 767–773.
- 39 N. CAMILLONE III, C. E. D. CHIDSEY, G.-Y. LIU, *et al.*, *J. Chem. Phys.* **1993**, *98*, 3503–3511.
- 40 P. FENTER, P. EISENBERGER, *Phys. Rev. Lett.* **1993**, *70*, 2447–2450.

- 41 P. FENTER, A. EBERHARDT, P. EISENBERGER, *Science*, **1994**, 266, 1216–1218.
- 42 M. S. YEGANEH, S. M. DOUGAL, R. S. POLLIZZOTTI, *et al.*, *Phys. Rev. Lett.* **1995**, 74, 1811–1814.
- 43 R. HEINZ, J. P. RABE, *Langmuir* **1995**, 11, 506–511.
- 44 H. RIELEY, G. K. KENDALL, R. G. JONES, *et al.*, *Langmuir* **1999**, 15, 8856–8866.
- 45 K. K. UNGER, C. DU FRESNE VON HOHENESCHE, R. DITZ, *Gas and Liquid Chromatography* in: *Handbook of Porous Solids* (F. SCHÜTH, K. SING, J. WEITKAMP; eds.) Wiley-VCH, Weinheim **2002**, 2623–2699.
- 46 J. SAGIV, *J. Am. Chem. Soc.* **1980**, 102, 92–98.
- 47 E. F. VANSANT, P. VAN DER VOORT, K. C. VRANCKEN, *Characterization and Chemical Modification of the Silica Surface*, in: *Studies in Surface Science and Catalysis*, 93, Elsevier, Amsterdam, **1995**.
- 48 K. K. UNGER, *Porous Silica*, Elsevier, Amsterdam, **1979**.
- 49 J. KÖHLER, J. J. KIRKLAND, *J. Chromatogr.* **1987**, 385, 125–150.
- 50 W. KERN, D. A. PUOTINEN, *RCA Review* **1970**, 31, 187–189.
- 51 R. JORDAN, K. GRAF, H. RIEGLER, K. K. UNGER, *Chem. Commun.* **1996**, 1025–1026.
- 52 L. C. SANDER, S. A. WISE, *J. Chromatogr.* **1984**, 316, 163–181.
- 53 I. HALLER, *J. Am. Chem. Soc.* **1978**, 100, 8050–8055.
- 54 K. D. LORK, K. K. UNGER, J. N. KINKEL, *J. Chromatogr.* **1986**, 352, 199–221.
- 55 K. ALBERT, E. BAYER, *J. Chromatogr.* **1991**, 544, 345–370.
- 56 J. N. KINKEL, K. K. UNGER, *J. Chromatogr.* **1984**, 316, 193–200.
- 57 M. J. WIRTH, H. O. FATUNMBI, in: *Chemically Modified Surfaces* (J. J. PESEK, I. E. LEIGH; eds.), Royal Society of Chemistry, Cambridge, UK, **1994**, 203–209.
- 58 J. D. LE GRANDE, J. L. MARKHAM, C. R. KURKJIAN, *Langmuir* **1993**, 9, 1746–1753.
- 59 P. SILBERZAHN, L. LÉGER, D. AUSSERRÉ, *et al.*, *Langmuir* **1991**, 7, 1647–1651.
- 60 M. J. STEVENS, *Langmuir* **1999**, 15, 2773–2778.
- 61 D. L. ALLARA, in *Polymer Surfaces and Interfaces*, 2, (W. J. FEAST, H. S. MUNRO, R. W. RICHARDS, eds.) Wiley, Chichester, **1993**, 27–46.
- 62 A. ULMAN, S. D. EVANS, Y. SHNIDMAN, *et al.*, *J. Am. Chem. Soc.* **1991**, 113, 1499–1506.
- 63 A. JARZEBINSKA, R. ROWINSKI, I. ZAWISZA, *et al.*, *Anal. Chim. Acta* **1999**, 396, 1–12.
- 64 a) C. E. D. CHIDSEY, *Science* **1991**, 251, 919–922. b) H. O. FINKLEA, D. D. HAN-SHEW, *J. Am. Chem. Soc.* **1992**, 114, 3173–3181. c) G. K. ROWE, S. E. CREAGER, *Langmuir* **1991**, 7, 2307–2312.
- 65 a) M. MRKSICH, J. R. GRUNWELL, G. M. WHITESIDES, *J. Am. Chem. Soc.* **1995**, 117, 12009–12010. b) K. MOTESHAREI, D. C. MYLES, *J. Am. Chem. Soc.* **1994**, 116, 7413–7414. c) J. SPINKE, M. LILEY, H.-J. GUDER, *et al.*, *Langmuir* **1993**, 9, 1821–1825.
- 66 a) M. MRKSICH, G. M. WHITESIDES, *Annu. Rev. Biophys. Biomol. Struct.* **1996**, 25, 55–78. b) M. N. YOUSAF, M. MRKSICH, *J. Am. Chem. Soc.* **1999**, 121, 4286–4287.
- 67 a) C. D. TIDWELL, S. I. ERTEL, B. D. RATNER, *et al.*, *Langmuir* **1997**, 13, 3404–3413. b) C. S. CHEN, M. MRKSICH, S. HUANG, *et al.*, D. E. Ingber, *Biotech. Progr.* **1998**, 14, 356–363. c) B. T. HOUSEMAN, M. MRKSICH, *J. Org. Chem.* **1998**, 63, 7552–7555.
- 68 J. ZACCARO, J. F. KANG, A. ULMAN, *et al.*, *Langmuir* **2000**, 16, 3791–3796.
- 69 S. KIM, G. Y. CHOI, A. ULMAN, *et al.*, *Langmuir* **1997**, 13, 6650–6856.
- 70 A. R. BISHOP, R. G. NUZZO, *Curr. Opin. Colloid Interface Sci.* **1996**, 1, 127–136.
- 71 L. BERTILSSON, B. LIEDBERG, *Langmuir* **1993**, 9, 141–149.
- 72 A. ULMAN, S. D. EVANS, Y. SHNIDMAN, *et al.*, *Adv. Colloid Interface Sci.* **1992**, 39, 175–224.
- 73 a) B. LIEDBERG, P. TENGVALL, *Langmuir* **1995**, 11, 3821–3827. b) B. LIEDBERG, M. WIRDE, Y.-T. TAO, *et al.*, *Langmuir* **1997**, 13, 5329–5334.
- 74 H. ZIMMERMANN, A. LINDGREN, W. L. SCHUHMAN, *et al.*, *Chem. Eur. J.* **2000**, 6, 592–599.
- 75 J. MADDOZ-GRPIDE, J. M. ABAD, J. FERNÁNDEZ-RECIO, *et al.*, *J. Am. Chem. Soc.* **2000**, 122, 9808–9817.

- 76 F. W. SCHELLER, U. WOLLENBERGER, C. LEI, *et al.*, *Rev. Mol. Biotechnology* **2002**, *82*, 411–424.
- 77 I. O. BENITEZ, B. BUJOLI, L. J. CAMUS, *et al.*, *J. Am. Chem. Soc.* **2002**, *124*, 4363–4370.
- 78 K. TÖLLNER, R. POPOVITZ-BIRO, M. LAHAV, *et al.*, *Science* **1997**, *278*, 2100.
- 79 C. D. BAIN, E. B. TROUGHTON, Y.-T. TAO, *et al.*, *J. Am. Chem. Soc.* **1989**, *111*, 321–335.
- 80 P. E. LAIBINIS, G. M. WHITESIDES *J. Am. Chem. Soc.* **1992**, *114*, 1990–1995.
- 81 T. H. ONG, R. N. WARD, P. B. DAVIES, *et al.*, *J. Am. Chem. Soc.* **1992**, *114*, 6243–6245.
- 82 S. D. EVANS, R. SHARMA, A. ULMAN, *Langmuir* **1991**, *7*, 156–161.
- 83 a) N. KACKER, S. K. KUMAR, D. L. ALLARA, *Langmuir* **1997**, *13*, 6366–6369. b) J. HAUTMAN, M. L. KLEIN, *Phys. Rev. Lett.* **1991**, *67*, 1763–1766. c) J. HAUTMAN, J. P. BAREMAN, W. MAR, *et al.*, *J. Chem. Soc. Faraday Trans.* **1991**, *87*, 2031–2037.
- 84 J. I. SIEPMANN, I. R. McDONALD, *Phys. Rev. Lett.* **1993**, *70*, 453–456.
- 85 a) J. GENZER, K. EFIMENKO, *Science* **2000**, *290*, 2130–2133. b) J. Genzer, E. SIVANIAH, E. J. KRAMER, *et al.*, *Langmuir* **2000**, *16*, 1993–1997. c) J. GENZER, E. SIVANIAH, E. J. KRAMER, *et al.*, *Macromolecules* **2000**, *33*, 1882–1887.
- 86 a) Y.-T. KIM, R. L. MCCARLEY, A. J. BARD, *J. Phys. Chem.* **1992**, *96*, 7416–7421. b) Y. S. OBENG, M. E. LAING, A. C. FRIEDLI, *et al.*, *J. Am. Chem. Soc.* **1992**, *114*, 9943–9953.
- 87 E. SABATANI, J. COHEN-BOULAKIA, M. BRUENING, *et al.*, *Langmuir* **1993**, *9*, 2974–2981.
- 88 a) A.-A. DHIRANI, R. W. ZEHNER, R. P. HSUNG, *et al.*, *J. Am. Chem. Soc.* **1996**, *118*, 3319–3320. b) R. W. ZEHNER, L. R. SITA, *Langmuir* **1997**, *13*, 2973–2979. c) R. W. ZEHNER, B. F. PEARSON, R. P. HSUNG, L. R. SITA, *Langmuir* **1999**, *15*, 1121–1127.
- 89 S. B. SACHS, S. P. DUDEK, C. E. D. CHIDSEY, *J. Am. Chem. Soc.* **1997**, *119*, 10563–10564.
- 90 S. C. CHANG, I. CHAO, Y. T. TAO, *J. Am. Chem. Soc.* **1994**, *116*, 6792–6805.
- 91 Y. T. TAO, C. C. WU, J. Y. EU, *et al.*, *Langmuir* **1997**, *13*, 4018–4023.
- 92 R. P. SCARINGE, IN: *Electron Crystallography of Organic Molecules* (J. R. FRYER, D. L. DORSET, eds.), Kluwer, Dordrecht, **1990**.
- 93 C. Y. YOUNG, R. PINDAK, N. A. CLARK, *et al.*, *Phys. Rev. Lett.* **1978**, *40*, 773–776.
- 94 A. ULMAN, R. SCARINGE, *Langmuir* **1992**, *8*, 894–897.
- 95 T. Y. B. LEUNG, P. V. SCHWARTZ, G. SCOLES, *et al.*, *Surf. Sci.* **2000**, *458*, 34–52.
- 96 J. F. KANG, S. LIAO, R. JORDAN, *et al.*, *J. Am. Chem. Soc.* **1998**, *120*, 9662–9667.
- 97 J. F. KANG, R. JORDAN, A. ULMAN, *Langmuir* **1998**, *14*, 3983–3985.
- 98 J. F. KANG, A. ULMAN, S. LIAO, *et al.*, *Langmuir* **1999**, *15*, 2095–2098.
- 99 J. F. KANG, A. ULMAN, R. JORDAN, *et al.*, *Langmuir* **1999**, *15*, 5555–5559.
- 100 S. FREY, V. STADLER, K. HEISTER, *et al.*, *Langmuir* **2001**, *17*, 2408–2415.
- 101 M. ZARNIKOV, M. GRUNZE, *J. Phys.: Condens. Mater.* **2001**, *13*, 11333–11365 and references therein.
- 102 a) G. J. KLUTH, M. M. SUNG, R. MABOUDIAN, *Langmuir* **1997**, *13*, 3775–3780. b) G. J. KLUTH, M. SANDER, M. M. SUNG, *et al.*, *J. Vac. Sci. Technol. A* **1998**, *16*, 932–936.
- 103 M. CALISTRI-YEH, E. J. KRAMER, R. SHARMA, *et al.*, *Langmuir* **1996**, *12*, 2747–2755.
- 104 a) S. BAXTER, A. B. D. CASSIE, *Text- Ind.* **1945**, *36*, T35. b) A. B. D. CASSIE, S. BAXTER, *Trans. Faraday Soc.* **1944**, *40*, 546–552.
- 105 J. N. ISRAELACHVILI, M. L. GEE, *Langmuir* **1989**, *5*, 288–289.
- 106 S. WU, *Polymer Interfaces and Adhesion*, Marcel Dekker, New York **1982**.
- 107 M. P. SOMASHEKARAPPA, S. SAMPARATH *Chem. Commun.* **2002**, 1262–1263.
- 108 A. ULMAN (ed.) *Self-assembled Monolayers of Thiols, Thin Films*, Vol. 24, Academic Press, San Diego, **1998**, 1pp.
- 109 H. A. BIEBUYCK, G. M. WHITESIDES, *Langmuir* **1994**, *10*, 4581–4587.
- 110 N. B. LARSEN, H. BIEBUYCK, E. DELAMARCHE, *et al.*, *J. Am. Chem. Soc.* **1997**, *119*, 3017–3026.
- 111 H. SCHMID, B. MICHEL, *Macromolecules* **2000**, *33*, 3042–3049.
- 112 R. D. PINER, J. ZHU, F. XU, *et al.*, *Science* **1999**, *283*, 661–663.

- 113 S. HONG, J. ZHU, C.A. MIRKIN, *Science* **1999**, *286*, 523–525.
- 114 S. HONG, J. ZHU, C.A. MIRKIN, *Langmuir* **1999**, *15*, 7897–7900.
- 115 G.Y. LIU, S. XU, Y. QIAN, *Acc. Chem. Res.* **2000**, *33*, 457–466.
- 116 a) J.W. ZHAO, K. UOSAKI, *Langmuir* **2001**, *17*, 7784–7788. b) J.W. ZHAO, K. UOSAKI, *Nano Lett.* **2002**, *2*, 137–140.
- 117 C.A. MIRKIN, S. HONG, L. DEMERS, *CHEMPHYSICHEM* **2001**, *2*, 37–39.
- 118 M.J. LERCEL, H.G. CRAIGHEAD, A.N. PARIKH, *et al.*, *Appl. Phys. Lett.* **1996**, *68*, 1504–1506.
- 119 A. GÖLZHÄUSER, W. GEYER, V. STADLER, *et al.*, *J. Vac. Sci. Technol. B* **2000**, *18*, 3414–3418.
- 120 A. GÖLZHÄUSER, W. ECK, W. GEYER, *et al.*, *Adv. Mater.* **2001**, *13*, 806–809.
- 121 W. GEYER, V. STADLER, W. ECK, *et al.*, *J. Vac. Sci. Technol. B* **2001**, *19*, 2732–2735.
- 122 W. ECK, V. STADLER, W. GEYER, *et al.*, *Adv. Mater.* **2000**, *12*, 805–808.
- 123 G. WITTSTOCK, W. SCHUHMAN *Anal. Chem.* **1997**, *69*, 5059–5066.
- 124 C. BLACKLEDGE, D.A. ENGBERTSON, J.D. McDONALD *Langmuir* **2000**, *16*, 8317–8323.
- 125 V. CHECHIK, R.M. CROOKS, C.J.M. STIRLING, *Adv. Mater.* **2000**, *12*, 1161–1171.
- 126 see e.g. a) K.L. PRIME, G.M. WHITESIDES, *Science* **1991**, *252*, 1164–1167. b) L. HÄUSSLING, W. KNOLL, H. RINGSDORF, *et al.*, *Makromol. Chem. Macromol. Symp.* **1991**, *46*, 145–155. c) R. SINGHVI, A. KUMAR, G.P. LOPEZ, *et al.*, *Science* **1994**, *264*, 696–698. d) M.J. WIRTH, R.W.P. FAIRBANK, H.O. FATUNMBI, *Science* **1997**, *275*, 44–47. e) J. LAHIRI, L. ISAACS, B. GRZYBOWSKI, J.D. CARBECK, *et al.*, *Langmuir* **1999**, *15*, 7186–7198. f) N. HIGASHI, M. TAKAHASHI, M. NIWA, *Langmuir* **1999**, *15*, 111–115. g) R.M. NYQUIST, A.S. EBERHARDT, L.A. SILKS III, *et al.*, *Langmuir* **2000**, *16*, 1793–1800. h) L. HÄUSSLING, B. MICHEL, H. RINGSDORF, *et al.*, *Angew. Chem.* **1990**, *103*, 568–571; *Angew. Chem. Int. Ed.* **1991**, *30*, 569–572. i) C. ROBERTS, C.S. CHEN, M. MRKSICH, *et al.*, *J. Am. Chem. Soc.* **1998**, *120*, 6548–6555. j) D.D. SCHLERETH, R.P.H. KOOYMAN, *J. Electroanal. Chem.* **1998**, *444*, 231–240. k) J. LAHIRI, L. ISAACS, J. TIEN, *et al.*, *Anal. Chem.* **1999**, *71*, 777–790. l) B.T. HOUSEMAN, M. MRKSICH, *Angew. Chem.* **1999**, *111*, 876–880; *Angew. Chem. Int. Ed.* **1999**, *38*, 782–785.
- 127 a) T. IHARA, M. NAKAYAMA, M. MURATA, *et al.*, *Chem. Commun.* **1997**, 1609–1610. b) A. BARDEA, F. PATOLSKY, A. DAGAN, *et al.*, *Chem. Commun.* **1999**, 21–22. c) A.B. STEEL, T.M. HERNE, M.J. TARLOV, *Anal. Chem.* **1998**, *70*, 4670–4677. c) C. BERGGREN, G. JOHANSSON, *Anal. Chem.* **1997**, *69*, 3651–3657. d) R. BLONDER, E. KATZ, Y. COHEN, *et al.*, *Anal. Chem.* **1996**, *68*, 3151–3157. e) R. BLONDER, S. LEVI, G. TAO, *et al.*, *J. Am. Chem. Soc.* **1997**, *119*, 10467–10478.
- 128 W.T. MÜLLER, D.L. KLEIN, T. LEE, *et al.*, *Science* **1995**, *268*, 272–273.
- 129 M. SASTRY, M. RAO, K.N. GANESH, *Acc. Chem. Res.* **2002**, *35*, 847–855.
- 130 V.L. COVLIN, A.N. GOLDSTEIN, A.P. ALIVISATOS, *J. Am. Chem. Soc.* **1992**, *114*, 5221–5230.
- 131 P. GHOSH, M.L. AMIRPOUR, W.M. LACKOWSKI, *et al.*, *Angew. Chem.* **1999**, *111*, 1697–1700; *Angew. Chem. Int. Ed.* **1999**, *38*, 1592–1595.
- 132 M. MRKSICH, *Cell. Mol. Life Sci.* **1998**, *54*, 653–662.
- 133 S. FINK, F.C.J. VAN VEGGEL, D.N. REINHOUTD, *Adv. Mater.* **2000**, *12*, 1315–1328.
- 134 F. AUER, M. SCOTTI, A. ULMAN, *et al.*, *Langmuir* **2000**, *16*, 7554–7557.
- 135 a) B. SELLERGREN, A. SWIETLOW, T. ARNEBRANT, *et al.*, *Anal. Chem.* **1996**, *68*, 402–407. b) F. AUER, D.W. SCHUBERT, M. STAMM, *et al.*, B. SELLERGREN, *Chem. Eur. J.*, **1999**, *5*, 1150–1159.
- 136 S.J. GREEN, J.J. STOKES, M.J. HOSTETLER, *et al.*, *J. Phys. Chem.* **1997**, *101*, 2663–2668.
- 137 For an overview see: a) J.H. FENDLER (ed.) *Nanoparticles and Nanostructured Films*, Wiley-VCH, Weinheim, **1998**. b) Special Issue on “Nanostructured Materials: *Chem. Mater.* **1996**, *8*.
- 138 a) J. SCHMITT, G. DECHER, W.J. DRESICK, *et al.*, *Adv. Mater.* **1997**, *9*, 61–65. b) J. SCHMITT, P. MÄCHTLE, D. ECK, *et al.*, *Langmuir* **1999**, *15*, 3256–3266 and references therein. c) C.J. LOWETH, W.P. CALDWELL, X. PENG, *et al.*, *Angew. Chem.* **1999**, *111*, 1925–1929; *Angew. Chem. Int.*

- Ed. 1999, 38, 1808–1812. d) R. P. Andres, J. D. Bielefeld, J. I. Henderson, *et al.*, *Science* 1996, 273, 1690–1693.
- 139 S. CONNOLLY, D. FITZMAURICE, *Adv. Mater.* 1999, 11, 1202–1205.
- 140 For reviews on the different aspects refer to e.g.: a) J. BELLONI, *Curr. Opin. Colloid Interface Sci.* 1996, 2, 184. b) L. BRUST, *Curr. Opin. Colloid Interface Sci.* 1996, 2, 197. c) E. MATIJEVIĆ, *Curr. Opin. Colloid Interface Sci.* 1996, 1, 176–183. d) H. HABERLAND (ed.), *Clusters of atoms and molecules*; Springer-Verlag, New York, 1994. e) G. SCHMID (ed.), *Clusters and Colloids. From Theory to Applications*, VCH, New York, 1994. f) G. SCHMIDT, *Chem. Rev.* 1992, 92, 1709–1707. g) L. N. LEWIS, *Chem. Rev.* 1993, 93, 2693–2730. h) U. KREIBIG, M. VOLLMER (eds.), *Optical Properties of Metal Clusters*; Springer-Verlag, New York, 1995.
- 141 a) M. BRUST, M. WALKER, D. BETHELL, *et al.*, *J. Chem. Soc. Chem. Commun.* 1994, 801–802. b) M. BRUST, J. FINK, D. BETHELL, *et al.*, *J. Chem. Soc. Chem. Commun.* 1995, 1655–1656. c) M. BRUST, D. BETHELL, D. J. SCHIFFRIN, *et al.*, *J. Adv. Mater.* 1995, 7, 795–797. d) D. BETHELL, M. BRUST, D. J. SCHIFFRIN, *et al.*, *J. Electroanal. Chem.* 1996, 409, 137–143.
- 142 see e.g.: M. Y. BEREZIN, K.-T. WAN, R. M. FRIEDMAN, *et al.*, *J. Mol. Cat. A: Chem.* 2000, 158, 567–576.
- 143 H. LI, Y.-Y. LUK, M. MRKSICH, *Langmuir* 1999, 15, 4957–4959.
- 144 a) C. K. YEE, R. JORDAN, A. ULMAN, *et al.*, *Langmuir* 1999, 15, 3486–3491. b) C. K. YEE, M. SCOTTI, A. ULMAN, *et al.*, *J. Sokolov, Langmuir*; 1999; 15, 4314–4316.
- 145 a) M. J. HOSTELTER, S. J. GREEN, J. J. STOKES, *et al.*, *J. Am. Chem. Soc.* 1996, 118, 4212–4213. b) ref. 135 (d). c) R. S. INGRAM, M. J. HOSTELTER, R. W. MURRAY, *J. Am. Chem. Soc.* 1997, 119, 9175–9178.
- 146 A. BADIA, L. CUCCIA, L. DEMERS, *et al.*, *J. Am. Chem. Soc.* 1997, 119, 2682–2692.
- 147 L. MOTTE, M. P. PILENI, *J. Phys. Chem. B* 1998, 102, 4104–4109.
- 148 A. BADIA, W. GAO, S. SINGH, *et al.*, *Langmuir* 1996, 12, 1262–1269.
- 149 W. D. LUEDTKE, U. LANDMAN, *J. Phys. Chem.* 1996, 100, 13323–13329.
- 150 L. HÄUSSLING, W. KNOLL, H. RINGSORF, *et al.*, *Makromol. Chem., Macromol. Symp.* 1991, 46, 145–155.
- 151 a) J. SPINKE, J. YANG, H. WOLF, *et al.*, *Biophys. J.* 1992, 63, 1667–1671. b) C. ERDELEN, L. HÄUSSLING, R. NAUMANN, *et al.*, *Langmuir* 1994, 10, 1246–1250. c) N. BUNJES, E. K. SCHMIDT, A. JONCZYK, *et al.*, *Langmuir* 1997, 13, 6188–6194.
- 152 W. KNOLL, C. W. FRANK, C. HEIBEL, *et al.*, *Reviews in Molecular Biotechnology* 2000, 74, 137–158.
- 153 E. SACKMANN, *Science* 1996, 271, 43–48.
- 154 R. JORDAN, K. MARTIN, H. J. RÄDER, *et al.*, *Macromolecules* 2001, 34, 8858–8865.
- 155 R. JORDAN, K. GRAF, H. RIEGLER, in preparation.
- 156 a) A. FÖRTIG, R. JORDAN, O. PURRUCKER, *et al.*, *Polym. Preprints* 2003, in press. b) O. PURUCKER, M. TANAKA, A. FÖRTIG, *et al.*, submitted..
- 157 a) G. DECHER, *Science* 1997, 277, 1232–1237 and references therein. b) G. DECHER, J. D. HONG, *Ber. Bunsenges. Phys. Chem.* 1991, 95, 1430–1434.
- 158 I. C. SANCHEZ (ed.), *Physics of polymer surfaces and interfaces*, Butterworth-Heinemann, Boston, 1992.
- 159 a) M. VAN DER WAARDEN. *J. Colloid Sci.* 1950, 5, 317–325. b) M. VAN DER WAARDEN. *J. Colloid Sci.* 1951, 6, 443–443. c) E. L. MACKOR. *J. Colloid Sci.* 1951, 6, 492–495. d) E. L. MACKOR, J. H. VAN DER WAALS, *J. Colloid Sci.* 1952; 7, 535–550. e) E. J. CLAYFIELD, E. C. LUMB. *J. Colloid Interface Sci.* 1966, 22, 269. f) E. J. CLAYFIELD, E. C. LUMB. *J. Colloid Interface Sci.* 1966, 22, 285.
- 160 R. ISRAELS, F. A. M. LEERMAKERS, G. J. FLEER, *Macromolecules* 1995, 28, 1626–1642.
- 161 M. AMIJI, K. J. PARK. *Biomater Sci Polym Ed* 1993, 4, 217–221.
- 162 J.-F. JOANNY. *Langmuir* 1992, 8, 989–995.
- 163 M. HANSON, K. K. UNGER, *Trends Anal. Chem* 1992, 11, 368–373.
- 164 G. SCHOMBURG, *Trends Anal. Chem* 1991, 10, 163–169.
- 165 J. H. VAN ZANTEN, *Macromolecules* 1994, 27, 6797–6807.
- 166 L. CANALI, D. C. SHERRINGTON *Chem. Soc. Rev.* 1999, 28, 85–102.

- 167 D. ASTRUC, F. CHARDAC *Chem. Rev.* **2001**, *101*, 2991–3004.
- 168 a) E. B. ZHULINA, T. A. VILGIS, *Macromolecules* **1995**, *28*, 1008–1015. b) M. A. CARIGNANO, I. SZLEIFER, *Macromolecules* **1994**, *27*, 702–710.
- 169 a) C. F. LAUB, J. T. KOBERSTEIN, *Macromolecules* **1994**, *27*, 5016–5023. b) N. DAN, M. TIRRELL, *Macromolecules* **1993**, *26*, 6467–6473. c) E. KUMACHEVA, J. KLEIN, P. PINCUS, L. J. FETTERS, *Macromolecules* **1993**, *26*, 6477–6482.
- 170 S. T. MILNER, *Science* **1991**, *251*, 905–914.
- 171 P. PINCUS, *Macromolecules* **1991**, *24*, 2912–2919.
- 172 R. ISRAELS, F. A. M. LEERMAKERS, G. J. FLEER, *et al.*, *Macromolecules* **1994**, *27*, 3249–3261.
- 173 Y. ITO, Y. OCHIAI, Y. S. PARK, Y. IMANISHI, *J. Am. Chem. Soc.* **1997**, *119*, 1619–1623.
- 174 Y. G. TAKEI, T. AOKI, K. SANUI, *et al.*, *Macromolecules* **1994**, *27*, 6163–6166.
- 175 a) J. KLEIN, Y. KAMIYAMA, H. YOSHIKAWA *et al.*, *Macromolecules* **1993**, *26*, 5552–5560. b) D. R. M. WILLIAMS, *Macromolecules* **1993**, *26*, 5806–5098.
- 176 a) G. S. GREST, M. MURAT, *Macromolecules* **1993**, *26*, 3108–3117. b) Y. LIU, J. QUINN, M. H. RAFAILOVICH, *et al.*, *Macromolecules* **1995**, *28*, 6347–6348 and references therein.
- 177 Y. ITO, Y. S. PARK, Y. IMANISHI, *J. Am. Chem. Soc.* **1997**, *119*, 2739–2739.
- 178 Y. ITO, S. W. NISHI, Y. S. PARK, *et al.*, *Macromolecules* **1997**, *30*, 5856–5859.
- 179 a) S. I. JOEN, J. D. ANDRADE, *J. Colloid Interface Sci.* **1991**, *142*, 159–166. b) S. I. JEON, J. H. LEE, J. D. ANDRADE, *et al.*, *J. Colloid Interface Sci.* **1991**, *142*, 149–158.
- 180 a) S. ALEXANDER, *J. Phys. (Paris)* **1977**, *38*, 983–987. b) P.-G. DE GENNES IN *Solid state physics*, (SEITZ, TURNBULL; eds.), Academic Press, New York, **1978**.
- 181 a) P.-G. DE GENNES, *J. Phys. (Paris)* **1976**, *37*, 1445–1452. b) P. G. DE GENNES, *Macromolecules* **1980**, *13*, 1069–1075 and references therein.
- 182 S. T. MILNER, T. A. WITTEN, M. E. CATES, *Macromolecules* **1988**, *21*, 2610–2619.
- 183 a) M. A. CARIGNANO, I. SZLEIFER, *J. Chem. Phys.* **1993**, *98*, 5006–5018. b) M. A. CARIGNANO, I. SZLEIFER, *J. Chem. Phys.* **1994**, *100*, 3210–3223.
- 184 a) P.-Y. LAI, K. J. BINDER, *J. Chem. Phys.* **1991**, *95*, 9288–9299. b) P.-Y. LAI, K. J. BINDER, *J. Chem. Phys.* **1992**, *97*, 586–592 and references therein.
- 185 see e.g.: R. R. NETZ, M. SCHICK, *Macromolecules* **1998**, *31*, 5105–5122.
- 186 see e.g.: A. HALPERIN, M. TIRELL, T. P. LODGE, *Adv. Polym. Sci.* **1992**, *100*, 31–71 and references therein.
- 187 B. ZHAO, W. J. BRITAIN, *Prog. Polym. Sci.* **2000**, *25*, 677–710.
- 188 R. R. NETZ, D. ADELMANN IN: *Oxide Surfaces* (J. WINGRAVE, ed.), Marcel Dekker, New York **2001**.
- 189 R. ISRAELS, D. GERSAPPE, M. FASOLKA, *et al.*, *Macromolecules* **1994**, *27*, 6679–6682.
- 190 E. M. SEVICK, D. R. M. WILLIAMS, *Macromolecules* **1994**, *27*, 5285–5290.
- 191 a) N. DAN, M. TIRRELL, *Macromolecules* **1993**, *26*, 4310–4315. b) G. F. BELDER, G. TEN BRINKE, G. HADZIIOANNOU, *Langmuir* **1997**, *13*, 4102–4105 and references therein.
- 192 a) W. ZHAO, G. KRAUSCH, M. H. RAFAILOVICH, J. SOKOLOV, *Macromolecules* **1994**, *27*, 2933–2935.
- 193 a) J. R. DORGAN, M. STAMM, C. TOPRACIOGLU, *et al.*, *Macromolecules* **1993**, *26*, 5321–5330. b) J. C. DIJT, M. A. C. STUART, G. J. FLEER, *Macromolecules* **1994**, *27*, 3207–3218. c) J. C. DIJT, M. A. C. STUART, G. J. FLEER, *Macromolecules* **1994**, *27*, 3219–3229.
- 194 R. JORDAN, A. ULMAN, J. F. KANG, *et al.*, *J. Am. Chem. Soc.* **1999**, *121*, 1016–1022.
- 195 J. JAGUR-GRODZINSKI, *Prog. Polym. Sci.* **1992**, *17*, 361–415.
- 196 N. TSUBOKAWA, *Prog. Polym. Sci.* **1992**, *17*, 417–470 and references therein.
- 197 N. TSUBOKAWA, K. FUKJIKI, Y. SONE, *Polym. J.* **1988**, *20*, 213–220.
- 198 K. FUJIKI, N. TSUBOKAWA, Y. SONE, *Polym. J.* **1990**, *22*, 661–670.
- 199 K. FUJIKI, N. TSUBOKAWA, Y. SONE, *J. Macromol. Sci., Chem.* **1991**, *A28*, 715–731.
- 200 N. TSUBOKAWA, K. FUKJIKI, Y. SONE, *J. Polym. Sci., Polym. Chem. Ed.* **1986**, *24*, 191–194.

- 201 N. TSUBOKAWA, K. FUKJIKI, Y. SONE, *J. Macromol. Sci., Chem.* **1988**, A25, 1159–1171.
- 202 K. NOLLEN, V. KADEN, K. HAMANN, *Angew. Makromol. Chem.* **1969**, 6, 1–23.
- 203 N. FERY, R. HOENE, K. HAMANN, *Angew. Chem.* **1972**, 84, 359–360.
- 204 N. FERY, R. LAIBLE, K. HAMANN, *Angew. Makromol. Chem.* **1973**, 34, 81–109.
- 205 E. DIETZ, N. FERY, K. HAMANN, *Angew. Makromol. Chem.* **1974**, 35, 115–129.
- 206 R. LAIBLE, K. HAMANN, *Angew. Makromol. Chem.* **1975**, 48, 97–133.
- 207 R. LAIBLE, K. HAMANN, *Adv. Coll. Interface Sci.* **1980**, 13, 65–99.
- 208 N. TSUBOKAWA, K. MARUYAMA, Y. SONE, *et al.*, *Polym. J.* **1989**, 21, 475–481.
- 209 R. JANZEN, K. K. UNGER, W. MÜLLER, *et al.*, *J. Chromatogr.* **1990**, 522, 77–93.
- 210 W. MÜLLER, *J. Chromatogr.* **1990**, 510, 133–140.
- 211 W. MÜLLER, *Bioseparation* **1990**, 1, 265–282.
- 212 a) G. BOVEN, M. L. C. M. OOSTERLING, G. CHALLA, *et al.*, *Polymer*, **1990**, 31, 2377–2382. b) G. BOVEN, R. FOLKSMA, G. CHALLA, *et al.*, *Polym. Commun.* **1991**, 32, 50–53.
- 213 a) E. CARLIER, A. GUYOT, A. REVILLON, *et al.*, *React. Polym.* **1991**, 16, 41–49. b) E. CARLIER, A. GUYOT, A. REVILLON, *React. Polym.* **1991**, 16, 115–124.
- 214 A. SIDORENKO, S. MINKO, K. SCHENKMEUSER, *et al.*, *Langmuir* **1999**, 15, 8349–8355.
- 215 a) R. SCHMIDT, T. ZHAO, J.-B. GREEN, *et al.*, *Langmuir* **2002**, 18, 1281–1287. b) R. PAUL, R. SCHMIDT, J. FENG, *et al.*, *J. Polym. Sci. A: Polym. Chem.* **2002**, 40, 3284–3291.
- 216 B. PENG, D. JOHANNSMANN, J. RÜHE, *Macromolecules* **1999**, 32, 6759–6766.
- 217 D. H. JUNG, I. J. PARK, Y. K. CHOI, *et al.*, *Langmuir* **2002**, 18, 6133–6139.
- 218 J. RÜHE in: *Supramolecular Polymers* (A. CIFERRI, Ed.), Marcel Dekker, New York, **2000**, 565–613.
- 219 J. HYUN, A. CHILKOTI, *Macromolecules* **2001**, 34, 5644–5652.
- 220 L. K. ISTA, S. MENDEZ, V. H. PÉREZ-LUNA, *et al.*, *Langmuir* **2001**, 17, 2552–2555.
- 221 H. G. G. DEKKING, *Appl. Polym. Sci.* **1965**, 9, 1641–1651.
- 222 H. G. G. DEKKING, *Appl. Polym. Sci.* **1967**, 11, 23–36.
- 223 L. P. MEIER, R. A. SHELDEN, W. R. CASERI, *et al.*, *Macromolecules* **1994**, 27, 1637–1642.
- 224 U. VELTEN, S. TOSSATI, R. A. SCHELDEN, *et al.*, *Langmuir* **1999**, 15, 6940–6945.
- 225 U. VELTEN, R. A. SCHELDEN, W. R. CASERI, *et al.*, *Macromolecules* **1999**, 32, 3590–3597.
- 226 O. PRUCKER, J. RÜHE, *Macromolecules* **1998**, 31, 592–601.
- 227 O. PRUCKER, J. RÜHE, *Macromolecules* **1998**, 31, 602–613.
- 228 A. ROTERS, M. SCHIMMEL, J. RÜHE, *et al.*, *Langmuir* **1998**, 14, 3999–4004.
- 229 O. PRUCKER, J. RÜHE, *Langmuir* **1998**, 14, 6893–6898.
- 230 M. BIESALSKI, J. RÜHE, *Macromolecules* **1999**, 32, 2309–2316.
- 231 M. BIESALSKI, J. RÜHE, *Langmuir* **2000**, 16, 1943–1950.
- 232 A. LASCHITSCH, C. BOUCHARD, J. HABICHT, *et al.*, *Macromolecules* **1999**, 32, 1244–1251.
- 233 J. HABICHT, M. SCHMIDT, J. RÜHE, *et al.*, *Langmuir* **1999**, 15, 2460–2465.
- 234 O. PRUCKER, M. SCHIMMEL, G. TOVAR, *et al.*, *Adv. Mater.* **1998**, 10, 1073–1077.
- 235 G. TOVAR, S. PAUL, W. KNOLL, *et al.*, *J. Supramol. Sci.* **1995**, 2, 89–98.
- 236 O. PRUCKER, J. RÜHE, *MRS Symp. Proc.* **1993**, 304, 163.
- 237 J. RÜHE, *MACROMOL. SYMP.* **1997**, 126, 215.
- 238 O. PRUCKER, J. HABICHT, I.-J. PAK, *et al.*, *Mater. Sci. Eng. C* **1999**, 8-9, 291–297.
- 239 J. ZHANG, C. Q. CUI, T. B. LIM, *et al.*, *Macromol. Chem. Phys.* **2000**, 201, 1653–1661.
- 240 W. HUANG, G. SKANTH, G. L. BAKER, *et al.*, *Langmuir* **2001**, 17, 1731–1736.
- 241 a) U. SCHMELMER, R. JORDAN, W. GEYER, *et al.*, *Angew. Chem.* **2003**, 115, 577–581; *Angew. Chem. Int. Ed.* **2003**, 42, 559–563. b) R. JORDAN, J. F. KANG, A. ULMAN, *et al.*, *Polym. Preprints* **2003**, in press. c) R. JORDAN, U. SCHMELMER, A. PAUL, *et al.*, *Polym. Preprints* **2003**, in press. d) U. SCHMELMER, R. JORDAN, A. PAUL, *et al.*, *Polym. Preprints* **2003**, in press.
- 242 a) E. B. ZHULINA, O. V. BORISOV, T. M. BIRSHTEIN, *J. Phys II* **1992**, 2, 63–74.

- b) O. V. BORISOV, E. B. ZHULINA, T. M. BIRSHTEIN, *Macromolecules* **1994**, *27*, 4795–4803. c) E. B. ZHULINA, T. M. BIRSHTEIN, O. V. BORISOV, *Macromolecules* **1995**, *28*, 1491–1499. d) V. A. PRYAMITSYN, F. A. M. LEERMAKERS, E. B. ZHULINA, *Macromolecules* **1997**, *30*, 584–589. e) R. ISRAELS, F. A. M. LEERMAKERS, G. J. FLEER, *et al.*, *Macromolecules* **1994**, *27*, 3249–3261. f) 165.
- 243 F. REHFELDT, M. TANAKA, L. PAGNONI, *et al.*, *Langmuir* **2002**, *18*, 4908–4914.
- 244 T. COSGROVE, K. RYAN, *Langmuir* **1990**, *6*, 136–1342.
- 245 T. COSGROVE, T. G. HEATH, K. RYAN, *et al.*, *Macromolecules* **1987**, *20*, 2879–2882.
- 246 T. KIDCHOB, S. KIMURA, Y. IMANISHI, *J. Control. Rel.* **1998**, *50*, 205–214.
- 247 X. GUO, A. WEISS, M. BALLAUF, *Macromolecules* **1999**, *32*, 6043–6046.
- 248 a) S. MINKO, G. GALFIJCHUK, A. SIDORENKO, *et al.*, *Macromolecules* **1999**, *32*, 4525–4531. b) S. MINKO, A. SIDORENKO, M. STAMM, *et al.*, *Macromolecules* **1999**, *32*, 4532–4538. c) A. SIDORENKO, S. MINKO, G. GALFIJCHUK, *et al.*, *Macromolecules* **1999**, *32*, 4539–4543. d) S. MINKO, I. A. LUZINOV, I. Y. EVCHUK, *et al.*, *Polymer* **1996**, *37*, 177–181. e) I. A. LUZINOV, I. Y. EVCHUK, S. S. MINKO, *et al.*, *J. Appl. Polym. Sci.* **1998**, *67*, 299–305. f) I. A. LUZINOV, A. VORONOV, S. S. MINKO, *et al.*, *J. Appl. Polym. Sci.* **1996**, *61*, 1101–1109. g) I. A. LUZINOV, S. S. MINKO, V. SENKOVSKY, *et al.*, *Macromolecules* **1998**, *31*, 3945–3952.
- 249 G. MINO, S. KAIZERMANN, *J. Polym. Sci.* **1958**, *31*, 242–243.
- 250 G. MINO, S. KAIZERMANN, E. RASMUSSEN, *J. Polym. Sci.* **1959**, *38*, 393–401.
- 251 T. MATSUDA, N. SAITO, T. SUGAWARA, *Macromolecules* **1996**, *29*, 7446–7451.
- 252 O. NUYKEN, R. WEIDNER, *Adv. Polym. Sci.* **1986**, *73/74*, 147–199 and references therein.
- 253 P. C. WIELAND, O. NUYKEN, M. SCHMIDT, *et al.*, *Macromol. Rapid Commun.* **2001**, *22*, 1255–1260.
- 254 M. L. C. M. OOSTERLING, A. SEIN, A. J. SCHOUTEN, *Polymer* **1992**, *33*, 4394–4400.
- 255 K. OHKITA, N. NAKAYAMA, T. OHTAKI, *Coatings Technol.* **1983**, *55*, 35–39.
- 256 N. TSUBOKAWA, *J. Macromol. Sci.- Chem.* **1987**, *A24*, 763–775.
- 257 N. TSUBOKAWA, T. YOSHIHARA, Y. SONE, *J. Polym. Sci. A-Polym. Chem.* **1992**, *30*, 561–567.
- 258 D. BRAUN, A. KAMPFRATH, *Angew. Makromol. Chem.* **1984**, *120*, 1–41.
- 259 E. SCHOMAKER, A. J. ZWARTEVEEN, G. CHALLA, *et al.*, *Polym. Commun.* **1988**, *29*, 158–160.
- 260 a) S. T. MILNER, *Europhys. Lett.* **1988**, *7*, 695–699. b) S. T. MILNER, T. A. WITTEN, M. E. CATES, *Macromolecules* **1988**, *21*, 2610–2619.
- 261 Y. LIU, M. H. RAFAILOVICH, J. SOKOLOV, *et al.*, *Phys. Rev. Lett.* **1994**, *73*, 440–443.
- 262 A. R. LEIBLER, *Proc. of the OUMS-Conference on Ordering in Macromolecular Systems*, Osaka, June **1983**.
- 263 M. D. INGALL, C. H. HONEYMAN, J. V. MERCURE, *et al.*, *J. Am. Chem. Soc.* **1999**, *121*, 3607–3613.
- 264 R. P. QUIRK, R. T. MATHERS, *Polym. Bull.* **2001**, *45*, 471–477.
- 265 Q. ZHOU, S. WANG, X. FAN, J. MAYS, *et al.*, *Langmuir* **2002**, *18*, 3324–3331.
- 266 Q. ZHOU, X. FAN, C. XIA, *et al.*, *Chem. Mat.* **2001**, *13*, 2465–2467.
- 267 X. FAN, Q. ZHOU, C. XIA, *et al.*, *Langmuir* **2002**, *18*, 4511–4518.
- 268 A. VIDAL, J. B. DONNET, J. P. KENNEDY, *J. Polym. Sci., Polym. Lett. Ed.* **1977**, *15*, 585–588.
- 269 A. VIDAL, A. GUYOT, J. P. KENNEDY, *Polym. Bull.* **1980**, *2*, 315–20.
- 270 A. VIDAL, A. GUYOT, J. P. KENNEDY, *Polym. Bull.* **1982**, *6*, 401–407.
- 271 S. SPANGE, *Prog. Polym. Sci.* **2000**, *25*, 718–849.
- 272 R. JORDAN, A. ULMAN, *J. Am. Chem. Soc.* **1998**, *120*, 243–247.
- 273 R. JORDAN, N. WEST, A. ULMAN, *et al.*, *Macromolecules* **2001**, *34*, 1606–1611.
- 274 S. KOBAYASHI, S. IJIMA, T. IGARASHI, *et al.*, *Macromolecules* **1987**, *20*, 1729–1739.
- 275 R. JORDAN, unpublished results.
- 276 C. ERDELEN, L. HÄUSSLING, R. NAUMANN, *et al.*, *Langmuir* **1994**, *10*, 1246–1250.
- 277 A. C. TEMPELTON, M. J. HOSTETLER, C. T. KRAFT, *et al.*, *J. Am. Chem. Soc.* **1998**, *120*, 1906–1911.



- 278 K. MATYJASZEWSKI, P. MILLER, N. SHUKLA, *et al.*, *Macromolecules* **1999**, *32*, 8716–8724.
- 279 T. LEHMANN, J. RÜHE, *Macromol. Symp.* **1999**, *142*, 1–12.
- 280 B. ZHAO, W.J. BRITAIN, *J. Am. Chem. Soc.* **1999**, *121*, 3557–3558.
- 281 B. ZHAO, W.J. BRITAIN, *Macromolecules* **2000**, *33*, 342–348.
- 282 B. ZHAO, W.J. BRITAIN, *Macromolecules* **2000**, *33*, 8813–8820.
- 283 B. ZHAO, W.J. BRITAIN, W. ZHOU, S.Z.D. CHENG, *J. Am. Chem. Soc.* **2000**, *122*, 2407–2408.
- 284 B. ZHAO, W.J. BRITAIN, W. ZHOU, *et al.*, *Macromolecules* **2000**, *33*, 8821–8827.
- 285 C.J. HAWKER, *Acc. Chem. Res.* **1997**, *30*, 373–382.
- 286 a) T. OTSU, M. YOSHIDA. *Makromol. Chem. Rapid Commun.* **1982**, *3*, 127–132.  
b) T. OTSU, M. YOSHIDA, T. TAZAKI. *Makromol. Chem. Rapid Commun.* **1982**, *3*, 133–140.
- 287 K. MATYJASZEWSKI, In *Controlled/Living Radical Polymerization*; MATYJASZEWSKI, K., Ed.; ACS Symposium Series 768; American Chemical Society: Washington, DC, **2000**.
- 288 M.W. WEIMER, H. CHEN, E.P. GIANNELIS, *et al.* *J. Am. Chem. Soc.* **1999**, *121*, 1615–1616.
- 289 M. HUSEMAN, E.E. MALMSTROM, M. MCNAMARA, *et al.*, *Macromolecules* **1999**, *32*, 1424–1431.
- 290 M. HUSEMANN, M. MORRISON, D. BENOIT, *et al.*, C.J. HAWKER, *J. Am. Chem. Soc.* **2000**, *122*, 1844–1845.
- 291 Y. NAKAYAMA, T. MATSUDA, *Macromolecules* **1996**, *29*, 8622–8630.
- 292 Y. NAKAYAMA, T. MATSUDA, *Macromolecules* **1999**, *32*, 5405–5410.
- 293 H.J. LEE, Y. NAKAYAMA, T. MATSUDA, *Macromolecules* **1999**, *32*, 6989–6995.
- 294 S. KIDOAKI, S. OHYA, Y. NAKAYAMA, *et al.*, *Langmuir* **2001**, *17*, 2402–2407.
- 295 Y. NAKAYAMA, M. SUDO, K. UCHIDA, *et al.*, *Langmuir* **2002**, *18*, 2601–2606.
- 296 B. DE BOER, H.K. SIMON, M.P.L. WERTS, *et al.*, *Macromolecules* **2000**, *33*, 349–356.
- 297 M. NIWA, M. DATE, N. HIGASHI, *Macromolecules* **1996**, *29*, 3681–3685.
- 298 X. HUANG, M.J. WIRTH, *Anal. Chem.* **1997**, *69*, 4577–4580.
- 299 X. HUANG, L.J. DONESKI, M.J. WIRTH, *Anal. Chem.* **1998**, *70*, 4023–4029.
- 300 X. HUANG, M.J. WIRTH, *Macromolecules* **1999**, *32*, 1694–1696.
- 301 T. WU, K. EFIMENKO, J. GENZER, *Macromolecules* **2001**, *34*, 684–686.
- 302 M. EJAZ, S. YAMAMOTO, K. OHNO, *et al.*, *Macromolecules* **1998**, *31*, 5934–5936.
- 303 M. EJAZ, K. OHNO, Y. TSUJII, *et al.*, *Macromolecules* **2000**, *33*, 2870–2874.
- 304 S. YAMAMOTO, M. EJAZ, Y. TSUJII, *et al.*, *Macromolecules* **2000**, *33*, 5602–5607.
- 305 S. YAMAMOTO, M. EJAZ, Y. TSUJII, *et al.*, *Macromolecules* **2000**, *33*, 5608–5612.
- 306 S. YAMAMOTO, Y. TSUJII, T. FUKUDA, *Macromolecules* **2000**, *33*, 5995–5998.
- 307 M. EJAZ, S. YAMAMOTO, Y. TSUJII, *et al.*, *Macromolecules* **2002**, *35*, 1412–1418.
- 308 S. YAMAMOTO, Y. TSUJII, T. FUKUDA, *Macromolecules* **2002**, *35*, 6077–6079.
- 309 D. GOPIREDDY, S.M. HUSSON, *Macromolecules* **2002**, *35*, 4218–4221.
- 310 T. VON WERNE, T.E. PATTEN, *J. Am. Chem. Soc.* **1999**, *121*, 7409–7410.
- 311 T. VON WERNE, T.E. PATTEN, *J. Am. Chem. Soc.* **2001**, *123*, 7497–7505.
- 312 C. PERRUCHOT, M.A. KHAN, A. KAMITSI, *et al.*, *Langmuir* **2001**, *17*, 4479–4481.
- 313 H. BÖTTCHER, M.L. HALLENSLEBEN, S. NUSS, *et al.*, *Polym. Bull.* **2000**, *44*, 223–229.
- 314 H. BÖTTCHER, M.L. HALLENSLEBEN, R. JANKE, *et al.*, ATRP 'Living/Controlled Radical Grafting of Solid Particles to Create New Properties' in: *Tailored Polymers and Applications*, (Y. YAGCI, M.K. MISHRA, O. NUYKEN, K. ITO, G. WNEK eds.), VSP Publishers, New York **2000**.
- 315 H. MORI, A. BÖKER, G. KRAUSCH, *et al.*, *Macromolecules* **2001**, *34*, 6871–6882.
- 316 X. KONG, T. KAWAI, J. ABE, *et al.*, *Macromolecules* **2001**, *34*, 1837–1844.
- 317 J.D. JEYAPRAKASH, S. SAMUEL, R. DHAMODHARAN, *et al.*, *Macromol. Rapid Commun.* **2002**, *23*, 277–281.
- 318 S.G. BOYES, W.J. BRITAIN, X. WENG, *et al.*, *Macromolecules* **2002**, *35*, 4960–4967.
- 319 R.R. SHAH, D. MERRECEYES, M. HUSEMANN, *et al.*, *Macromolecules* **2000**, *33*, 597–605.
- 320 J.-B. KIM, M.L. BRUENING, G.L. BAKER, *J. Am. Chem. Soc.* **2000**, *122*, 7616–7617.

- 321 W. HUANG, G. L. BAKER, M. L. BRUENING, *Angew. Chem.* **2001**, *113*, 1558–1560; *Angew. Chem. Int. Ed.* **2001**, *40*, 1510–1512.
- 322 S. NUSS, H. BÖTTCHER, H. WURM, *et al.*, *Angew. Chem.* **2001**, *113*, 4137–4139; *Angew. Chem. Int. Ed.* **2001**, *40*, 4016–4018.
- 323 W. HUANG, J.-B. KIM, M. L. BRUENING, *et al.*, *Macromolecules* **2002**, *35*, 1175–1179.
- 324 J.-B. KIM, W. HUANG, M. L. BRUENING, *et al.*, *Macromolecules* **2002**, *35*, 4799–4805.
- 325 D. M. JONES, A. A. BROWN, W. T. S. HUCK, *Langmuir* **2002**, *18*, 1265–1269.
- 326 Y. TSUJII, M. EJAZ, K. SATO, *et al.*, *Macromolecules* **2001**, *34*, 8872–8878.
- 327 M. BAUM, W. J. BRITAIN, *Macromolecules* **2002**, *35*, 610–615.
- 328 G. ZHENG, H. D. H. STÖVER, *Macromolecules* **2002**, *35*, 6828–6834.
- 329 R. A. SEDJO, B. K. MIROUS, W. J. BRITAIN, *Macromolecules* **2000**, *33*, 1492–1493.
- 330 S. ANGOT, N. AYRES, S. A. F. BON, *et al.*, *Macromolecules* **2001**, *34*, 768–774.
- 331 K. M. VAETH, R. J. JACKMANN, A. J. BLACK, *et al.*, *Langmuir* **2000**, *16*, 8495–8500.
- 332 D. FU, L.-T. WENG, B. DU, *et al.*, *Adv. Mater.* **2002**, *14*, 339–343.
- 333 N. TSUBOKAWA, K. KOBAYASHI, Y. SONE, *Polym. J.* **1987**, *19*, 1147–1155.
- 334 R. KROKER, K. HAMANN, *Angew. Makromol. Chem.* **1970**, *13*, 1–22.
- 335 E. DIETZ, N. FERY, K. HAMANN, *Angew. Makromol. Chem.* **1974**, *115*–129.
- 336 M. L. C. M. OOSTERLING, E. WILLEMS, A. J. SCHOUTEN, *Polymer* **1995**, *36*, 4463–4470.
- 337 S. H. WIERINGA, A. J. SCHOUTEN, *Macromolecules* **1996**, *29*, 3032–3034.
- 338 A. HEISE, H. MENZEL, H. YIM, *et al.*, *Langmuir* **1997**, *13*, 723–728.
- 339 Y. C. CHANG, C. W. FRANK, *Macromol. Symp.* **1997**, *118*, 641–646.
- 340 Y.-C. CHANG, C. W. FRANK, G. G. FORSTMANN *et al.*, *J. Chem. Phys.* **1999**, *111*, 6136–6143.
- 341 L. HARTMANN, T. KRATZMÜLLER, H.-G. BRAUN, *et al.*, *Macromol. Rapid Commun.* **2000**, 795–868.
- 342 T. KRATZMÜLLER, D. APPELHANS, H.-G. BRAUN, *Adv. Mater.* **1999**, *11*, 555–557.
- 343 J. K. WHITESSELL, H. K. CHANG, *Science* **1993**, *261*, 73–76.
- 344 J. K. WHITESSELL, H. K. CHANG, *Mol. Cryst. Liq. Cryst.* **1994**, *240*, 251–258.
- 345 J. K. WHITESSELL, H. K. CHANG, C. S. WHITESSELL, *Angew. Chem.* **1994**, *106*, 921–924; *Angew. Chem. Int. Ed.* **1994**, *33*, 871–874.
- 346 M. HUSEMANN, D. MECERREYES, C. J. HAWKER, *et al.*, *Angew. Chem.* **1999**, *111*, 685–687; *Angew. Chem. Int. Ed.* **1999**, *38*, 647–649.
- 347 I. S. CHOI, R. LANGER, *Macromolecules* **2001**, *34*, 5361–5363.
- 348 W. R. HERTLER, D. Y. SOGAH, F. H. BOETTCHER, *Macromolecules* **1990**, *23*, 1264–1268.
- 349 D. L. HUBER, K. E. GONSAIVES, G. CARLSON, *et al.* in: *Interfacial aspects of multi-component polymer materials* (D. J. Lohse, T. P. Russell, L. H. Sperling, eds.), Plenum Press, New York **1997**, 107–134.
- 350 K. LOOS, V. VON BRAUNMÜHL, R. STADLER, *et al.*, *Macromol. Rapid Commun.* **1997**, *18*, 927–938.
- 351 T. CHEN, G. KUMAR, M. T. HARRIS, *et al.*, *Biotechnology and Bioengineering* **2000**, *70*, 565–573.
- 352 R. M. CROOKS, *CHEMPHYSICHEM* **2001**, *2*, 644–654.